

Generalized Pseudospectral Shattering and Inverse-Free Matrix Pencil Diagonalization

James Demmel*

Ioana Dumitriu[†]Ryan Schneider^{*‡}

Abstract

We present a randomized, inverse-free algorithm for producing an approximate diagonalization of any $n \times n$ matrix pencil (A, B) . The bulk of the algorithm rests on a randomized divide-and-conquer eigensolver for the generalized eigenvalue problem originally proposed by Ballard, Demmel, and Dumitriu [Technical Report 2010]. We demonstrate that this divide-and-conquer approach can be formulated to succeed with high probability provided the input pencil is sufficiently well-behaved, which is accomplished by generalizing the recent pseudospectral shattering work of Banks, Garza-Vargas, Kulkarni, and Srivastava [Foundations of Computational Mathematics 2022]. In particular, we show that perturbing and scaling (A, B) regularizes its pseudospectra, allowing divide-and-conquer to run over a simple random grid and in turn producing an accurate diagonalization of (A, B) in the backward error sense. The main result of the paper states the existence of a randomized algorithm that with high probability (and in exact arithmetic) produces invertible S, T and diagonal D such that $\|A - SDT^{-1}\|_2 \leq \varepsilon$ and $\|B - ST^{-1}\|_2 \leq \varepsilon$ in at most $O(\log^2(\frac{n}{\varepsilon}) T_{\text{MM}}(n))$ operations, where $T_{\text{MM}}(n)$ is the asymptotic complexity of matrix multiplication. This not only provides a new set of guarantees for highly parallel generalized eigenvalue solvers but also establishes nearly matrix multiplication time as an upper bound on the complexity of inverse-free, exact-arithmetic matrix pencil diagonalization.

Keywords: Matrix pencil, generalized eigenvalue problem, diagonalization, pseudospectra

AMS MSC2020 Codes: 15A22, 65F15

Communicated by Peter Buergisser.

*Department of Mathematics, University of California Berkeley

[†]Department of Mathematics, University of California San Diego

[‡]Corresponding author (ryan.schneider@berkeley.edu)

Contents

1	Introduction	3
1.1	The Generalized Eigenvalue Problem	3
1.2	Divide-and-Conquer Eigensolvers	3
1.3	Pseudospectra and Random Matrix Theory	4
1.4	Matrix Pencil Diagonalization	5
1.5	Complexity and Numerical Stability	6
1.6	Outline	6
2	Background	7
2.1	Matrix Pencils, Eigenvalues, and Eigenvectors	7
2.2	Pseudospectra	9
3	Pseudospectral Shattering for Matrix Pencils	12
3.1	Preliminaries	13
3.2	Multi-Parameter Tail Bound	14
3.3	Shattering	16
4	Inverse-Free Divide-and-Conquer	20
4.1	Motivation	21
4.2	Numerical Building Blocks	22
4.2.1	Implicit Repeated Squaring (IRS)	22
4.2.2	RURV and GRURV	23
4.2.3	DEFLATE	24
4.3	Divide-and-Conquer Routine	26
5	Randomized Pencil Diagonalization	35
5.1	Diagonalization Routine	35
5.2	Forward Error Guarantee and Asymptotic Complexity	39
6	Numerical Examples	41
6.1	Model Problems	42
6.2	Large n and Infinite Eigenvalues	45
6.3	Singular Pencils	47
7	Conclusion	48
8	Acknowledgements	49
A	Alternative Versions of Bauer-Fike for Matrix Pencils	49
B	Finite-Precision Analysis	51
B.1	Black-Box Assumptions	51
B.2	Finite-Precision Shattering	52
B.3	Two-Matrix GRURV	54

1 Introduction

1.1 The Generalized Eigenvalue Problem

Given matrices $A, B \in \mathbb{C}^{n \times n}$ with $\det(A - xB) \in \mathbb{C}[x]$ not identically zero, the generalized eigenvalue problem seeks pairs $(\lambda, v) \in \mathbb{C} \times \mathbb{C}^n$ with $v \neq 0$ such that

$$Av = \lambda Bv. \tag{1.1.1}$$

As the name implies, this is a generalization of the standard, single-matrix eigenvalue problem, which we recover by setting $B = I$. Solutions to (1.1.1) yield a generalized eigenvalue λ and a generalized eigenvector v of the matrix pencil (A, B) . As in the standard eigenvalue problem, generalized eigenvalues and eigenvectors arise in a variety of research disciplines, ranging from signal processing [38,46] and binary classification [32,43] to linear differential equations [33].

Unlike the single-matrix case, however, the generalized eigenvalue problem may admit eigenvalues at infinity, which arise when B is singular. Even more strange behavior occurs when the characteristic polynomial $\det(A - xB)$ is identically zero, in which case the pencil (A, B) is *singular* and (1.1.1) cannot be used to define eigenvalues and eigenvectors. While the singular case is not the primary focus of this paper, our results apply generally, and we will return to the challenge of computing eigenvalues/eigenvectors for singular pencils later on.

When B is invertible, the pencil (A, B) and the matrix $B^{-1}A$ have the same set of eigenvalues and eigenvectors. This prompts a natural approach to the problem: explicitly form $B^{-1}A$ and apply any method for solving the single-matrix eigenvalue problem. Though straightforward, this naive approach is unsatisfactory for a variety of reasons. First, many applications feature pencils where one (or both) of the matrices involved is singular. Even when this is not the case, numerical stability concerns still prompt us to avoid taking inverses (see Section 1.5). With this in mind, our focus will be on methods that work with the pencil (A, B) rather than the matrix $B^{-1}A$.

The standard method for solving the generalized eigenvalue problem is the QZ algorithm of Moler and Stewart [44], which obtains generalized eigenvalues and eigenvectors of (A, B) by first producing its generalized Schur form via shifted QR. A significant amount of research has focused on exploring the performance of this approach as well as developing a variety of extensions [39, 61, 62]. The main drawback to QZ is its relative difficulty to parallelize. Efforts to do so [1] require a non-trivial reworking of the numerical details and to our knowledge are not widely used. Methods for extracting only a certain subset of generalized eigenvalues/eigenvectors for sparse problems include the trace minimization algorithm [49], projection methods [48], and extensions of the Lanczos procedure [24].

In this paper, we present a naturally parallelizable method that, given any matrix pencil (A, B) , constructs a full set of approximate generalized eigenvalues and eigenvectors. For simplicity, we will drop the label “generalized” in the subsequent sections and simply refer to eigenvalues and eigenvectors of (A, B) .

1.2 Divide-and-Conquer Eigensolvers

To construct an easily parallelizable method, we employ a divide-and-conquer strategy that recursively splits the original problem (A, B) into smaller ones with disjoint spectra. By ensuring that these subproblems share no eigenvalues (and have no overlapping eigenspaces), we can handle them in parallel. Moreover, as long as the spectrum of each subproblem is contained in its predecessor’s, we can reconstruct a full set of eigenvalues/eigenvectors for (A, B) from those of the smallest subproblems, which are either 1×1 and therefore trivial or small enough to handle with existing techniques.

One step of divide-and-conquer consists of the following:

1. Divide the eigenvalues into two disjoint sets (opposite sides of a line, inside/outside a circle, etc.).
2. Compute unitary projectors onto the corresponding eigenspaces.
3. Apply the projectors to the original problem, splitting it in two.

Note that if we are able to consistently split the eigenvalues into sets of roughly equal size, only $O(\log(n))$ steps of divide-and-conquer are required to find a full set of eigenvalues/eigenvectors.

Parallel divide-and-conquer eigensolvers have a rich history in the literature. Early approaches for dense matrices followed work of Beavers and Denman [12], which demonstrated that the matrix sign function of Roberts [45] could be used to compute projectors onto certain eigenspaces. While it is possible to adapt the sign function for the generalized eigenvalue problem [29], it traditionally requires taking inverses which, as mentioned above, we’d prefer to avoid. An alternative, inverse-free method was outlined by Malyshev [42] and subsequently explored, for both pencils and individual matrices, in work of Bai, Demmel, and Gu [4]. In this approach, spectral projectors are approximated by repeatedly and implicitly squaring $A^{-1}B$, where eigenvalues are split by the unit circle.

The requirement to have unitary projectors in each step of divide-and-conquer is non-trivial. In fact, neither the sign function nor the inverse-free, repeated squaring approach of Malyshev produce explicitly unitary projectors; instead, rank-revealing factorizations are applied to guarantee a unitary result. The rank-revealing aspect is important here, as the rank of each projector tells us how many eigenvalues lie in a corresponding region of the complex plane. While there are many ways to compute a rank-revealing factorization [13, 31, 54], we are specifically interested in a randomized, rank-revealing URV factorization introduced by Demmel, Dumitriu, and Holtz [17], which is simple to implement and particularly compatible with inverse-free computations [6].

The method we present combines this randomized, rank-revealing factorization with the inverse-free approach of Malyshev. A technical report of Ballard, Demmel, and Dumitriu [6] already explored this combination, though it left one fundamental question unanswered: how do we reliably split the spectrum at each step? The importance of this cannot be understated, as divide-and-conquer can only hope to be efficient if the split is significant (i.e., close to 50/50) at each step. And while we might hope that randomly selecting a dividing line/circle may work with high probability, the method will fail if whatever we choose intersects the spectrum or even pseudospectrum. Our most important contribution, we resolve this problem by adapting recent work of Banks et al. [9], demonstrating that by adding a bit of randomness to the problem we can state the inverse-free procedure in a way that succeeds with high probability.

1.3 Pseudospectra and Random Matrix Theory

The pseudospectrum of a matrix or matrix pencil consists of all eigenvalues of nearby matrices/pencils. We will define them precisely in Section 2.2, but for now we can think of the ϵ -pseudospectrum as containing the eigenvalues of matrices or pencils that are, in a spectral norm sense, ϵ -away. In general, each pseudospectrum consists of connected components in \mathbb{C} containing at least one true eigenvalue, to which they collapse as $\epsilon \rightarrow 0$. For more background, see the standard reference [58].

Looking toward floating-point implementations where error may accumulate at each step, we expect that divide-and-conquer eigensolvers are most likely to fail when the ϵ -pseudospectra for small ϵ (say close to machine precision) cover large areas of the complex plane, in which case it becomes difficult to select a dividing line/circle that will significantly split the spectrum without causing the process to break down. This is particularly important for matrix pencils, since infinite eigenvalues are a possibility.

To work around this, our algorithm begins by adding small perturbations to the input matrices, swapping the pencil (A, B) for $(\tilde{A}, \tilde{B}) = (A + \gamma G_1, B + \gamma G_2)$, where γ is a tuning parameter and G_1 and G_2 are independent, complex Ginibre random matrices – i.e., matrices whose entries are independent and identically distributed (i.i.d.) standard complex Gaussian with mean zero and variance $1/n$. It is well-known that random matrices with i.i.d. entries have a number of useful properties [5, 20, 21]; not only are they almost surely invertible, but in many cases distributions for their smallest singular values are known [47, 57]. The perturbation applied to (A, B) leverages these properties to regularize the problem, replacing what could be a poorly-conditioned input pencil with one whose eigenvalue problem is well-behaved (in a way to be defined precisely later).

The concept of using a random perturbation to regularize a matrix – considered a linear algebra extension of smoothed analysis – has been well-studied [2, 25, 50]. Of particular relevance here, Banks et al. [10] showed that adding a Ginibre perturbation to a matrix provides a probabilistic bound on its smallest singular value while also controlling its eigenvector condition number. In a subsequent work [9] they demonstrated that these perturbations also regularize ϵ -pseudospectra, breaking them into small connected components around distinct eigenvalues. Banks et al. used this phenomena, referred to as *pseudospectral shattering*, as the basis for a divide-and-conquer eigensolver, which proceeds as follows:

1. Perturb the input matrix, shattering its pseudospectra into distinct components.
2. Construct a random grid that covers the spectrum of the matrix. Shattering implies that a fine enough grid does not intersect the pseudospectra, and moreover each eigenvalue of the perturbed matrix is contained in a unique grid box with high probability.
3. Run divide-and-conquer (using the sign function), each time splitting the eigenvalues by a grid line.

This rough outline obscures the numerical details but captures the core idea: by perturbing, we obtain a matrix whose pseudospectra are sufficiently well-behaved for divide-and-conquer to succeed using a simple random grid. We generalize these results here, proving our own version of pseudospectral shattering for matrix pencils and using it to complete the divide-and-conquer algorithm posed by Ballard, Demmel, and Dumitriu [6].

This is not the first approach that solves the generalized eigenvalue problem by perturbing the input matrices. A method of Hochstenbach, Mehl, and Plestenjak [36], for example, finds eigenvalues via QZ by first applying rank-completing perturbations, if applicable. Note that because our perturbations are random, and because we use a random rank-revealing factorization, convergence is only possible with high probability.

1.4 Matrix Pencil Diagonalization

The decision to perturb the input matrices also impacts accuracy, where only backward-error guarantees will be available. In particular, the eigensolver we present approximates the eigenvalues/eigenvectors of the nearby pencil (\tilde{A}, \tilde{B}) rather than those of (A, B) . While perturbation results for the generalized eigenvalue problem are well-developed in the literature, see for example [55, Chapter VI], little can be said about the accuracy of an individual eigenvalue or eigenvector found this way in the absence of additional information (e.g., a condition number). Ultimately, the eigenvalues of (\tilde{A}, \tilde{B}) may vary significantly from those of (A, B) even when $\|A - \tilde{A}\|_2$ and $\|B - \tilde{B}\|_2$ are small. Take the following 2×2 matrices as an example:

$$A = B = \begin{pmatrix} 1 & 0 \\ 0 & 10^{-10} \end{pmatrix}, \quad \tilde{A} = \begin{pmatrix} 1 & 0 \\ 0 & 1.5 \times 10^{-10} \end{pmatrix}, \quad \tilde{B} = \begin{pmatrix} 1 & 0 \\ 0 & 5 \times 10^{-11} \end{pmatrix}. \quad (1.4.1)$$

By construction, $\|A - \tilde{A}\|_2 = \|B - \tilde{B}\|_2 = 5 \times 10^{-11}$ while $\Lambda(A, B) = \{1\}$ and $\Lambda(\tilde{A}, \tilde{B}) = \{1, 3\}$ – i.e., a tiny perturbation in A and B results in macroscopic changes to the eigenvalues. This is a consequence of the instability of the second eigenvalue of (A, B) , which itself is due to the near singularity of B . Guarantees are even worse when the matrix B is actually singular. In particular, our algorithm always produces a set of finite eigenvalues, even though the input pencil may have one or many eigenvalues at infinity.

With this in mind, we consider the related problem of joint diagonalization. A pair of nonsingular matrices S and T jointly diagonalize A and B , or equivalently diagonalize the pencil (A, B) , if $S^{-1}AT$ and $S^{-1}BT$ are both diagonal. The connection to the generalized eigenvalue problem is fairly straightforward, as the pencils (A, B) and $(S^{-1}AT, S^{-1}BT)$ have the same set of eigenvalues. Moreover any matrix pencil with a full set of distinct eigenvalues can be diagonalized by matrices S and T containing its left and right eigenvectors, respectively [55, Corollary VI.1.12].

It is in this context that our method produces provably accurate results, in a backward-error sense, regardless of the input pencil (A, B) . The main result of the paper (presented technically as [Theorem 5.1](#) and [Proposition 5.3](#) below) may be summarized as follows:

Theorem 1.1. *Let $(A, B) \in \mathbb{C}^{n \times n} \times \mathbb{C}^{n \times n}$ be any matrix pencil and let $\varepsilon < 1$ be any desired (backward) diagonalization accuracy. There exists an exact-arithmetic, inverse-free, and randomized divide-and-conquer algorithm that takes as inputs (A, B) and ε and produces matrices $D, S, T \in \mathbb{C}^{n \times n}$ such that D is diagonal, S and T are nonsingular, and*

$$\|A - SDT^{-1}\|_2 \leq \varepsilon \quad \text{and} \quad \|B - ST^{-1}\|_2 \leq \varepsilon$$

with probability at least $1 - O(\frac{1}{n})$. This algorithm requires at most $O(\log^2(\frac{n}{\varepsilon})T_{\text{MM}}(n))$ operations, where $T_{\text{MM}}(n)$ is the complexity of $n \times n$ matrix multiplication.

Note that [Theorem 1.1](#) is fully general, and in particular applies to edge cases like $A = B = 0$. As we will see, this result provides forward error guarantees on approximate eigenvalues and eigenvectors when B is invertible and (A, B) has a full set of distinct eigenvalues ([Theorem 5.2](#)).

1.5 Complexity and Numerical Stability

The complexity $O(\log^2(\frac{n}{\epsilon})T_{\text{MM}}(n))$ in [Theorem 1.1](#) implies that our algorithm runs in *nearly matrix multiplication time*, meaning its asymptotic complexity is the same as matrix multiplication up to logarithmic factors. This is accomplished by showing that (1) one step of divide-and-conquer runs in nearly matrix multiplication time, and (2) that only $O(\log(n))$ steps are needed to obtain the approximate diagonalization. As alluded to earlier, (2) is guaranteed as long as the eigenvalue split at each step is significant. Claim (1), meanwhile, stems from using only QR and matrix multiplication, both of which can be implemented stably in $O(T_{\text{MM}}(n))$ operations (see work of Demmel, Dumitriu, and Holtz [[17](#)]). In fact, matrix multiplication and QR have $O(T_{\text{MM}}(n))$ implementations that are respectively forward and backwards stable – i.e., the relative forward/backward error is bounded by machine precision \mathbf{u} times an appropriate condition number.

This combination of efficiency and stability is our motivation for stating an inverse-free approach. While it is possible to invert a matrix in $O(T_{\text{MM}}(n))$ operations, such implementations are only logarithmically stable [[17](#), §3], meaning a polylogarithmic increase in precision is required to obtain the same error as a truly backward stable version. Accordingly, the pseudospectral method of Banks et al., which requires inversion to compute the sign function, is built on a logarithmically stable black-box inversion algorithm [[9](#), Definition 2.7]. This lack of stability carries over into their floating-point analysis, which yields a slightly weaker-than-logarithmic stability guarantee for the divide-and-conquer routine as a whole.

We do not present a full finite-precision analysis of our algorithm in this paper (though we do outline progress in that direction in [Appendix B](#)). Nevertheless, we anticipate that the inverse-free approach presented here can produce a logarithmically stable method for computing an approximate diagonalization of any matrix or pencil, including the singular case. In addition, we present examples in [Sections 3](#) and [6](#) in which the use of inversion (in double precision) introduces nontrivial – and potentially catastrophic – errors. In light of these examples, we make the case that an inverse-free algorithm is likely to perform significantly better on arbitrary pencils. As a result, we position our work as a more stable generalization of the algorithm presented by Banks et al. [[9](#)].

Up to this point, efficiency has been characterized by the number of arithmetic operations performed. We could alternatively focus on communication costs, both between multiple processors and/or between levels of memory hierarchy. This is especially relevant for the algorithm presented here, which is highly parallel and primed for memory-constrained applications; in particular, divide-and-conquer can be used to reduce a problem to fit in available fast memory. With this in mind, we could consider a communication-optimal implementation in the vein of Ballard et al. [[8](#)]. In fact, the variant of our approach presented by Ballard, Demmel, and Dumitriu [[6](#)] was shown to achieve asymptotic communication lower bounds for $O(n^3)$ eigensolvers (again, a consequence of avoiding inversion). While we won't analyze in detail the communication costs of our algorithm, we mention this here to emphasize the flexibility of the high level strategy: the method may be easily reformulated to minimize communication costs if desired.

1.6 Outline

To improve readability, we summarize the main contributions of each of the remaining sections here.

1. In [Section 2](#), we define the pseudospectrum of a matrix pencil and explore some of its properties, culminating in our version of Bauer-Fike [[11](#)] for pencil pseudospectra ([Theorem 2.20](#)).
2. In [Section 3](#), we prove pseudospectral shattering for matrix pencils ([Theorem 3.12](#)). The proof presented is a fairly straightforward generalization of the single-matrix case done by Banks et al. [[9](#)].
3. In [Section 4](#), we state our divide-and-conquer eigensolver and prove that it succeeds with high probability in exact arithmetic ([Theorem 4.8](#)).
4. In [Section 5](#), we use the eigensolver to construct an algorithm that produces an accurate diagonalization of any matrix pencil with high probability, thereby proving [Theorem 1.1](#).
5. In [Section 6](#) we present a handful of numerical experiments to demonstrate that the algorithm works in finite precision.
6. Finally in the appendices, we consider alternative versions of Bauer-Fike for matrix pencils ([Appendix A](#)) and discuss progress towards a floating-point analysis of the algorithm ([Appendix B](#)).

2 Background

2.1 Matrix Pencils, Eigenvalues, and Eigenvectors

In this section, we review necessary background information from linear algebra as presented in the standard references [37, 55]. Here and in the subsequent sections, $\|\cdot\|_2$ is the spectral norm, A^H and A^{-H} denote the Hermitian transpose and inverse Hermitian transpose of A , respectively, and $\kappa(A)$ is the spectral norm condition number of A . Throughout, (A, B) is a matrix pencil with $A, B \in \mathbb{C}^{n \times n}$, $\Lambda(A)$ and $\Lambda(A, B)$ denote the spectrum of A and (A, B) , and $\rho(A)$ is the spectral radius. Note that while non-square pencils are of interest in certain applications, we do not consider them here. Finally, we assume familiarity with the basic definitions of the single-matrix eigenvalue problem.

Definition 2.1. The matrix pencil (A, B) is regular if its characteristic polynomial $\det(A - xB) \in \mathbb{C}[x]$ is not identically zero. If (A, B) is not regular, it is singular.

In the following definitions we assume that (A, B) is regular. For a discussion of singular pencils, see [Remark 2.12](#).

Definition 2.2. A nonzero vector $v \in \mathbb{C}^n$ is a right eigenvector of (A, B) if $Av = \lambda Bv$ for some $\lambda \in \mathbb{C}$. In this case the eigenvalue λ is a root of the characteristic polynomial $\det(A - xB)$ and (λ, v) is an eigenpair of (A, B) . Similarly, a nonzero vector w is a left eigenvector of (A, B) if $w^H A = \lambda w^H B$.

Technically, [Definition 2.2](#) only defines finite eigenpairs; missing are the infinite eigenvalues that correspond to nontrivial vectors in the null space of B , which in some sense formally satisfy $\frac{1}{\lambda}Av = Bv$ (though of course infinity cannot be a root of the characteristic polynomial). Ultimately, eigenvectors with infinite eigenvalues are included for completeness: since the characteristic polynomial of (A, B) has degree less than n if B is singular, we only obtain a full set of n eigenvalues for (A, B) if we include those at infinity. As is standard, we will use “eigenvector” to refer to right eigenvectors unless stated otherwise.

Throughout, we are interested in factorizations of A and B that reveal the eigenvalues of (A, B) . First, we consider a generalization of Schur form to matrix pencils.

Definition 2.3. $(A, B) = (UT_A V^H, UT_B V^H)$ is a generalized Schur form of (A, B) if $U, V \in \mathbb{C}^{n \times n}$ are unitary and T_A and T_B are upper triangular.

(A, B) and its Schur form are equivalent, meaning they have the same set of eigenvalues – given by $T_A(i, i)/T_B(i, i)$ – where zeros on the diagonal of T_B correspond to eigenvalues at infinity. It is not hard to show that (A, B) is guaranteed to have a Schur form (see for example [55, Theorem VI.1.9]). As in the single-matrix case, we can build a generalized Schur decomposition by constructing V so that any leading set of columns is an orthonormal basis for a space spanned by a collection of right eigenvectors of (A, B) . In fact, the columns of V span right deflating subspaces for the pencil.

Definition 2.4. Subspaces $\mathcal{X}, \mathcal{Y} \subseteq \mathbb{C}^n$ are right and left deflating subspaces of (A, B) , respectively, if $\dim(\mathcal{X}) = \dim(\mathcal{Y})$ and $\text{span}\{Ax, Bx : x \in \mathcal{X}\} = \mathcal{Y}$.

The right and left deflating subspaces of (A, B) generalize the invariant eigenspaces of an individual matrix. That is, a collection of eigenvectors of (A, B) span a right deflating subspace that is “mapped” to a corresponding left deflating subspace by A and B . Despite the similarity in naming, the left deflating subspace of (A, B) corresponding to a set of right eigenvectors is not usually spanned by left eigenvectors.

Note that if $(A, B) = (UT_A V^H, UT_B V^H)$ then the first k columns of U span the left deflating subspace corresponding to the first k columns of V (this follows from $AV = UT_A$ and $BV = UT_B$ since T_A and T_B cannot both have a zero in the same diagonal entry). Moreover, if we take the first k columns of U as a right deflating subspace of (A^H, B^H) then the first k columns of V span the corresponding left deflating subspace since $A^H U = VT_A^H$ and $B^H U = VT_B^H$. In this way, taking a Hermitian transpose swaps left and right deflating subspaces.

Moving beyond Schur form, we next generalize diagonalization to pencils.

Definition 2.5. Nonsingular matrices S and T diagonalize (A, B) if $S^{-1}AT = D_1$ and $S^{-1}BT = D_2$ are both diagonal.

Once again, (A, B) and its diagonalization (D_1, D_2) have the same spectrum, with infinite eigenvalues corresponding to zeros on the diagonal of D_2 . Moreover, the columns of T and rows of S^{-1} contain right and left eigenvectors of (A, B) . As in the single-matrix problem, not every pencil is diagonalizable. Instead, the diagonalization given in [Definition 2.5](#) is a special case of the Kronecker canonical form [\[40\]](#), which generalizes Jordan form to matrix pencils. Of particular use here, note that if B is invertible and T contains right eigenvectors of (A, B) then $S = BT$ produces a diagonalization with $D_2 = I$.

To prove pseudospectral shattering in [Section 3](#), we will need the following definitions related to the eigenvalues/eigenvectors of an individual matrix. While each of these generalizes to pencils in a fairly straightforward way, we state them first for the single-matrix case to match how they are used in the analysis to come.

Definition 2.6. The eigenvector condition number of a diagonalizable matrix M is $\kappa_V(M) = \inf_V \kappa(V)$, where the infimum is taken over nonsingular matrices V that diagonalize M .

Definition 2.7. Let $\lambda_1(M), \dots, \lambda_n(M)$ be the eigenvalues of M repeated according to multiplicity. The eigenvalue gap of M is $\text{gap}(M) = \min_{i \neq j} |\lambda_i(M) - \lambda_j(M)|$.

Under the right conditions, we can also define a condition number for each eigenvalue of a diagonalizable matrix.

Definition 2.8. If λ_i is an eigenvalue of a matrix M with distinct eigenvalues and v_i and w_i are right and left eigenvectors corresponding to λ_i normalized so that $w_i^H v_i = 1$, then the condition number of λ_i is

$$\kappa(\lambda_i) = \|v_i w_i^H\|_2 = \|v_i\|_2 \|w_i\|_2.$$

Together, the eigenvector/eigenvalue condition numbers and the eigenvalue gap give an indication of how well-behaved the corresponding eigenvalue problem is. To generalize this to the eigenvalues/eigenvectors of a matrix pencil, we can adapt $\kappa_V(M)$ and $\text{gap}(M)$ as follows.

Definition 2.9. The (right) eigenvector condition number of a diagonalizable pencil (A, B) is $\kappa_V(A, B) = \inf_T \kappa(T)$, where the infimum is taken over all invertible T containing a full set of right eigenvectors of (A, B) .

Definition 2.10. Let $\lambda_1(A, B), \dots, \lambda_n(A, B)$ be the eigenvalues of (A, B) repeated according to multiplicity. The eigenvalue gap of (A, B) is $\text{gap}(A, B) = \min_{i \neq j} |\lambda_i(A, B) - \lambda_j(A, B)|$.

Of course, these definitions are not the only possible condition numbers for generalized eigenvalues and eigenvectors [\[3,34\]](#). We justify our choice in [Section 5.1](#), where we show that a backward error diagonalization of a suitably well-behaved pencil provides forward error approximations of its eigenvalues and eigenvectors in terms of $\kappa_V(A, B)$ and $\text{gap}(A, B)$ ([Theorem 5.2](#)). Note that when B is invertible, $\kappa_V(A, B) = \kappa_V(B^{-1}A)$ and $\text{gap}(A, B) = \text{gap}(B^{-1}A)$.

Finally, we consider an important building block of divide-and-conquer eigensolvers: spectral projectors.

Definition 2.11. P is a spectral projector of the matrix M if $P^2 = P$ and $MP = PM$.

The simplest spectral projector is vw^H for v and w right and left eigenvectors of M corresponding to the same eigenvalue λ and scaled so that $w^H v = 1$. In this case, we have by Cauchy's integral formula

$$vw^H = \frac{1}{2\pi i} \oint_{\Gamma} (z - M)^{-1} dz \tag{2.1.1}$$

for Γ any closed, rectifiable curve that separates λ from the rest of the spectrum of M . More generally, any spectral projector can be expressed as

$$P = V \begin{pmatrix} I_k & 0 \\ 0 & 0 \end{pmatrix} V^{-1} \tag{2.1.2}$$

for V a matrix containing the right eigenvectors of M , again appropriately scaled.

As mentioned above, an important step of any divide-and-conquer eigensolver is the approximation of spectral projectors onto certain sets of eigenvectors. For our purposes, since (A, B) and $B^{-1}A$ have the same eigenvectors if B is nonsingular, it will be sufficient to approximate the spectral projectors of $B^{-1}A$ without explicitly forming it.

Remark 2.12. When (A, B) is singular, $\lambda \in \mathbb{C}$ is a finite eigenvalue if $\text{rank}(A - \lambda B) < \text{rank}(A - xB)$, where the latter is computed over the field of fractions of $\mathbb{C}[x]$. From there, all of the definitions given above can be suitably adapted to singular pencils (see for example [19, 27, 59]). Because our algorithm begins with a perturbation – which guarantees almost surely that the perturbed pencil is regular – a deeper discussion of singular pencils is beyond the scope of this paper. Nevertheless, our main error bound still applies to input pencils that are singular, and in Section 6 we will explore the practical challenges of recovering eigenvalues in this case.

To wrap up this section, we state a few general linear algebra results/facts that will be useful later on. First is the stability of singular values, which follows from Weyl’s inequality [55, Corollary IV.4.9]

Lemma 2.13 (Stability of Singular Values). *If $\sigma_i(M)$ is the i -th singular value of a matrix M , then for any $M_1, M_2 \in \mathbb{C}^{n \times n}$*

$$|\sigma_i(M_1) - \sigma_i(M_2)| \leq \|M_1 - M_2\|_2, \quad 1 \leq i \leq n.$$

Second, we note that the spectral norm is often generalized to pencils by setting $\|(A, B)\|_2$ equal to the norm of the $n \times 2n$ matrix obtained by concatenating A and B . Throughout we use the loose upper bound $\|(A, B)\|_2 \leq \|A\|_2 + \|B\|_2$.

2.2 Pseudospectra

In this section, we define pseudospectra for both individual matrices and matrix pencils. We start with the single-matrix case, where the definition is standard.

Definition 2.14. For any $\epsilon > 0$, the ϵ -pseudospectrum of M is

$$\Lambda_\epsilon(M) = \{z : \text{there exists } u \neq 0 \text{ with } (M + E)u = zu \text{ for some } \|E\|_2 \leq \epsilon\}.$$

Each pseudospectrum $\Lambda_\epsilon(M)$ consists of connected components in \mathbb{C} containing at least one eigenvalue of M . As $\epsilon \rightarrow 0$ these connected components collapse to the true eigenvalues of the matrix. If M is diagonalizable, we can quantify this explicitly via the Bauer-Fike Theorem [11].

Theorem 2.15 (Bauer-Fike). *If $\lambda_1, \dots, \lambda_n$ are the eigenvalues of $M \in \mathbb{C}^{n \times n}$ and V is any invertible matrix that diagonalizes M , then*

$$\bigcup_{i=1}^n B_\epsilon(\lambda_i) \subseteq \Lambda_\epsilon(M) \subseteq \bigcup_{i=1}^n B_{\epsilon\kappa(V)}(\lambda_i)$$

where $B_r(z)$ is the ball of radius r centered at z .

To extend this to matrix pencils, we must first decide how to define $\Lambda_\epsilon(A, B)$ – the ϵ -pseudospectrum of the pencil (A, B) . Unlike the single matrix case there is no standard choice here (see Trefethen and Embree [58, Chapter 45] for a discussion of various options). In this paper, we follow a definition originally due to Frayssé et al. [28].

Definition 2.16. For any $\epsilon > 0$, the ϵ -pseudospectrum of (A, B) is

$$\Lambda_\epsilon(A, B) = \{z : \text{there exists } u \neq 0 \text{ with } (A + \Delta A)u = z(B + \Delta B)u \text{ for some } \|\Delta A\|_2, \|\Delta B\|_2 \leq \epsilon\}.$$

There are several equivalent ways to state Definition 2.16, which we use throughout when convenient.

Theorem 2.17 (Frayssé et al. 1996). *The following are equivalent:*

1. $z \in \Lambda_\epsilon(A, B)$.
2. There exists a unit vector u such that $\|(A - zB)u\|_2 \leq \epsilon(1 + |z|)$.
3. $\|(A - zB)^{-1}\|_2 \geq \frac{1}{\epsilon(1 + |z|)}$.
4. $\sigma_n(A - zB) \leq \epsilon(1 + |z|)$.

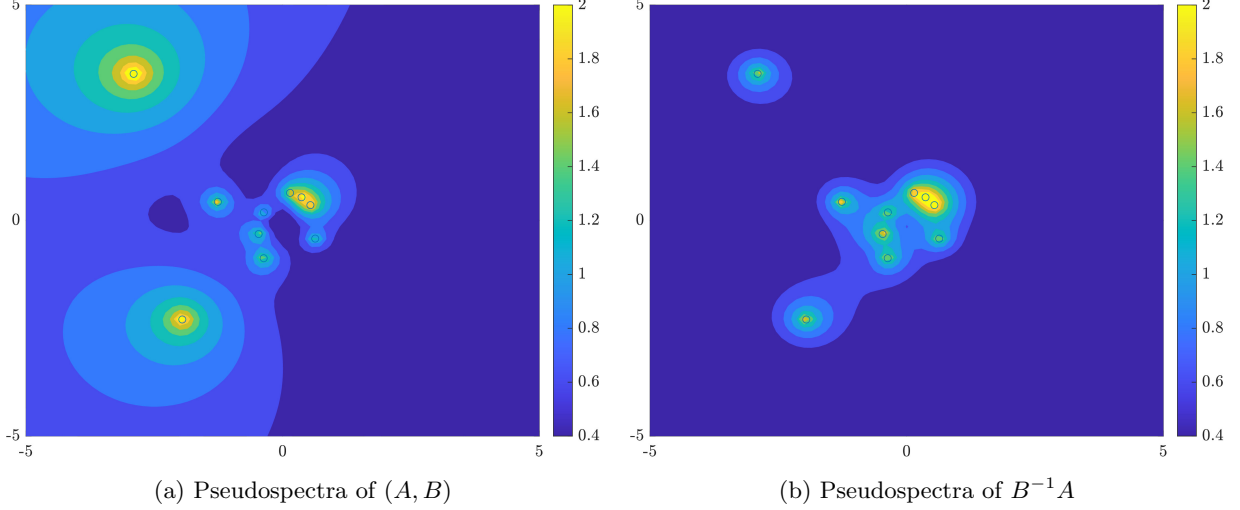


Figure 1: Pseudospectra of (A, B) and $B^{-1}A$ for Gaussian $A, B \in \mathbb{C}^{10 \times 10}$ following Definition 2.16 and Definition 2.14, respectively. Eigenvalues are plotted with open circles. Pseudospectra were obtained by graphing the level curves of $\log_{10} [(1 + |z|) \|(A - zB)^{-1}\|_2]$ and $\log_{10} [\|(B^{-1}A - zI)^{-1}\|_2]$ in Matlab R2023a.

Figure 1 plots the pseudospectra of (A, B) and $B^{-1}A$ for one (randomly chosen) pair $A, B \in \mathbb{C}^{10 \times 10}$. Clearly, the pseudospectra of (A, B) and $B^{-1}A$ differ significantly. Informally, we might say that the pseudospectra of (A, B) are less well-behaved than those of $B^{-1}A$, despite the fact that both coalesce around the same set of eigenvalues. In the remainder of this section, we pursue bounds on $\Lambda_\epsilon(A, B)$.

Lemma 2.18. $\Lambda_\epsilon(A, B)$ is bounded if and only if $\epsilon < \sigma_n(B)$.

Proof. Let $\epsilon < \sigma_n(B)$ and suppose $\Lambda_\epsilon(A, B)$ is unbounded. By Theorem 2.17, any nonzero $z \in \Lambda_\epsilon(A, B)$ satisfies

$$\frac{1}{\epsilon(1 + |z|)} \leq \|(A - zB)^{-1}\|_2 = \frac{1}{|z|} \left\| \left(\frac{1}{z}A - B \right)^{-1} \right\|_2 \implies \frac{|z|}{\epsilon(1 + |z|)} \leq \left\| \left(\frac{1}{z}A - B \right)^{-1} \right\|_2. \quad (2.2.1)$$

Since $\Lambda_\epsilon(A, B)$ is unbounded, we can take a limit $z \rightarrow \infty$ in this inequality to obtain

$$\frac{1}{\epsilon} \leq \|(-B)^{-1}\|_2 = \frac{1}{\sigma_n(B)}, \quad (2.2.2)$$

which implies $\epsilon \geq \sigma_n(B)$, a contradiction.

To prove the converse, suppose now $\epsilon \geq \sigma_n(B)$ and let $U\Sigma V^H$ be the singular value decomposition of B . If $D \in \mathbb{C}^{n \times n}$ is a diagonal matrix with $D(i, i) = 0$ for $1 \leq i \leq n - 1$ and $D(n, n) = -\sigma_n(B)$, then $\|UDV^H\|_2 = \sigma_n(B) \leq \epsilon$ and therefore eigenvalues of $(A, B + UDV^H)$ belong to $\Lambda_\epsilon(A, B)$. But by construction $B + UDV^H$ is singular, which means $(A, B + UDV^H)$ is singular and/or has an eigenvalue at infinity. In both cases $\Lambda_\epsilon(A, B)$ must be unbounded. \square

We next derive an upper bound on $\Lambda_\epsilon(A, B)$ when it exists. Keeping in mind that we plan to perturb our matrices, and will therefore have access to a lower bound on $\sigma_n(B)$ with high probability, we prove the following lemma.

Lemma 2.19. If $\epsilon < \sigma_n(B)$ then any $z \in \Lambda_\epsilon(A, B)$ satisfies

$$|z| \leq \frac{\epsilon \|B^{-1}\|_2 + \|B^{-1}A\|_2}{1 - \epsilon \|B^{-1}\|_2}.$$

Proof. Suppose $|z| > \|B^{-1}A\|_2$ and consider $\frac{B^{-1}A}{z} - I$. For any vector x ,

$$\left\| \frac{B^{-1}A}{z} x \right\|_2 \leq \frac{\|B^{-1}A\|_2}{|z|} \|x\|_2 \quad (2.2.3)$$

by matrix/vector norm compatibility, so

$$\|x\|_2 - \left\| \frac{B^{-1}A}{z} x \right\|_2 \geq \|x\|_2 - \frac{\|B^{-1}A\|_2}{|z|} \|x\|_2 \geq 0, \quad (2.2.4)$$

where we know $\|x\|_2 - (\|B^{-1}A\|_2/|z|)\|x\|_2$ is positive since $|z| > \|B^{-1}A\|_2$. Thus, applying this result and the reverse triangle inequality,

$$\sigma_n \left(\frac{B^{-1}A}{z} - I \right) = \min_{\|x\|_2=1} \left\| \left(\frac{B^{-1}A}{z} - I \right) x \right\|_2 \geq \min_{\|x\|_2=1} \left[\|x\|_2 - \frac{\|B^{-1}A\|_2}{|z|} \|x\|_2 \right] = 1 - \frac{\|B^{-1}A\|_2}{|z|} \quad (2.2.5)$$

and therefore

$$\left\| \left(\frac{B^{-1}A}{z} - I \right)^{-1} \right\|_2 = \frac{1}{\sigma_n \left(\frac{B^{-1}A}{z} - I \right)} \leq \frac{1}{1 - \frac{\|B^{-1}A\|_2}{|z|}}. \quad (2.2.6)$$

If $z \in \Lambda_\epsilon(A, B)$, we then have

$$\frac{1}{\epsilon(1+|z|)} \leq \frac{\|B^{-1}\|_2}{|z|} \left\| \left(\frac{B^{-1}A}{z} - I \right)^{-1} \right\|_2 \leq \frac{\|B^{-1}\|_2}{|z|} \frac{1}{1 - \frac{\|B^{-1}A\|_2}{|z|}} = \frac{\|B^{-1}\|_2}{|z| - \|B^{-1}A\|_2}, \quad (2.2.7)$$

which, rearranging to solve for $|z|$, is equivalent to

$$|z| \leq \frac{\epsilon\|B^{-1}\|_2 + \|B^{-1}A\|_2}{1 - \epsilon\|B^{-1}\|_2}. \quad (2.2.8)$$

Since we assumed $|z| > \|B^{-1}A\|_2$, we have proved that $z \in \Lambda_\epsilon(A, B)$ for $\epsilon < \sigma_n(B)$ implies

$$|z| \leq \max \left\{ \|B^{-1}A\|_2, \frac{\epsilon\|B^{-1}\|_2 + \|B^{-1}A\|_2}{1 - \epsilon\|B^{-1}\|_2} \right\} = \frac{\epsilon\|B^{-1}\|_2 + \|B^{-1}A\|_2}{1 - \epsilon\|B^{-1}\|_2} \quad (2.2.9)$$

which finishes the proof. \square

While this gives a nice upper bound for the pseudospectrum as a whole, the upper bound in Bauer-Fike is in terms of balls around the eigenvalues. If we add an assumption that $B^{-1}A$ is diagonalizable, we can convert the bound just obtained to a similar result, obtaining our version of Bauer-Fike for matrix pencils.

Theorem 2.20 (Bauer-Fike for Matrix Pencils). *Suppose $B^{-1}A$ is diagonalizable with eigenvalues $\lambda_1, \dots, \lambda_n$ and invertible right eigenvector matrix V . For $\epsilon < \sigma_n(B)$ let*

$$r_\epsilon = \epsilon\kappa(V)\|B^{-1}\|_2 \left(1 + \frac{\epsilon\|B^{-1}\|_2 + \|B^{-1}A\|_2}{1 - \epsilon\|B^{-1}\|_2} \right)$$

and further set

$$r_i = \begin{cases} \frac{1}{\|B\|_2} & \text{if } A = 0 \\ \max \left\{ \frac{1}{\|B\|_2}, \frac{|\lambda_i|}{\|A\|_2} \right\} & \text{otherwise} \end{cases}$$

for $1 \leq i \leq n$. Then,

$$\bigcup_{i=1}^n B_{\epsilon r_i}(\lambda_i) \subseteq \Lambda_\epsilon(A, B) \subseteq \bigcup_{i=1}^n B_{r_\epsilon}(\lambda_i).$$

Proof. To obtain the first containment we note that for any $|\Delta\lambda| \leq \epsilon/\|B\|_2$ the pencil $(A + \Delta\lambda B, B)$ has eigenvalues $\lambda_i + \Delta\lambda$ while $\Lambda(A + \Delta\lambda B, B) \subseteq \Lambda_\epsilon(A, B)$. Similarly, if $A \neq 0$ then $(A + \Delta\lambda A, B)$ has eigenvalues $\lambda_i(1 + \Delta\lambda)$ and $\Lambda(A + \Delta\lambda A, B) \subseteq \Lambda_\epsilon(A, B)$ as long as $|\Delta\lambda| \leq \epsilon/\|A\|_2$. For the remaining containment we appeal to [Theorem 2.17](#): any $z \in \Lambda_\epsilon(A, B)$ satisfies

$$\frac{1}{\epsilon(1 + |z|)} \leq \|(A - zB)^{-1}\|_2 \leq \|B^{-1}\|_2 \|(B^{-1}A - zI)^{-1}\|_2. \quad (2.2.10)$$

Applying the fact that V diagonalizes $B^{-1}A$, meaning $B^{-1}A = V\Lambda V^{-1}$ for a diagonal matrix Λ , this expression becomes

$$\frac{1}{\epsilon(1 + |z|)} \leq \|B^{-1}\|_2 \|(V\Lambda V^{-1} - zI)^{-1}\|_2 \leq \kappa(V) \|B^{-1}\|_2 \|(\Lambda - zI)^{-1}\|_2. \quad (2.2.11)$$

Inverting and rearranging, we then have

$$\sigma_n(\Lambda - zI) \leq \epsilon \kappa(V) \|B^{-1}\|_2 (1 + |z|). \quad (2.2.12)$$

We complete the proof by noting

$$\sigma_n(\Lambda - zI) = \min_{\lambda_i \in \Lambda(A, B)} |\lambda_i - z| \quad (2.2.13)$$

and replacing $|z|$ in [\(2.2.12\)](#) with the upper bound provided by [Lemma 2.19](#). \square

[Theorem 2.20](#) is not the only version of Bauer-Fike derived for the generalized eigenvalue problem (see [Appendix A](#)). Nevertheless, it is useful here since it leverages the assumptions we'll have available to us in the following sections. In particular, the perturbations applied to (A, B) to obtain (\tilde{A}, \tilde{B}) guarantee with high probability that \tilde{B} is nonsingular (with a lower bound on $\sigma_n(\tilde{B})$ known) and that $\tilde{B}^{-1}\tilde{A}$ is diagonalizable.

3 Pseudospectral Shattering for Matrix Pencils

Following the convention used by Banks et al. [\[9\]](#), define a grid on the complex plane as follows.

Definition 3.1. The grid $g = \text{grid}(z_0, \omega, s_1, s_2)$ is the boundary of a $s_1 \times s_2$ lattice in the complex plane consisting of $\omega \times \omega$ -sized squares with lower left corner $z_0 \in \mathbb{C}$. The grid lines of g are parallel to either the real or the complex axis.

In this section, we show that with high probability the ϵ -pseudospectrum of a scaled and perturbed matrix pencil is shattered with respect to a random grid g (constructed according to [Definition 3.1](#)) for sufficiently small ϵ , where shattering is defined as follows.

Definition 3.2. $\Lambda_\epsilon(A, B)$ is shattered with respect to a grid g if $\Lambda_\epsilon(A, B) \cap g = \emptyset$ and each eigenvalue of (A, B) is contained in a unique box of g .

Throughout, we consider perturbations made by Ginibre random matrices and make use of results from random matrix theory for this ensemble.

Definition 3.3. A random matrix $G \in \mathbb{C}^{n \times n}$ is Ginibre if its entries are i.i.d. with distribution $\mathcal{N}_{\mathbb{C}}(0, \frac{1}{n})$.

Note that $\mathcal{N}_{\mathbb{C}}(0, \frac{1}{n})$ in [Definition 3.3](#) is a complex normal distribution. In practice, we can construct a Ginibre matrix by drawing a complex Gaussian matrix and normalizing by $\frac{1}{\sqrt{n}}$.

For the remainder of this section, let $(\tilde{A}, \tilde{B}) = (A + \gamma G_1, B + \gamma G_2)$ for G_1, G_2 two independent, complex Ginibre matrices, $0 < \gamma < \frac{1}{2}$, and $A, B \in \mathbb{C}^{n \times n}$ with $\|A\|_2, \|B\|_2 \leq 1$. The norm requirement here is applied to simplify the analysis and can be assumed without loss of generality since our input matrices can be normalized if necessary. We are interested in showing shattering for the pseudospectra of the scaled pencil $(\tilde{A}, n^\alpha \tilde{B})$, where α is a positive constant. As we will see, the choice to scale \tilde{B} is required to obtain usable bounds on the locations of the eigenvalues of $(\tilde{A}, n^\alpha \tilde{B})$. Later on, we will comment on how this choice of scaling affects the results.

3.1 Preliminaries

We begin by discussing some singular value bounds that will be useful later. The first of these is a bound on the norm (i.e., largest singular value) of a complex Ginibre matrix due to Banks et al. [10, Lemma 2.2].

Lemma 3.4 (Banks et al. 2021). *For G an $n \times n$ complex Ginibre matrix, $\mathbb{P}[\|G\|_2 \geq 2\sqrt{2} + t] \leq 2e^{-nt^2}$.*

The same paper also provides a lower tail bound on the smallest singular value of a matrix after it is perturbed by a Ginibre matrix [10, Lemma 3.3].

Lemma 3.5 (Banks et al. 2021). *Let G be an $n \times n$ complex Ginibre matrix. Then for any $M \in \mathbb{C}^{n \times n}$ and any $\gamma, t > 0$, $\mathbb{P}[\sigma_n(M + \gamma G) < t] \leq n^2 \frac{t^2}{\gamma^2}$.*

Finally, we use the following result from their subsequent work [9, Corollary 3.3].

Lemma 3.6 (Banks et al. 2022). *Let G be an $n \times n$ complex Ginibre matrix. Then for any $M \in \mathbb{C}^{n \times n}$ and any $\gamma, t > 0$, $\mathbb{P}[\sigma_{n-1}(M + \gamma G) < t] \leq 4(\frac{tn}{\gamma})^8$.*

These are the main results from random matrix theory that we will use. Note that Lemma 3.5 implies that \tilde{B} is almost surely invertible, meaning with probability one we may assume that \tilde{B}^{-1} exists. Moreover, Lemma 3.4 and Lemma 3.5 allow us to control the location of the eigenvalues of $(\tilde{A}, n^\alpha \tilde{B})$ as follows.

Lemma 3.7. *The eigenvalues of $(\tilde{A}, n^\alpha \tilde{B})$ are contained in $B_3(0)$ – the ball of radius three centered at the origin – with probability at least $1 - \frac{n^{2-2\alpha}}{\gamma^2} - 2e^{-n}$.*

Proof. Consider $X = n^{-\alpha} \tilde{B}^{-1} \tilde{A}$. Since X and $(\tilde{A}, n^\alpha \tilde{B})$ have the same eigenvalues, it is sufficient to bound the probability that $\Lambda(X)$ is not contained in $B_3(0)$. To do this, we note

$$\rho(X) \leq \|X\|_2 = n^{-\alpha} \|\tilde{B}^{-1} \tilde{A}\|_2 \leq \frac{1}{n^\alpha \sigma_n(\tilde{B})} \|\tilde{A}\|_2 \leq \frac{1}{n^\alpha \sigma_n(\tilde{B})} (\|A\|_2 + \gamma \|G_1\|_2). \quad (3.1.1)$$

Now $\|A\|_2 \leq 1$ so, conditioning on the event $\|G_1\|_2 \leq 4$, we have $\|A + \gamma G_1\|_2 \leq 3$. Thus, if $\Lambda(X) \not\subseteq B_3(0)$ and therefore $\rho(X) > 3$, we obtain $n^\alpha \sigma_n(\tilde{B}) < 1$. Consequently,

$$\mathbb{P}[\Lambda(X) \not\subseteq B_3(0) \mid \|G_1\|_2 \leq 4] \leq \mathbb{P}\left[n^\alpha \sigma_n(\tilde{B}) < 1\right] \leq \frac{n^{2-2\alpha}}{\gamma^2}, \quad (3.1.2)$$

where the last inequality comes from Lemma 3.5. By Bayes' Theorem, we therefore have

$$\mathbb{P}[\Lambda(X) \not\subseteq B_3(0), \|G_1\|_2 \leq 4] \leq \frac{n^{2-2\alpha}}{\gamma^2}. \quad (3.1.3)$$

At the same time, applying Lemma 3.4, we have

$$\mathbb{P}[\Lambda(X) \not\subseteq B_3(0), \|G_1\|_2 > 4] \leq \mathbb{P}[\|G_1\|_2 > 4] \leq 2e^{-n(4-2\sqrt{2})^2} \leq 2e^{-n}. \quad (3.1.4)$$

Putting these two results together, we conclude

$$\mathbb{P}[\Lambda(X) \not\subseteq B_3(0)] \leq \frac{n^{2-2\alpha}}{\gamma^2} + 2e^{-n} \quad (3.1.5)$$

which completes the proof. \square

With this in place, we can now consider building our random grid g over $B_3(0)$ which (with an appropriate choice of α and γ) will contain every eigenvalue of $(\tilde{A}, n^\alpha \tilde{B})$ with high probability. Given a grid box size ω , we define the random grid $g = \text{grid}(z, \omega, \lceil 8/\omega \rceil, \lceil 8/\omega \rceil)$ for z a point chosen uniformly at random from the square with bottom left corner $-4 - 4i$ and side length ω . The construction here is somewhat arbitrary; for convenience we choose g so that it roughly covers the smallest box with integer side length that contains $B_3(0)$ (with some buffer space).

3.2 Multi-Parameter Tail Bound

As in [Lemma 3.7](#), let $X = n^{-\alpha} \tilde{B}^{-1} \tilde{A}$. The bulk of the proof of shattering in the following section rests on a multi-parameter tail bound for $\kappa_V(X)$ and $\text{gap}(X)$, which we derive here. We start with two intermediate results. The first concerns the second to last singular value of $yI - X$ for $y \in \mathbb{C}$.

Lemma 3.8. *For any $t > 0$ and any $y \in \mathbb{C}$,*

$$\mathbb{P}[\sigma_{n-1}(yI - X) < t \mid \|G_2\|_2 \leq 4] \leq 4 \left(\frac{t(1+4\gamma)n^{\alpha+1}}{\gamma} \right)^8$$

Proof. We begin by rewriting $yI - X$ as

$$yI - X = n^{-\alpha} \tilde{B}^{-1} \left(n^\alpha y \tilde{B} - A - \gamma G_1 \right). \quad (3.2.1)$$

Using standard singular value inequalities, we then have

$$\sigma_{n-1}(yI - X) \geq \sigma_n \left(n^{-\alpha} \tilde{B}^{-1} \right) \sigma_{n-1} \left(n^\alpha y \tilde{B} - A - \gamma G_1 \right). \quad (3.2.2)$$

Now conditioning on $\|G_2\|_2 \leq 4$, we have $\|\tilde{B}\|_2 \leq 1 + 4\gamma$. Thus, $\sigma_n(n^{-\alpha} \tilde{B}^{-1}) \geq \frac{1}{n^\alpha(1+4\gamma)}$ and therefore

$$\sigma_{n-1}(yI - X) \geq \frac{1}{n^\alpha(1+4\gamma)} \sigma_{n-1} \left(n^\alpha y \tilde{B} - A - \gamma G_1 \right). \quad (3.2.3)$$

Consequently, we observe

$$\mathbb{P}[\sigma_{n-1}(yI - X) < t \mid \|G_2\|_2 \leq 4] \leq \mathbb{P} \left[\sigma_{n-1} \left(n^\alpha y \tilde{B} - A - \gamma G_1 \right) < tn^\alpha(1+4\gamma) \right]. \quad (3.2.4)$$

Setting $M = n^\alpha y \tilde{B} - A$ and applying [Lemma 3.6](#) (noting that M is independent of G_1 and that G_1 and $-G_1$ have the same distribution) we have

$$\mathbb{P}[\sigma_{n-1}(yI - X) < t \mid \|G_2\|_2 \leq 4] \leq 4 \left(\frac{t(1+4\gamma)n^{\alpha+1}}{\gamma} \right)^8 \quad (3.2.5)$$

for any $t > 0$. □

Next, we show that given any measurable set $S \subset \mathbb{C}$, we can bound the expected value of $\sum_{\lambda_i \in S} \kappa(\lambda_i)^2$, where the sum is taken over eigenvalues of X . This gives us some control over $\kappa_V(X)$; in particular, taking V to be the eigenvector matrix of X scaled so that each column is a unit vector, we observe

$$\kappa_V(X) \leq \kappa(V) \leq \|V\|_F \|V^{-1}\|_F \leq \sqrt{n \sum_{i=1}^n \kappa(\lambda_i)^2}. \quad (3.2.6)$$

Note that with probability one X has a full set of distinct eigenvalues and is therefore diagonalizable. The proof of this result follows closely a proof of Banks et al. for the single matrix case [[10](#), Theorem 1.5].

Lemma 3.9. *Let $\lambda_1, \dots, \lambda_n$ be the eigenvalues of X . For any measurable set $S \subset \mathbb{C}$,*

$$\mathbb{E} \left[\sum_{\lambda_i \in S} \kappa(\lambda_i)^2 \mid \|G_2\|_2 \leq 4 \right] \leq \left(\frac{(1+4\gamma)n^{\alpha+1}}{\gamma} \right)^2 \frac{\text{vol}(S)}{\pi}.$$

Proof. By [Definition 2.14](#), we know for any $z \in \mathbb{C}$

$$\mathbb{P}[z \in \Lambda_\epsilon(X)] = \mathbb{P}[\sigma_n(zI - X) < \epsilon]. \quad (3.2.7)$$

Following the same argument made in [Lemma 3.8](#), swapping [Lemma 3.6](#) for [Lemma 3.5](#), we therefore have

$$\mathbb{P}[z \in \Lambda_\epsilon(X) \mid \|G_2\|_2 \leq 4] \leq \left(\frac{\epsilon(1+4\gamma)n^{\alpha+1}}{\gamma} \right)^2. \quad (3.2.8)$$

Consider now the measurable set $S \subset \mathbb{C}$. Using [\(3.2.8\)](#), we observe

$$\begin{aligned} \mathbb{E}[\text{vol}(\Lambda_\epsilon(X) \cap S) \mid \|G_2\|_2 \leq 4] &= \mathbb{E} \left[\int_S \mathbb{1}_{z \in \Lambda_\epsilon(X) \mid \|G_2\|_2 \leq 4} dz \right] \\ &= \int_S \mathbb{P}[z \in \Lambda_\epsilon(X) \mid \|G_2\|_2 \leq 4] dz \\ &\leq \left(\frac{\epsilon(1+4\gamma)n^{\alpha+1}}{\gamma} \right)^2 \text{vol}(S). \end{aligned} \quad (3.2.9)$$

Applying this result alongside [\[10, Lemma 3.2\]](#) and Fatou's Lemma for conditional expectation, we conclude

$$\begin{aligned} \mathbb{E} \left[\sum_{\lambda_i \in S} \kappa(\lambda_i)^2 \mid \|G_2\|_2 \leq 4 \right] &= \mathbb{E} \left[\liminf_{\epsilon \rightarrow 0} \frac{\text{vol}(\Lambda_\epsilon(X) \cap S)}{\pi \epsilon^2} \mid \|G_2\|_2 \leq 4 \right] \\ &\leq \liminf_{\epsilon \rightarrow 0} \frac{\mathbb{E}[\text{vol}(\Lambda_\epsilon(X) \cap S \mid \|G_2\|_2 \leq 4)]}{\pi \epsilon^2} \\ &\leq \left(\frac{(1+4\gamma)n^{\alpha+1}}{\gamma} \right)^2 \frac{\text{vol}(S)}{\pi}, \end{aligned} \quad (3.2.10)$$

which completes the proof. \square

With these in place, we are now ready to prove the main multi-parameter tail bound. In this result, as in the previous two, $X = n^{-\alpha} \tilde{B}^{-1} \tilde{A}$ for our perturbed pencil (\tilde{A}, \tilde{B}) . Again, this follows closely the proof of an equivalent tail bound of Banks et al. [\[9, Theorem 3.6\]](#).

Theorem 3.10. *For any $t, \delta > 0$,*

$$\mathbb{P}[\kappa_V(X) < t, \text{gap}(X) > \delta] \geq \left[1 - \frac{9(1+4\gamma)^2 n^{2\alpha+3}}{t^2 \gamma^2} - 1296 \delta^6 \left(\frac{t(1+4\gamma)n^{\alpha+1}}{\gamma} \right)^8 \right] \left[1 - \frac{n^{2-2\alpha}}{\gamma^2} - 4e^{-n} \right].$$

Proof. We condition on the events $\|G_2\|_2 \leq 4$ and $\Lambda_\epsilon(X) \subseteq B_3(0)$. Combining [Lemma 3.4](#) and [Lemma 3.7](#), we know these occur with probability at least $1 - \frac{n^{2-2\alpha}}{\gamma^2} - 4e^{-n}$. Define now the events:

- $E_{\text{gap}} = \{\text{gap}(X) < \delta\}$
- $E_\kappa = \{\kappa_V(X) > t\}$.

We are interested in bounding the probability of $E_{\text{gap}} \cup E_\kappa$. To do this, we construct a minimal $\frac{\delta}{2}$ -net \mathcal{N} covering $B_3(0)$, which exists with $|\mathcal{N}| \leq \frac{324}{\delta^2}$ (see for example [\[60, Corollary 4.2.11\]](#)). By construction

$$E_{\text{gap}} \subset \{|D(y, \delta) \cap \Lambda(X)| \geq 2 \text{ for some } y \in \mathcal{N}\} \quad (3.2.11)$$

where $D(y, \delta)$ is the ball of radius δ centered at y . Now if $D(y, \delta)$ contains two eigenvalues of X , [\[9, Lemma 3.5\]](#) implies $\sigma_{n-1}(yI - X) < \delta \kappa_V(X)$, where we note again that X is almost surely diagonalizable. Thus, if $\text{gap}(X) < \delta$ either $\sigma_{n-1}(yI - X) < \delta t$ for at least one $y \in \mathcal{N}$ or $\kappa_V(X) > t$. In other words, defining the event $E_y = \{\sigma_{n-1}(yI - X) < \delta t\}$ for $y \in \mathcal{N}$,

$$E_{\text{gap}} \subset E_\kappa \cup \bigcup_{y \in \mathcal{N}} E_y \implies E_{\text{gap}} \cup E_\kappa \subset E_\kappa \cup \bigcup_{y \in \mathcal{N}} E_y. \quad (3.2.12)$$

By a union bound, we then have

$$\mathbb{P}[E_{\text{gap}} \cup E_{\kappa}] \leq \mathbb{P}[E_{\kappa}] + |\mathcal{N}| \max_{y \in \mathcal{N}} \mathbb{P}[E_y]. \quad (3.2.13)$$

To bound $\mathbb{P}[E_{\kappa}]$, we first use (3.2.6) to obtain

$$\mathbb{P}[E_{\kappa}] \leq \mathbb{P} \left[t < \sqrt{n \sum_{i=1}^n \kappa(\lambda_i)^2} \right] = \mathbb{P} \left[\sum_{i=1}^n \kappa(\lambda_i)^2 > \frac{t^2}{n} \right]. \quad (3.2.14)$$

Applying Markov's inequality and Lemma 3.9 (recalling that we've conditioned on $\Lambda(X) \subseteq B_3(0)$) we then have

$$\mathbb{P}[E_{\kappa}] \leq \frac{n}{t^2} \mathbb{E} \left[\sum_{\lambda_i \in B_3(0)} \kappa(\lambda_i)^2 \right] \leq \frac{9(1+4\gamma)^2 n^{2\alpha+3}}{t^2 \gamma^2}. \quad (3.2.15)$$

Similarly, Lemma 3.8 implies

$$\mathbb{P}[E_y] \leq 4 \left(\frac{\delta t (1+4\gamma) n^{\alpha+1}}{\gamma} \right)^8 \quad (3.2.16)$$

for all $y \in \mathcal{N}$. Putting everything together, we conclude

$$\mathbb{P}[E_{\text{gap}} \cup E_{\kappa}] \leq \frac{9(1+4\gamma)^2 n^{2\alpha+3}}{t^2 \gamma^2} + 4 \left(\frac{\delta t (1+4\gamma) n^{\alpha+1}}{\gamma} \right)^8 \frac{324}{\delta^2} \quad (3.2.17)$$

so we have shown

$$\mathbb{P}[\kappa_V(X) < t, \text{gap}(X) > \delta \mid \Lambda(X) \subseteq B_3(0), \|G_2\|_2 \leq 4] \geq 1 - \frac{9(1+4\gamma)^2 n^{2\alpha+3}}{t^2 \gamma^2} - 1296 \delta^6 \left(\frac{t(1+4\gamma) n^{\alpha+1}}{\gamma} \right)^8. \quad (3.2.18)$$

Noting

$$\mathbb{P}[\kappa_V(X) < t, \text{gap}(X) > \delta] \geq \mathbb{P}[\kappa_V(X) < t, \text{gap}(X) > \delta, \Lambda(X) \subseteq B_3(0), \|G_2\|_2 \leq 4], \quad (3.2.19)$$

we obtain the final result by Bayes' Theorem. \square

Remark 3.11. Note that we could replace $\kappa_V(X)$ in Theorem 3.10 with $\kappa(V)$ for any eigenvector matrix V satisfying (3.2.6). In particular, as was used to derive the inequality, this applies to the scaling where each column of V has unit length.

Informally, Theorem 3.10 says that for the right choice of t and δ (i.e., polynomial in n and inverse polynomial in n , respectively) the eigenvector condition number of X is not too large and its eigenvalue gap is not too small. Since the eigenvalues and eigenvectors of X and $(\tilde{A}, n^\alpha \tilde{B})$ are the same, this eigenvector and eigenvalue stability is inherited by our perturbed and scaled pencil.

3.3 Shattering

We are now ready to prove shattering for the pseudospectra of $(\tilde{A}, n^\alpha \tilde{B})$.

Theorem 3.12. *Let $A, B \in \mathbb{C}^{n \times n}$ with $\|A\|_2 \leq 1$ and $\|B\|_2 \leq 1$. Let $(\tilde{A}, \tilde{B}) = (A + \gamma G_1, B + \gamma G_2)$ for G_1, G_2 two independent complex Ginibre matrices and $0 < \gamma < \frac{1}{2}$. Let g be the grid*

$$g = \text{grid}(z, \omega, \lceil 8/\omega \rceil, \lceil 8/\omega \rceil) \quad \text{with} \quad \omega = \frac{\gamma^4}{4} n^{-\frac{8\alpha+13}{3}},$$

where z is chosen uniformly at random from the square with bottom left corner $-4 - 4i$ and side length ω . Then $\|\tilde{A}\|_2 \leq 3$, $\|\tilde{B}\|_2 \leq 3$, and $\Lambda_\epsilon(\tilde{A}, n^\alpha \tilde{B})$ is shattered with respect to g for

$$\epsilon = \frac{\gamma^5}{64n^{\frac{11\alpha+25}{3}} + \gamma^5}$$

with probability at least $\left[1 - \frac{82}{n} - \frac{531441}{16n^2}\right] \left[1 - \frac{n^{2-2\alpha}}{\gamma^2} - 4e^{-n}\right]$.

Proof. As in the previous section, let $X = n^{-\alpha} \tilde{B}^{-1} \tilde{A}$. We condition on the following events: $n^\alpha \sigma_n(\tilde{B}) \geq 1$, $\|G_1\|_2 \leq 4$, and $\|G_2\|_2 \leq 4$. As noted above, these events occur with probability at least $1 - \frac{n^{2-2\alpha}}{\gamma^2} - 4e^{-n}$ and, following the argument made in [Lemma 3.7](#), guarantee that $\Lambda(X) \subseteq B_3(0)$. Consequently, we know with probability one each eigenvalue of X , and therefore of $(\tilde{A}, n^\alpha \tilde{B})$, is contained in a box of g . At the same time,

$$\|\tilde{A}\|_2 = \|A + \gamma G_1\|_2 \leq \|A\|_2 + \gamma \|G_1\|_2 \leq 3 \quad (3.3.1)$$

and similarly $\|\tilde{B}\|_2 \leq 3$.

Suppose now $\kappa_V(X) < \frac{n^{\alpha+2}}{\gamma}$, $\text{gap}(X) > \gamma^4 n^{-\frac{8\alpha+13}{3}}$, and

$$\min_{\lambda_i \in \Lambda(X)} \text{dist}_g(\lambda_i) > \frac{\omega}{4n^2}, \quad (3.3.2)$$

where $\text{dist}_g(\lambda_i) = \min_{y \in g} |\lambda_i - y|$. By [\(3.2.18\)](#), we know the first two of these occur under our assumptions with probability at least

$$1 - \frac{9(1+4\gamma)^2 n^{2\alpha+3}}{\left(\frac{n^{\alpha+2}}{\gamma}\right)^2 \gamma^2} - 1296 \left(\frac{\gamma^4}{n^{\frac{8\alpha+13}{3}}}\right)^6 \left(\frac{\left(\frac{n^{\alpha+2}}{\gamma}\right)(1+4\gamma)n^{\alpha+1}}{\gamma}\right)^8, \quad (3.3.3)$$

which, applying $\gamma < \frac{1}{2}$, simplifies to $1 - \frac{81}{n} - \frac{531441}{16n^2}$. Similarly, by a simple geometric argument (using the fact that the eigenvalues of X are uniformly distributed in their grid boxes),

$$\mathbb{P} \left[\min_{\lambda_i \in \Lambda(X)} \text{dist}_g(\lambda_i) > \frac{\omega}{4n^2} \right] \geq 1 - \frac{1}{n}. \quad (3.3.4)$$

Thus, these events occur under our assumptions with probability at least $1 - \frac{82}{n} - \frac{531441}{16n^2}$, which means by Bayes' Theorem that we have $n^\alpha \sigma_n(\tilde{B}) \geq 1$, $\|G_1\|_2 \leq 4$, $\|G_2\|_2 \leq 4$, $\kappa_V(X) < \frac{n^{\alpha+2}}{\gamma}$, $\text{gap}(X) > \gamma^4 n^{-\frac{8\alpha+13}{3}}$, and [\(3.3.2\)](#) with probability at least $\left[1 - \frac{82}{n} - \frac{531441}{16n^2}\right] \left[1 - \frac{n^{2-2\alpha}}{\gamma^2} - 4e^{-n}\right]$.

To complete the proof, we now show that these events guarantee shattering. To do this, we first observe that if $\text{gap}(X) > \gamma^4 n^{-\frac{8\alpha+13}{3}}$ then no two eigenvalues can share a grid box of g . At the same time, [\(3.3.2\)](#) implies that the ball of radius $\frac{\omega}{4n^2}$ around each eigenvalue does not intersect g . Therefore, it is sufficient to show that $\Lambda_\epsilon(\tilde{A}, n^\alpha \tilde{B})$ is contained in these balls, which we can do by appealing to [Theorem 2.20](#), our version of Bauer-Fike for matrix pencils. In particular, noting that we can replace $\kappa(V)$ with $\kappa_V(X)$ by taking an infimum, [Theorem 2.20](#) implies that $(\tilde{A}, n^\alpha \tilde{B})$ is contained in balls of radius

$$r_\epsilon = \epsilon \kappa_V(X) \|n^{-\alpha} \tilde{B}^{-1}\|_2 \left(1 + \frac{\epsilon \|n^{-\alpha} \tilde{B}^{-1}\|_2 + \|X\|_2}{1 - \epsilon \|n^{-\alpha} \tilde{B}^{-1}\|_2} \right). \quad (3.3.5)$$

Applying our bounds $\|n^{-\alpha} \tilde{B}^{-1}\|_2 = \frac{1}{n^\alpha \sigma_n(\tilde{B})} \leq 1$, $\|X\|_2 \leq 3$, and $\kappa_V(X) \leq \frac{n^{\alpha+2}}{\gamma}$, we obtain shattering as long as

$$r_\epsilon \leq \epsilon \left(\frac{n^{\alpha+2}}{\gamma} \right) \left(\frac{4}{1-\epsilon} \right) \leq \frac{\omega}{4n^2} = \frac{\gamma^4}{16n^{\frac{8\alpha+19}{3}}} \quad (3.3.6)$$

or, equivalently, $\epsilon \leq \frac{\gamma^5}{64n^{\frac{11\alpha+25}{3}} + \gamma^5}$. \square

This result clarifies the impact of the n^α scaling. On one hand, increasing α drives the term $\frac{n^{2-2\alpha}}{\gamma^2}$ in our probability bound to zero, assuming γ is fixed. Said another way, a larger choice of α allows us to take γ smaller without losing our guarantee of shattering. In particular, we need

$$\gamma > n^{1-\alpha} \quad (3.3.7)$$

to ensure that the probability in [Theorem 3.12](#) is not vacuous. This is important, as we'd like to perturb our matrices as little as possible. Nevertheless, we pay a penalty for increasing α in ω and ϵ , both of which

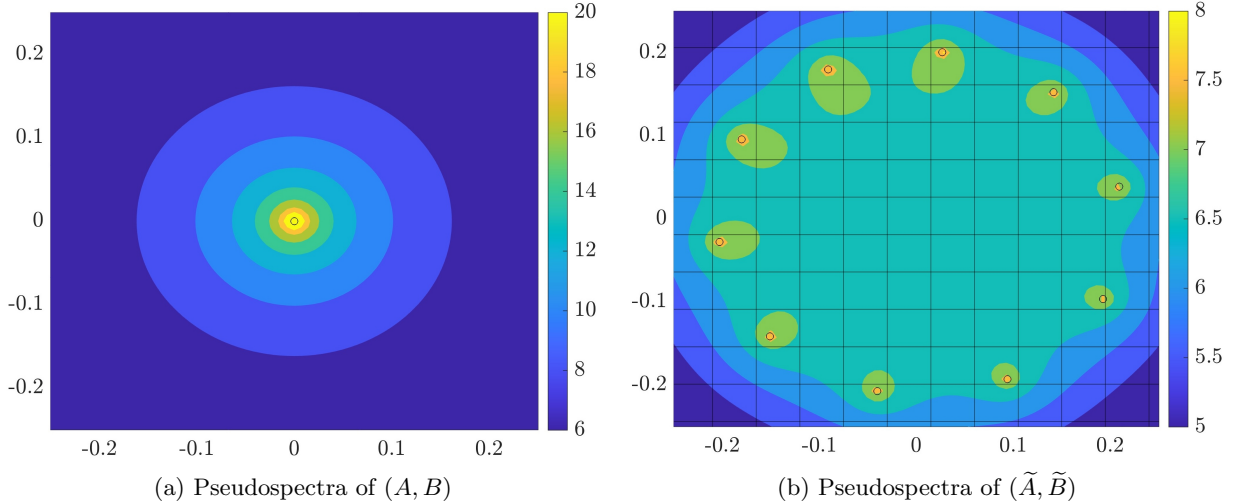


Figure 2: Pseudospectra of a pencil (A, B) before and after perturbation. Here, A is a 10×10 Jordan block, B is the identity matrix, and the perturbed matrices are $\tilde{A} = A + 10^{-7}G_1$ and $\tilde{B} = B + 10^{-7}G_2$ for G_1 and G_2 two independent, complex Gaussian matrices. Once again eigenvalues are plotted with open circles. A grid that shatters the 10^{-8} -pseudospectrum of (\tilde{A}, \tilde{B}) is superimposed over figure (b).

shrink as α increases. This trade-off reflects a fundamental geometric reality: the more we scale by, the closer the eigenvalues of $(\tilde{A}, n^\alpha \tilde{B})$ are driven to zero (and therefore to each other), meaning we'll need a finer grid and a smaller pseudospectrum to guarantee shattering.

Figure 2 demonstrates pseudospectral shattering on a 10×10 example. We observe here all of the same phenomena as in single-matrix shattering: small perturbations turn a pencil with a poorly conditioned eigenvalue problem – here only one eigenvalue repeated ten times – to one with a full set of distinct eigenvalues. Note in particular how much faster the pseudospectra of (\tilde{A}, \tilde{B}) coalesce around the eigenvalues as $\epsilon \rightarrow 0$.

Because Theorem 3.10 applies to the product matrix $X = n^{-\alpha} \tilde{B}^{-1} \tilde{A}$, our proof of shattering only works with $(\tilde{A}, n^\alpha \tilde{B})$ as a pencil via the version of Bauer-Fike used. Consequently, swapping Theorem 2.20 for Theorem 2.15, the same proof implies the following pseudospectral shattering result for X .

Proposition 3.13. *Let $A, B \in \mathbb{C}^{n \times n}$ and let $0 < \gamma < \frac{1}{2}$. Suppose $(\tilde{A}, \tilde{B}) = (A + \gamma G_1, B + \gamma G_2)$ for G_1, G_2 two independent complex Ginibre matrices and let $X = n^{-\alpha} \tilde{B}^{-1} \tilde{A}$ for $\alpha > 0$. Then $\Lambda_\epsilon(X)$ is shattered with respect to the grid g (as defined in Theorem 3.12) for $\epsilon = \frac{\gamma^5}{16} n^{-\frac{11\alpha+25}{3}}$ with probability at least $\left[1 - \frac{82}{n} - \frac{531441}{16n^2}\right] \left[1 - \frac{n^{2-2\alpha}}{\gamma^2} - 4e^{-n}\right]$.*

Proposition 3.13 implies an alternative strategy for diagonalizing (A, B) : form the product matrix X and apply single-matrix divide-and-conquer as defined by Banks et al. [9, Algorithm EIG] using the grid g and the corresponding pseudospectral guarantee. While this is fairly straightforward – and even implies the same asymptotic complexity for the diagonalization as we derive in the subsequent sections – it is not viable in general due to potential numerical instability. If B is poorly conditioned and γ is small, inverting \tilde{B} to form X will incur significant error in finite precision.

This phenomenon is illustrated in Figure 3, which plots the pseudospectra of both (\tilde{A}, \tilde{B}) and $\tilde{B}^{-1} \tilde{A}$ for a 10×10 example in which B is initially singular. The difference between the two is striking; while $\Lambda_\epsilon(\tilde{A}, \tilde{B})$ easily separates the eigenvalues, $\Lambda_\epsilon(\tilde{B}^{-1} \tilde{A})$ covers large regions of the complex plane, even for small ϵ . This indicates that the guarantee provided by Proposition 3.13 is more vulnerable in finite precision than Theorem 3.12. Indeed, we prove in Appendix B that higher precision is needed to guarantee shattering for the product matrix X . As mentioned in the introduction, this increase in precision is our motivation for bypassing this approach to the problem and prioritizing inverse-free computations.

In the remainder of this section, we develop two perturbation results: one for pseudospectral shattering (Lemma 3.14) and one for individual eigenvalues and eigenvectors (Lemma 3.15). These follow closely [9, Lemmas 5.8 and 5.9] and will be useful in the next section.

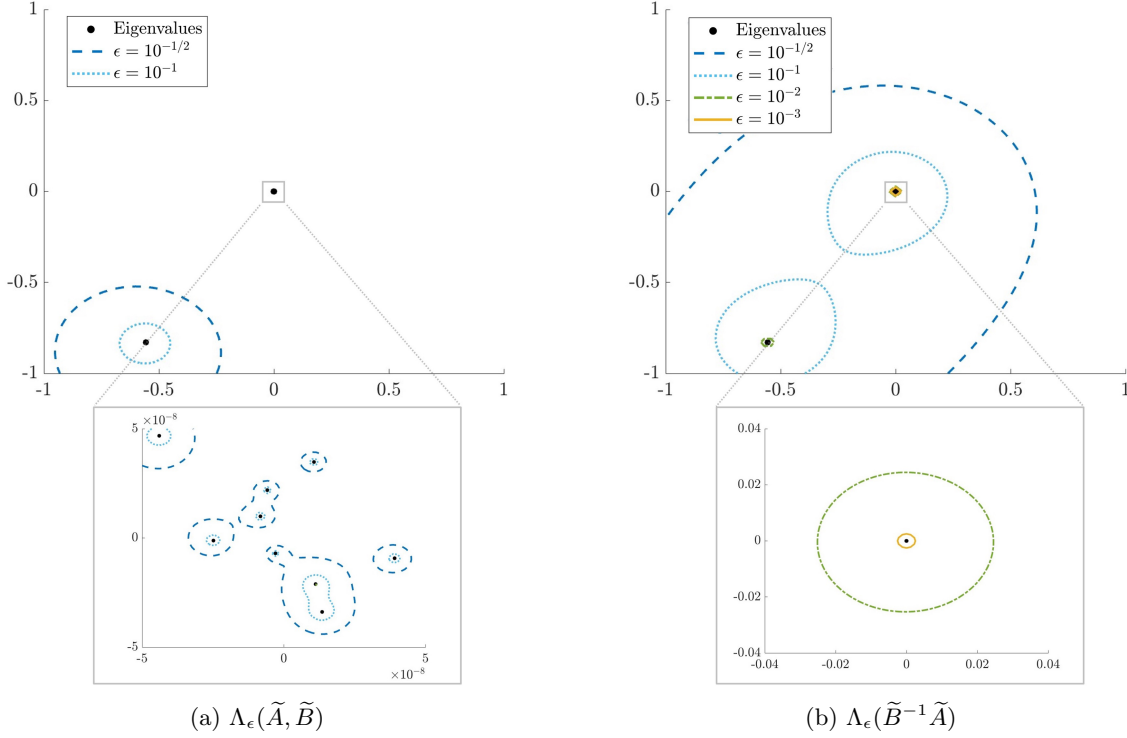


Figure 3: Pseudospectra of a 10×10 pencil (\tilde{A}, \tilde{B}) and its corresponding product matrix $\tilde{B}^{-1}\tilde{A}$. Here, $\tilde{A} = A + 10^{-7}G_1$ and $\tilde{B} = B + 10^{-7}G_2$ for A and B drawn randomly and B modified to be singular (without changing its remaining singular values). In both plots, \tilde{B} is scaled so that the maximum eigenvalue has modulus one. In addition, we provide a subplot focused around the origin to examine the pseudospectra around the small eigenvalues of (\tilde{A}, \tilde{B}) , which correspond to finite eigenvalues of (A, B) . In plot (a), we omit the pseudospectra for $\epsilon = 10^{-2}$ and $\epsilon = 10^{-3}$ since they are too close to the eigenvalues to be visible.

Lemma 3.14. *Suppose (A, B) is regular and $\Lambda_\epsilon(A, B)$ is shattered with respect to a finite grid g . If $\|A - A'\|_2, \|B - B'\|_2 \leq \eta < \epsilon$ then each eigenvalue of (A', B') shares a grid box with exactly one eigenvalue of (A, B) and $\Lambda_{\epsilon-\eta}(A', B')$ is also shattered with respect to g .*

Proof. If $z \in \Lambda_{\epsilon-\eta}(A', B')$ then z is an eigenvalue of a pencil (C, D) with $\|A' - C\|_2, \|B' - D\|_2 \leq \epsilon - \eta$. In this case,

$$\|A - C\|_2 \leq \|A - A' + A' - C\|_2 \leq \|A - A'\|_2 + \|A' - C\|_2 \leq \eta + \epsilon - \eta = \epsilon \quad (3.3.8)$$

and similarly $\|B - D\|_2 \leq \epsilon$, which implies $z \in \Lambda_\epsilon(A, B)$. Thus, $\Lambda_{\epsilon-\eta}(A', B') \subseteq \Lambda_\epsilon(A, B)$, which guarantees that $\Lambda_{\epsilon-\eta}(A', B')$ is also shattered with respect to g . To show that each eigenvalue of (A', B') shares a grid box with exactly one eigenvalue of (A, B) , consider $A_t = A + t(A' - A)$ and $B_t = B + t(B' - B)$ for $t \in [0, 1]$. Since (A, B) is regular (and moreover $\epsilon < \sigma_n(B)$ since $\Lambda_\epsilon(A, B)$ is bounded), (A_t, B_t) continuously deforms the eigenvalues of (A, B) to eigenvalues of (A', B') while staying within $\Lambda_\eta(A, B) \subseteq \Lambda_\epsilon(A, B)$. Since $\Lambda_\epsilon(A, B)$ is shattered with respect to g and therefore no two eigenvalues of (A, B) share a grid box, this ensures that each eigenvalue of (A', B') belongs to a grid box with a unique eigenvalue of (A, B) \square

Lemma 3.15. *Suppose (A, B) is regular and $\Lambda_\epsilon(A, B)$ is shattered with respect to a finite grid g with boxes of side length ω . If $\|A - A'\|_2, \|B - B'\|_2 \leq \eta < \epsilon$ then for any right unit eigenvector v' of (A', B') there exists a right unit eigenvector v of (A, B) such that*

1. *The eigenvalue of (A', B') corresponding to v' shares a grid box of g with the eigenvalue of (A, B) that corresponds to v .*
2. $\|v' - v\| \leq \frac{\sqrt{8}\omega}{\pi} \frac{\eta}{\epsilon(\epsilon-\eta)} (1 + \|B^{-1}A\|_2) \|B\|_2.$

Proof. Let λ' be the eigenvalue of (A', B') corresponding to v' . By [Lemma 3.14](#), λ' shares a grid box of g with a unique eigenvalue of λ of (A, B) . Let v be the right unit eigenvector of (A, B) corresponding to λ . In addition, let w' and w be the left eigenvectors corresponding to v' and v respectively, normalized so that $w^H v = (w')^H v' = 1$. If Γ is the contour of the grid box containing both λ and λ' , then by [\(2.1.1\)](#)

$$\begin{aligned} v'(w')^H - vw^H &= \frac{1}{2\pi i} \oint_{\Gamma} (z - (B')^{-1}A')^{-1} dz - \frac{1}{2\pi i} \oint_{\Gamma} (z - B^{-1}A)^{-1} dz \\ &= \frac{1}{2\pi i} \oint_{\Gamma} (z - (B')^{-1}A')^{-1} - (z - B^{-1}A)^{-1} dz. \end{aligned} \quad (3.3.9)$$

By the resolvent identity

$$\begin{aligned} (z - (B')^{-1}A')^{-1} - (z - B^{-1}A)^{-1} &= (z - (B')^{-1}A')^{-1}((B')^{-1}A' - B^{-1}A)(z - B^{-1}A)^{-1} \\ &= (zB' - A')^{-1}B'((B')^{-1}A' - B^{-1}A)(zB - A)^{-1}B \\ &= (zB' - A)^{-1}(A' - B'B^{-1}A)(zB - A)^{-1}B, \end{aligned} \quad (3.3.10)$$

so, applying this along with the ML inequality above, we have

$$\|v'(w')^H - vw^H\|_2 \leq \frac{2\omega}{\pi} \sup_{z \in \Gamma} \|(zB' - A')^{-1}(A' - B'B^{-1}A)(zB - A)^{-1}B\|_2. \quad (3.3.11)$$

Now $\Lambda_{\epsilon}(A, B)$ is shattered with respect to g and therefore does not intersect Γ , so we know $\|(zB - A)^{-1}\|_2 \leq \frac{1}{\epsilon(1+|z|)} \leq \frac{1}{\epsilon}$ for all $z \in \Gamma$. Moreover, again by [Lemma 3.14](#), $\Lambda_{\epsilon-\eta}(A', B')$ is shattered with respect to g , so the same argument implies $\|(zB' - A')^{-1}\|_2 \leq \frac{1}{\epsilon-\eta}$ for all $z \in \Gamma$. Applying this to the previous inequality, we conclude

$$\|v'(w')^H - vw^H\|_2 \leq \frac{2\omega}{\pi} \frac{1}{\epsilon(\epsilon-\eta)} \|A' - B'B^{-1}A\|_2 \|B\|_2. \quad (3.3.12)$$

Writing $B' = B + E$ for some $\|E\|_2 \leq \eta$ since $\|B - B'\|_2 \leq \eta$, we have

$$\|A' - B'B^{-1}A\|_2 = \|A' - (B + E)B^{-1}A\|_2 \leq \|A' - A\|_2 + \|EB^{-1}A\|_2 \leq \eta(1 + \|B^{-1}A\|_2) \quad (3.3.13)$$

which yields a final upper bound

$$\|v'(w')^H - vw^H\|_2 \leq \frac{2\omega}{\pi} \frac{\eta}{\epsilon(\epsilon-\eta)} (1 + \|B^{-1}A\|_2) \|B\|_2. \quad (3.3.14)$$

Since without loss of generality we can assume $v^H v' \geq 0$ (if this is not true we can just rotate v), and using the fact that $\|v\| = \|v'\| = 1$, we complete the proof by observing

$$\|v' - v\|_2 = \sqrt{2 - 2v^H v'} \leq \sqrt{2} \|v'(w')^H - vw^H\|_2. \quad (3.3.15)$$

This inequality is nontrivial (see the proof of [\[9, Lemma 5.8\]](#) for the details). Combining it with [\(3.3.14\)](#), we conclude that v is the desired eigenvector of (A, B) with $\|v' - v\| \leq \frac{\sqrt{8}\omega}{\pi} \frac{\eta}{\epsilon(\epsilon-\eta)} (1 + \|B^{-1}A\|_2) \|B\|_2$. \square

4 Inverse-Free Divide-and-Conquer

In this section, we develop a divide-and-conquer eigensolver that, based on the pseudospectral shattering result proved in the previous section, produces approximations of the eigenvalues and eigenvectors of the perturbed and scaled pencil $(\tilde{A}, n^{\alpha}\tilde{B})$. We first provide motivation and background before stating the divide-and-conquer algorithm and proving convergence in exact arithmetic. In the next section, we use this divide-and-conquer routine to produce approximate diagonalizations for arbitrary pencils.

4.1 Motivation

Suppose we have a regular matrix pencil (A, B) to be split by divide-and-conquer. Let P_R be a rank- k spectral projector onto the span of a set of right eigenvectors of (A, B) and let $U_R \in \mathbb{C}^{n \times k}$ be a matrix whose orthonormal columns span $\text{range}(P_R)$. Similarly, let $U_L \in \mathbb{C}^{n \times k}$ be a matrix whose orthonormal columns span the left deflating subspace of (A, B) corresponding to $\text{range}(P_R)$. Since (λ, v) is an eigenpair of (A, B) if and only if (λ, w) is an eigenpair of $(U_L^H A U_R, U_L^H B U_R)$ for $v = U_R w$, we can find eigenpairs of (A, B) by solving the $k \times k$ problem $(U_L^H A U_R, U_L^H B U_R)$, whose spectra is contained in $\Lambda(A, B)$ and whose eigenvectors are in simple correspondence with those of (A, B) . This observation is the heart of divide-and-conquer, which proceeds as follows:

1. Locate a set of eigenvectors of (A, B) and compute the spectral projectors P_R and P_L onto the corresponding right and left deflating subspaces.
2. Apply a rank-revealing factorization to find matrices U_R and U_L consisting of orthonormal columns that span $\text{range}(P_R)$ and $\text{range}(P_L)$, respectively.
3. Reduce the problem (A, B) to $(U_L^H A U_R, U_L^H B U_R)$ and repeat for the other set of eigenvectors, then recur.

One question remains: how do we locate a set of eigenvectors to project onto? Pseudospectral shattering provides an answer. If we have a grid that shatters the pseudospectrum of our perturbed and scaled problem $(\tilde{A}, n^\alpha \tilde{B})$, we can search for a grid line that significantly¹ splits the spectrum; applying a Möbius transformation that sends that grid line to the unit circle and then repeatedly squaring the pencil to drive one set of eigenvalues to zero, we obtain a projector onto the eigenvectors belonging to the surviving eigenvalues. In this approach, finding a grid line that produces a significant split ensures that divide-and-conquer will succeed in $O(\log(n))$ steps.

For this to work without drawing a new grid at each step, we need shattering to be preserved as the problem shrinks in size. This is guaranteed by the following lemma.

Lemma 4.1. *Let P_R be a spectral projector for a regular matrix pencil (A, B) and let P_L be the projector onto the corresponding left deflating subspace. Let $U_L, U_R \in \mathbb{C}^{n \times k}$ be matrices whose orthonormal columns span the ranges of P_L and P_R respectively. Then*

$$\Lambda_\epsilon(U_L^H A U_R, U_L^H B U_R) \subseteq \Lambda_\epsilon(A, B).$$

Proof. If $z \in \Lambda_\epsilon(U_L^H A U_R, U_L^H B U_R)$ then there exists a unit vector $u \in \mathbb{C}^k$ such that

$$\|U_L^H (A - zB) U_R u\|_2 = \|(U_L^H A U_R - z U_L^H B U_R) u\|_2 \leq \epsilon(1 + |z|). \quad (4.1.1)$$

Let $y = U_R u \in \mathbb{C}^n$. Since U_R has orthonormal columns $\|y\|_2 = \|U_R u\|_2 = \|u\|_2 = 1$. Moreover, y is in the right deflating subspace $\text{range}(P_R)$, which means $(A - zB)y$ belongs to the corresponding left deflating subspace $\text{range}(P_L)$. Since the columns of U_L are an orthonormal basis for this subspace, we conclude

$$\|(A - zB)y\|_2 = \|U_L^H (A - zB)y\|_2 \leq \epsilon(1 + |z|) \quad (4.1.2)$$

and therefore $z \in \Lambda_\epsilon(A, B)$. □

Lemma 4.1 emphasizes the importance of the matrices U_L and U_R . While in principle many of the building blocks of divide-and-conquer hold for arbitrary matrices whose columns span deflating subspaces, its proof requires properties of matrices with orthonormal columns, meaning it would not be sufficient to simply compute the projectors P_R and P_L . On top of this, U_L and U_R have the added benefit of ensuring that the norms of $U_L^H A U_R$ and $U_L^H B U_R$ don't grow, allowing us to carry norm assumptions through the recursion.

¹Significant here means that at least a fifth of the eigenvalues lie on either side of the line.

4.2 Numerical Building Blocks

In this section, we review the numerical building blocks that allow us to compute the projectors P_R and P_L and subsequently the orthonormal bases contained in U_L and U_R . Note that, as mentioned in the introduction, each of these uses only QR and matrix multiplication.

4.2.1 Implicit Repeated Squaring (IRS)

We begin with Implicit Repeated Squaring (**IRS**), a routine for repeatedly squaring a product $A^{-1}B$ without forming it. **IRS** first appeared in the context of eigenvalue problems in initial explorations of inverse-free and parallel methods [4, 42]. It was subsequently stated as it appears in [Algorithm 1](#) under the name **IRS** in a technical report of Ballard, Demmel, and Dumitriu [6].

Algorithm 1 Implicit Repeated Squaring (**IRS**)

Input: $A, B \in \mathbb{C}^{n \times n}$ and p a positive integer

Output: $A_p, B_p \in \mathbb{C}^{n \times n}$ satisfying $A_p^{-1}B_p = (A^{-1}B)^{2^p}$

1: $A_0 = A$
 2: $B_0 = B$
 3: **for** $j = 0 : p - 1$ **do**
 4:

$$\begin{aligned} \begin{pmatrix} B_j \\ -A_j \end{pmatrix} &= \begin{pmatrix} Q_{11} & Q_{12} \\ Q_{21} & Q_{22} \end{pmatrix} \begin{pmatrix} R_j \\ 0 \end{pmatrix} \\ A_{j+1} &= Q_{12}^H A_j \\ B_{j+1} &= Q_{22}^H B_j \end{aligned}$$

5: **end for**
 6: **return** A_p, B_p

Assuming invertibility where needed, we can verify the guarantee of [Algorithm 1](#) by noting that line 4 ensures $Q_{12}^H B_j - Q_{22}^H A_j = 0$ and consequently $B_j A_j^{-1} = Q_{12}^{-H} Q_{22}^H$, which implies

$$A_{j+1}^{-1} B_{j+1} = A_j^{-1} Q_{12}^{-H} Q_{22}^H B_j = A_j^{-1} B_j A_j^{-1} B_j = (A_j^{-1} B_j)^2. \quad (4.2.1)$$

The connection to spectral projectors is fairly straightforward: if A is nonsingular, $A^{-1}B$ and (A, B) have the same set of eigenvectors, with each finite eigenvalue λ of $A^{-1}B$ corresponding to an eigenvalue λ^{-1} of (A, B) . Repeatedly squaring $A^{-1}B$ drives its eigenvalues to either zero or infinity, assuming (A, B) has no eigenvalues on the unit circle, without changing eigenvectors. Moreover, after p steps of repeated squaring we have

$$(A_p + B_p)^{-1} A_p = (I + A_p^{-1} B_p)^{-1} = (I + (A^{-1} B)^{2^p})^{-1}, \quad (4.2.2)$$

so the eigenvalues of $(A_p + B_p)^{-1} A_p$ are close to either zero or one, corresponding to eigenvalues that were originally inside, respectively outside, the unit disk. For clarity, [Table 1](#) shows the correspondence between eigenvalues of (A, B) and eigenvalues of the outputs of **IRS**.

Since $(A_p + B_p)^{-1} A_p$ has the same set of eigenvectors as $A^{-1}B$, it is not hard to show that $(A_p + B_p)^{-1} A_p$ approaches a projector $P_{R, |z| > 1}$ onto the right deflating subspace of (A, B) spanned by eigenvectors with eigenvalues outside the unit disk [4, §4]. Nevertheless, for divide-and-conquer to proceed we also need a projector onto the corresponding left deflating subspace. Luckily, this can be done by running **IRS** on (A^H, B^H) since taking a Hermitian transpose swaps right and left deflating spaces. In fact, if A_p and B_p are the outputs of p steps of repeated squaring on (A^H, B^H) , then

$$A_p^H (A_p + B_p)^{-H} = (I + (A^{-H} B^H)^{2^p})^{-H} \quad (4.2.3)$$

approaches a projector $P_{L, |z| > 1}$ onto the left deflating subspace corresponding to $P_{R, |z| > 1}$. And while taking a Hermitian transpose does change the eigenvalues, we can see from [Table 1](#) that repeated squaring on (A^H, B^H) drives corresponding eigenvalues to the same destination (either zero or one).

Eigenvalue Correspondence in IRS (Algorithm 1)							
(A, B)	$A^{-1}B$	$A_p^{-1}B_p$	$(A_p + B_p)^{-1}A_p$	(A^H, B^H)	$A^{-H}B^H$	$\mathcal{A}_p^{-1}\mathcal{B}_p$	$\mathcal{A}_p^H(\mathcal{A}_p + \mathcal{B}_p)^{-H}$
λ	λ^{-1}	λ^{-2p}	$(1 + \lambda^{-2p})^{-1}$	$\bar{\lambda}$	$(\bar{\lambda})^{-1}$	$(\bar{\lambda})^{-2p}$	$(1 + \lambda^{-2p})^{-1}$

Table 1: Correspondence between each eigenvalue λ of (A, B) and an eigenvalue of the matrices that appear when **IRS** is used to compute spectral projectors. Here, $[A_p, B_p] = \mathbf{IRS}(A, B, p)$ while $[\mathcal{A}_p, \mathcal{B}_p] = \mathbf{IRS}(A^H, B^H, p)$.

As mentioned, **IRS** breaks down if the input pencil has an eigenvalue on the unit circle. Considering such a problem to be ill-posed, Bai, Demmel, and Gu introduced the following distance $d_{(A,B)}$, whose reciprocal can be thought of as a condition number for the procedure.

Definition 4.2. The distance from (A, B) to the nearest ill-posed problem is

$$d_{(A,B)} = \inf \{ \|E\| + \|F\| : (A + E) - z(B + F) \text{ is singular for some } |z| = 1 \}.$$

Using $d_{(A,B)}$, they proved quadratic convergence for exact arithmetic **IRS**. Informally, this result states that to reach accuracy δ we need to take roughly $O(\log_2(1/\delta))$ steps of repeated squaring.

Theorem 4.3 (Bai-Demmel-Gu 1994). *Let A_p, B_p be the result of applying **IRS** to A, B . If*

$$p \geq \log_2 \left[\frac{\|(A, B)\|_2 - d_{(A,B)}}{d_{(A,B)}} \right]$$

then

$$\|(A_p + B_p)^{-1}A_p - P_{R,|z|>1}\|_2 \leq \|P_{R,|z|>1}\|_2 \frac{2^{p+3} \left(1 - \frac{d_{(A,B)}}{\|(A,B)\|_2}\right)^{2p}}{\max \left\{ 0, 1 - 2^{p+2} \left(1 - \frac{d_{(A,B)}}{\|(A,B)\|_2}\right)^{2p} \right\}}.$$

Note that because $d_{(A^H, B^H)} = d_{(A, B)}$ and $\|(A, B)\|_2 = \|(A^H, B^H)\|_2$, **Theorem 4.3** can be applied to the left projector by swapping $A, B, (A_p + B_p)^{-1}A_p$, and $P_{R,|z|>1}$ for $A^H, B^H, A_p^H(A_p + B_p)^{-H}$, and $P_{L,|z|>1}$, respectively.

4.2.2 RURV and GRURV

Once we have our spectral projectors P_R and P_L , we next need to apply a rank-revealing factorization to locate an orthonormal basis for the corresponding right and left deflating subspaces. To do this, we produce a (random) URV factorization of the projectors.

Definition 4.4. $A = URV$ is a URV factorization of the matrix $A \in \mathbb{C}^{n \times n}$ if R is upper triangular and $U, V \in \mathbb{C}^{n \times n}$ are unitary.

The URV factorization was first introduced by Stewart [54] as an alternative to the SVD with many of the same properties. Most important is its rank-revealing capability: when A has effective rank k (i.e., there is a significant gap between $\sigma_k(A)$ and $\sigma_{k+1}(A)$), $A = URV$ is a rank-revealing factorization with

$$R = \begin{pmatrix} R_{11} & R_{21} \\ 0 & R_{22} \end{pmatrix} \quad (4.2.4)$$

for R_{11} a $k \times k$ block if $\sigma_k(R_{11})$ is a “good” approximation to $\sigma_k(A)$ and $\sigma_1(R_{22})$ is a “good” approximation of $\sigma_{k+1}(A)$. We will make the meaning of “good” precise in the guarantees to come.

While there are many ways to compute a rank-revealing URV factorization (see for example [26, §3]) we are interested in the **RURV** algorithm of Demmel, Dumitriu, and Holtz [17], which is stated below as **Algorithm 2**. This randomized algorithm is simple to implement, backwards stable [7, Theorem 4.5], and capable of producing strongly rank-revealing factorizations (in the sense of Gu and Eisenstat [31]). In fact, Ballard et al. [7] proved the following result, which demonstrates that **RURV** matches the best-known guarantees for deterministic factorizations.

Algorithm 2 Randomized Rank-Revealing Factorization (**RURV**)**Input:** $A \in \mathbb{C}^{n \times n}$ **Output:** U unitary matrix, R upper triangular matrix, and V Haar such that $A = URV$ is a rank-revealing factorization of A .

-
- 1: Draw a random matrix B with i.i.d. $\mathcal{N}_{\mathbb{C}}(0, 1)$ entries
 - 2: $[V, \widehat{R}] = \mathbf{QR}(B)$
 - 3: $\widehat{A} = A \cdot V^H$
 - 4: $[U, R] = \mathbf{QR}(\widehat{A})$
 - 5: **return** U, R, V
-

Theorem 4.5 (Ballard et al. 2019). *Let $A \in \mathbb{C}^{n \times n}$ with singular values $\sigma_1, \sigma_2, \dots, \sigma_n$. Let R be the matrix produced by applying exact arithmetic **RURV** to A as in (4.2.4). Assume that $k, n - k > 30$. Then with probability $1 - \delta$ the following occur:*

$$\begin{aligned} \frac{\delta}{2.02} \frac{\sigma_k}{\sqrt{k(n-k)}} &\leq \sigma_k(R_{11}) \leq \sigma_k \\ \sigma_{k+1} &\leq \sigma_1(R_{22}) \leq 2.02 \frac{\sqrt{k(n-k)}}{\delta} \sigma_{k+1} \\ \|R_{11}^{-1} R_{12}\|_2 &\leq \frac{6.1 \sqrt{k(n-k)}}{\delta} + \frac{\sigma_{k+1}}{\sigma_k} \frac{50 \sqrt{k^3(n-k)^3}}{\delta^3}. \end{aligned}$$

The proof of [Theorem 4.5](#) boils down to bounding the smallest singular value of a $k \times k$ block of a Haar unitary matrix via [[17](#), Theorem 5.2]. The requirement $k, n - k > 30$ comes from the bound used by Ballard et al. [[7](#), Corollary 3.4]. Banks et al. subsequently demonstrated that this can be relaxed [[9](#), Proposition C.3], although the fundamental guarantees are the same: with high probability **RURV** produces a factorization such that $\sigma_k(R_{11})$ and $\sigma_1(R_{22})$ are at worst a multiplicative factor of $O(\sqrt{k(n-k)})$ away from $\sigma_k(A)$ and $\sigma_{k+1}(A)$, respectively.

Of course, the projectors we would like to apply **RURV** to are not simple matrices but rather products of the form $A^{-1}B$ or AB^{-1} (i.e., the approximate projectors $(A_p + B_p)^{-1}A_p$ and $\mathcal{A}_p^H(\mathcal{A}_p + \mathcal{B}_p)^{-H}$ from **IRS**). Since we avoid taking inverses, explicitly forming either of these products is not an option. Instead, a generalized version of **RURV** – referred to as **GRURV** and presented here as [Algorithm 3](#) – allows us to apply **RURV** to an arbitrary product of matrices and their inverses. Note that in this routine **RURV** is a version of **RURV** that replaces the QR factorization in line 4 of [Algorithm 2](#) with QL.

GRURV was first introduced in a technical report of Ballard, Demmel, and Dumitriu [[6](#)] specifically to apply **RURV** to spectral projectors found by **IRS**. Importantly, exact arithmetic **GRURV** is essentially equivalent to applying exact arithmetic **RURV** to the corresponding product [[7](#), Theorem 5.2], which allows us to access guarantees like [Theorem 4.5](#) for **GRURV** in exact arithmetic without any additional effort.

4.2.3 DEFLATE

We are now ready to state a routine that combines **IRS** and **GRURV** to accomplish items (1) and (2) from our outline of divide-and-conquer in [Section 4.1](#). Such a routine was first stated as **RGNEP** [[6](#), Algorithm 4], albeit in a different form than we present below. In particular, **RGNEP** assumed no knowledge of the number of eigenvalues of (A, B) inside/outside the unit circle (equivalently, the rank of the corresponding spectral projectors), instead multiplying by the full $n \times n$ unitary matrices produced by **GRURV** and deciding where to split the problem to minimize certain matrix norms. Since we will have access to information about the rank of the projectors being computed (this is how dividing grid lines are selected), we state an alternative **DEFLATE** ([Algorithm 4](#)), which simply takes the first k columns of the matrices computed by **GRURV**.

For **DEFLATE** to succeed, we need to know that the first k columns of the U-factor produced by **GRURV** span the range of the rank- k product it is applied to with high probability. We would also like a guarantee that the result for an approximate projector is close to the corresponding result for a true spectral projector (since **IRS** can only produce approximations of P_R or P_L).

Algorithm 3 Generalized Randomized Rank-Revealing Factorization (**GRURV**)**Input:** k a positive integer, $A_1, A_2, \dots, A_k \in \mathbb{C}^{n \times n}$, and $m_1, m_2, \dots, m_k \in \{1, -1\}$ **Output:** U unitary, R_1, R_2, \dots, R_k upper triangular, and V Haar such that $UR_1^{m_1}R_2^{m_2}\dots R_k^{m_k}V$ is a rank-revealing factorization of $A_1^{m_1}A_2^{m_2}\dots A_k^{m_k}$

```
1: if  $m_k = 1$  then
2:    $[U, R_k, V] = \mathbf{RURV}(A_k)$ 
3: else
4:    $[U, L_k, V] = \mathbf{RULV}(A_k^H)$ 
5:    $R_k = L_k^H$ 
6: end if
7:  $U_{\text{current}} = U$ 
8: for  $i = k - 1 : 1$  do
9:   if  $m_i = 1$  then
10:     $[U, R_i] = \mathbf{QR}(A_i \cdot U_{\text{current}})$ 
11:     $U_{\text{current}} = U$ 
12:   else
13:     $[U, R_i] = \mathbf{RQ}(U_{\text{current}}^H \cdot A_i)$ 
14:     $U_{\text{current}} = U^H$ 
15:   end if
16: end for
17: return  $U_{\text{current}}$ , optionally  $R_1, R_2, \dots, R_k, V$ 
```

Algorithm 4 Deflating Subspace Finder (**DEFLATE**)**Input:** $A, B \in \mathbb{C}^{n \times n}$, positive integers p and k **Requires:** $k \leq n$; (A, B) has no eigenvalues on the unit circle and exactly k eigenvalues outside it.**Output:** $U_R^{(k)}, U_L^{(k)} \in \mathbb{C}^{k \times n}$ with orthonormal columns that approximately span right and left deflating subspaces of (A, B) .

```
1:  $[A_p, B_p] = \mathbf{IRS}(A, B, p)$ 
2:  $U_R = \mathbf{GRURV}(2, A_p + B_p, A_p, -1, 1)$ 
3:  $[A_p, B_p] = \mathbf{IRS}(A^H, B^H, p)$ 
4:  $U_L = \mathbf{GRURV}(2, A_p^H, (A_p + B_p)^H, 1, -1)$ 
5:  $U_R^{(k)} = U_R(:, 1 : k)$ 
6:  $U_L^{(k)} = U_L(:, 1 : k)$ 
7: return  $U_R^{(k)}, U_L^{(k)}$ 
```

If we apply **RURV** to a rank- k matrix A , the first k columns of the U -factor almost surely span $\text{range}(A)$. The intuition behind this is fairly simple: multiplying by the Haar matrix in line 3 of **RURV** “mixes” the columns of A , distributing information so that the first k columns of A – and therefore the first k columns of U – are likely to span $\text{range}(A)$. On top of this, we have the following perturbation result in exact arithmetic, originally proved by Banks et al. [9, Proposition C.12].

Theorem 4.6 (Banks et al. 2022). *Let $A, A' \in \mathbb{C}^{n \times n}$ with $\|A - A'\|_2 \leq \delta$ and $\text{rank}(A) = \text{rank}(A^2) = k$. Let T and S contain the first k columns of the U -factors produced by applying exact arithmetic **RURV** to A and A' , respectively. Then for any $\theta \in (0, 1)$ with probability $1 - \theta^2$ there exists a unitary $W \in \mathbb{C}^{k \times k}$ such that*

$$\|S - TW^H\|_2 \leq \sqrt{\frac{8\sqrt{k(n-k)}}{\sigma_k(T^H A T)}} \cdot \sqrt{\frac{\delta}{\theta}}$$

Letting A be a rank- k spectral projector (in which case $\sigma_k(T^H A T) = 1$), **Theorem 4.6** says that the first k columns of the U -factor of an approximation A' of A are close to a rotation/reflection of the first k columns of the U -factor of A as long as $\|A - A'\|_2$ is sufficiently small.

Recalling that exact arithmetic **GRURV** is equivalent to exact arithmetic **RURV** on the corresponding product, these results generalize directly. Not only can we say that almost surely the first k columns of the U-factor produced by **GRURV** span the range of the product, but a perturbation result similar to [Theorem 4.6](#) holds. Combining these with our analysis of **IRS** yields the following exact arithmetic guarantee for **DEFLATE**.

Theorem 4.7. *Suppose (A, B) , p , and k satisfy the requirements of **DEFLATE**, where p is large enough to ensure error in repeated squaring is at most δ in lines 1 and 3. Let $U_R^{(k)}$ and $U_L^{(k)}$ be the outputs of running this algorithm in exact arithmetic. Then for any $\nu \in (0, 1)$, there exist $U_R, U_L \in \mathbb{C}^{n \times k}$ with orthonormal columns spanning right and left deflating subspaces of (A, B) , respectively, such that*

1. $\|U_R^{(k)} - U_R\|_2 \leq \sqrt{8\sqrt{k(n-k)}}\sqrt{\frac{\delta}{\nu}}$
2. $\|U_L^{(k)} - U_L\|_2 \leq \sqrt{8\sqrt{k(n-k)}}\sqrt{\frac{\delta}{\nu}}$

with probability at least $1 - 2\nu^2$.

Proof. Consider first $U_R^{(k)}$ and let A_p and B_p be the outputs of applying p steps of exact arithmetic repeated squaring to A and B . We know $(A_p + B_p)^{-1}A_p$ approaches a projector $P_{R,|z|>1}$ onto the right deflating subspace spanned by eigenvectors of (A, B) with eigenvalues outside the unit circle. Let $URV = P_{R,|z|>1}$ be a rank-revealing factorization of $P_{R,|z|>1}$ obtained via exact arithmetic **RURV** and let $U^{(k)}$ contain the first k columns of U . Since k is the number of eigenvalues with modulus greater than one, we know $k = \text{rank}(P_{R,|z|>1})$ and moreover $\text{range}(U^{(k)}) = \text{range}(P_{R,|z|>1})$ almost surely. Thus, since p is large enough to ensure $\|(A_p + B_p)^{-1}A_p - P_{R,|z|>1}\|_2 \leq \delta$ and exact arithmetic **GRURV** satisfies the same guarantees as exact **RURV**, we have by [Theorem 4.6](#) that with probability at least $1 - \nu^2$ there exists a unitary $W \in \mathbb{C}^{k \times k}$ such that

$$\|U_R^{(k)} - U^{(k)}W^H\|_2 \leq \sqrt{8\sqrt{k(n-k)}}\sqrt{\frac{\delta}{\nu}}. \quad (4.2.5)$$

Setting $U_R = U^{(k)}W^H$, we have inequality (1) with probability at least $1 - \nu^2$. Repeating the same argument for $U_L^{(k)}$, using this time the fact that $[A_p, B_p] = \mathbf{IRS}(A^H, B^H, p)$ implies $\|A_p^H(A_p + B_p)^{-H} - P_{L,|z|>1}\|_2 \leq \delta$ for $P_{L,|z|>1}$ a projector onto the left deflating subspace corresponding to $P_{R,|z|>1}$, we obtain result (2) also with probability at least $1 - \nu^2$. Taking a union bound, we have both 1 and 2 with probability at least $1 - 2\nu^2$. \square

4.3 Divide-and-Conquer Routine

With **IRS**, **GRURV**, and **DEFLATE** (and their exact arithmetic guarantees discussed above) we can now state our divide-and-conquer eigensolver, presented below as **EIG** ([Algorithm 5](#)). The main inputs for this routine are a pencil (A, B) and a grid g that shatters $\Lambda_\epsilon(A, B)$ for some $\epsilon > 0$. In practice, this will be our perturbed and scaled pencil $(\tilde{A}, n^\alpha \tilde{B})$ (hence the norm assumption on B has a factor of n^α attached) and the shattering grid guaranteed by [Theorem 3.12](#). Recall that shattering implies that (A, B) is both regular and diagonalizable.

Before proving exact arithmetic guarantees for **EIG**, we first provide a high-level overview of the algorithm to motivate why it works. Throughout, we rely on the analysis of each of the building blocks from the previous section as well as the requirements listed in [Algorithm 5](#).

1. Since **EIG** calls itself recursively, the first three lines check for our stopping criteria. We choose to continue divide-and-conquer until the pencil is 1×1 , though as mentioned in the introduction we could choose instead to stop once the pencil is small enough to be handled by another method.
2. The next four lines (4-7) set parameters for the algorithm. Most importantly, they determine how many steps of repeated squaring need to be taken to achieve the desired accuracy (i.e., the value of p in line 7).

Algorithm 5 Divide-and-Conquer Eigensolver (**EIG**)

Input: $n \in \mathbb{N}_+$, $A, B \in \mathbb{C}^{m \times m}$, $\epsilon > 0$, $\alpha > 1$, g an $s_1 \times s_2$ grid with box size ω , $\beta > 0$ a desired eigenvector accuracy, and $\theta \in (0, 1)$ a failure probability.

Requires: $m \leq n$, $\|A\|_2 \leq 3$, $\|B\|_2 \leq 3n^\alpha$, $g \subset \{z : |\operatorname{Re}(z)|, |\operatorname{Im}(z)| < 5\}$, and $\Lambda_\epsilon(A, B)$ shattered w.r.t. g .

Output: T an invertible matrix and (D_1, D_2) a diagonal pencil. The eigenvalues of (D_1, D_2) each share a grid box of g with a unique eigenvalue of (A, B) and each column of T is an approximate right unit eigenvector of (A, B) .

```
1: if  $m = 1$  then
2:    $T = 1$ ;  $D_1 = A$ ;  $D_2 = B$ 
3: else
4:    $\zeta = 2(\lfloor \log_2(\max\{s_1, s_2\}) + 1 \rfloor)$ 
5:    $\eta = \min \left\{ \frac{4\pi}{315\sqrt{8}} \frac{\beta\epsilon^2}{\omega n^\alpha}, \frac{1}{2\log_{5/4}(n)} \right\}$ 
6:    $\delta = \min \left\{ \sqrt{\frac{\theta}{10}} \frac{\epsilon^2}{7200n^{2\alpha+3}}, \frac{\theta}{2(\theta+10n^6\zeta)}, \sqrt{\frac{\theta}{10}} \frac{\eta^2}{288n^{2\alpha+3}} \right\}$ 
7:    $p = \left\lceil \max \left\{ 7, \log_2 \left( \frac{105n^\alpha}{\epsilon} - 1 \right), -2\log_2 \left( -\frac{1}{2} \log_2 \left( 1 - \frac{\epsilon}{105n^\alpha} \right) \right), 1 + \log_2 \left[ \frac{\log_2 \left( \frac{\delta\pi\epsilon}{12n^\alpha m\omega + \delta\pi\epsilon} \right)}{\log_2 \left( 1 - \frac{\epsilon}{105n^\alpha} \right)} \right] \right\} \right\rceil$ 
8:   Choose a grid line  $\operatorname{Re}(z) = h$  of  $g$ 
9:    $(\mathcal{A}, \mathcal{B}) = (A - (h-1)B, A - (h+1)B)$ 
10:   $[A_p, B_p] = \mathbf{IRS}(\mathcal{A}, \mathcal{B}, p)$ 
11:   $[U, R_1, R_2, V] = \mathbf{GRURV}(2, A_p + B_p, A_p, -1, 1)$ 
12:   $k = \# \left\{ i : \left| \frac{R_2(i,i)}{R_1(i,i)} \right| \geq \sqrt{\frac{\theta}{10\zeta}} \frac{1-\delta}{n^3} \right\}$ 
13:  if  $k < \frac{1}{5}m$  or  $k > \frac{4}{5}m$  then
14:    Return to step 8 and choose a new grid line, executing a binary search if necessary. If this fails,
    search over horizontal grid lines  $\operatorname{Im}(z) = h$ , this time setting  $(\mathcal{A}, \mathcal{B}) = (A - i(h-1)B, A - i(h+1)B)$ .
15:  else
16:     $[U_R^{(k)}, U_L^{(k)}] = \mathbf{DEFLATE}(\mathcal{A}, \mathcal{B}, p, k)$ 
17:     $(\mathcal{A}, \mathcal{B}) = (A - (h+1)B, A - (h-1)B)$   $\triangleright$  or  $(\mathcal{A}, \mathcal{B}) = (A - i(h+1)B, A - i(h-1)B)$ 
18:     $[U_R^{(m-k)}, U_L^{(m-k)}] = \mathbf{DEFLATE}(\mathcal{A}, \mathcal{B}, p, m-k)$ 
19:
     $(A_{11}, B_{11}) = \left( (U_L^{(k)})^H A U_R^{(k)}, (U_L^{(k)})^H B U_R^{(k)} \right)$ 
     $(A_{22}, B_{22}) = \left( (U_L^{(m-k)})^H A U_R^{(m-k)}, (U_L^{(m-k)})^H B U_R^{(m-k)} \right)$ 
20:     $g_R = \{z \in g : \operatorname{Re}(z) > h\}$   $\triangleright$  or  $g_R = \{z \in g : \operatorname{Im}(z) > h\}$ 
21:     $[\widehat{T}, \widehat{D}_1, \widehat{D}_2] = \mathbf{EIG}(n, A_{11}, B_{11}, \frac{4}{5}\epsilon, \alpha, g_R, \frac{1}{3}\beta, \theta)$ 
22:     $g_L = \{z \in g : \operatorname{Re}(z) < h\}$   $\triangleright$  or  $g_L = \{z \in g : \operatorname{Im}(z) < h\}$ 
23:     $[\widetilde{T}, \widetilde{D}_1, \widetilde{D}_2] = \mathbf{EIG}(n, A_{22}, B_{22}, \frac{4}{5}\epsilon, \alpha, g_L, \frac{1}{3}\beta, \theta)$ 
24:
    
$$T = \begin{pmatrix} U_R^{(k)} & U_R^{(m-k)} \end{pmatrix} \begin{pmatrix} \widehat{T} & 0 \\ 0 & \widetilde{T} \end{pmatrix}$$


$$D_1 = \begin{pmatrix} \widehat{D}_1 & 0 \\ 0 & \widetilde{D}_1 \end{pmatrix}$$


$$D_2 = \begin{pmatrix} \widehat{D}_2 & 0 \\ 0 & \widetilde{D}_2 \end{pmatrix}$$

25:  end if
26: end if
27: return  $T, D_1, D_2$ 
```

3. Lines 8-15 execute a search over g for a grid line that sufficiently splits the spectrum, which in our case means separating at least a fifth of the eigenvalues on each side. Since g shatters $\Lambda_\epsilon(A, B)$, a grid line that sufficiently splits the spectrum always exists.
4. We check a line $\text{Re}(z) = h$ of the grid by applying the Möbius transformation $S(z) = \frac{z-(h-1)}{z-(h+1)}$ to (A, B) (line 9). S maps the grid line to the unit circle while sending the half plane $\{\text{Re}(z) < h\}$ inside the unit disk. Applying this transformation to (A, B) sends eigenvalues to the left/right of the dividing line inside/outside the unit circle, respectively, without changing eigenvectors.
5. Lines 10 and 11 apply **IRS** and **GRURV** to the transformed pencil $(\mathcal{A}, \mathcal{B})$. This produces a rank-revealing factorization $UR_1^{-1}R_2V$ of the approximate projector onto the right deflating subspace corresponding to eigenvectors of $(\mathcal{A}, \mathcal{B})$ with eigenvalues outside the unit disk (equivalently eigenvectors of (A, B) with eigenvalues to the right of the selected grid line).
6. In line 12, we leverage the rank-revealing guarantees of **RURV**, and by extension **GRURV**, to read off the rank of the approximate projector. Note that we do this without forming $R_1^{-1}R_2$. The grid line is selected if this rank is between $\frac{1}{5}m$ and $\frac{4}{5}m$, where m is the size of the pencil (which shrinks as we recur).
7. In line 8 we assume that the grid line is vertical, however it is possible that only a horizontal grid line sufficiently splits the spectrum. This is covered in line 14. The remainder of the algorithm similarly assumes the split is vertical, though we note in lines 17, 20, and 22 the adjustments that need to be made if we split by $\text{Im}(z) = h$ instead of $\text{Re}(z) = h$.
8. Once a dividing line is identified, we call **DEFLATE** twice to compute orthonormal bases for both sets of spectral projectors. To recover eigenvectors corresponding to eigenvalues to the left of the line, we apply the alternative Möbius transformation $S(z) = \frac{z-(h+1)}{z-(h-1)}$.
9. In line 19 we compute the next pair of subproblems. We then pass these to **EIG** along with pieces of the grid g and slightly adjusted parameters. In particular, note that the ϵ for which $\Lambda_\epsilon(A, B)$ is shattered shrinks by a factor of $\frac{4}{5}$ at each step. As we will see, this is necessary to guarantee shattering since $U_R^{(k)}$, $U_L^{(k)}$, $U_R^{(m-k)}$ and $U_L^{(m-k)}$ are only approximations of the matrices used in [Lemma 4.1](#).
10. Once the recursion finishes, **EIG** reconstructs a diagonal pencil (D_1, D_2) and a set of approximate right eigenvectors T (line 24).

With this outline in mind, we are now ready to state and prove our main guarantee for **EIG**.

Theorem 4.8. *Let (A, B) and g be a pencil and grid satisfying the requirements of **EIG**. Then for any choice of $\theta \in (0, 1)$ and $\beta > 0$, exact-arithmetic **EIG** applied to (A, B) and g satisfies the following with probability at least $1 - \theta$.*

1. *The recursive procedure converges and each eigenvalue of the diagonal pencil (D_1, D_2) shares a grid box with a unique eigenvalue of (A, B) .*
2. *If $\sigma_n(B) \geq 1$, each column t_i of T satisfies $\|t_i - v_i\|_2 \leq \beta$ for some right unit eigenvector v_i of (A, B) .*

Proof. We start by bounding the probability that the first guarantee does not hold. Since **EIG** calls itself recursively, we do this by bounding the probability of failure for one step of divide-and-conquer. In this context, success requires two events: first, a dividing line that sufficiently splits the spectrum must be found; second, the subsequent calls to **EIG** must be valid, meaning the inputs satisfy the listed properties.

Computing the probabilities that these occur is fairly lengthy, so to improve readability we number the steps in the proof and provide in bold a description of what each step accomplishes. Throughout, we use the assumptions on the inputs – i.e., $A, B \in \mathbb{C}^{m \times m}$ with $m \leq n$, $\|A\|_2 \leq 3$, $\|B\|_2 \leq 3n^\alpha$, and $\Lambda_\epsilon(A, B)$ is shattered with respect to the grid g , which is $s_1 \times s_2$ consisting of boxes of size ω .

1. Any transformed pencil $(\mathcal{A}, \mathcal{B})$ in **EIG satisfies $d_{(\mathcal{A}, \mathcal{B})} \geq \frac{2}{5}\epsilon$.**

Consider first a vertical grid line $\text{Re}(z) = h$ and $(\mathcal{A}, \mathcal{B}) = (A - (h-1)B, A - (h+1)B)$ as in line 9. Suppose $z \in \Lambda_{\epsilon'}(\mathcal{A}, \mathcal{B})$ for some $\epsilon' > 0$. In this case, there exist matrices E and F with $\|E\|_2, \|F\|_2 \leq \epsilon'$ such that z is an eigenvalue of $(\mathcal{A} + E, \mathcal{B} + F)$. If we apply the Möbius transformation $S(z) = \frac{(h+1)z - (h-1)}{z-1}$ to this pencil, we observe that $S(z)$ is an eigenvalue of

$$((h+1)(\mathcal{A} + E) - (h-1)(\mathcal{B} + F), (\mathcal{A} + E) - (\mathcal{B} + F)), \quad (4.3.1)$$

or, equivalently,

$$(2A + (h+1)E - (h-1)F, 2B + E - F). \quad (4.3.2)$$

Dividing by two, we conclude that $S(z)$ is an eigenvalue of $(A + \frac{h+1}{2}E - \frac{h-1}{2}F, B + \frac{1}{2}E - \frac{1}{2}F)$, where

$$\left\| \frac{h+1}{2}E - \frac{h-1}{2}F \right\|_2 \leq \frac{|h+1|}{2}\|E\|_2 + \frac{|h-1|}{2}\|F\|_2 \leq \frac{\epsilon'}{2}(|h+1| + |h-1|) \quad (4.3.3)$$

and

$$\left\| \frac{1}{2}E - \frac{1}{2}F \right\|_2 \leq \frac{1}{2}(\|E\|_2 + \|F\|_2) \leq \epsilon'. \quad (4.3.4)$$

Thus, $S(z)$ belongs to $\Lambda_{\epsilon''}(A, B)$ for

$$\epsilon'' = \max \left\{ \epsilon', \frac{\epsilon'}{2}(|h+1| + |h-1|) \right\} \leq 5\epsilon', \quad (4.3.5)$$

which means the preimage of $\Lambda_{\epsilon/5}(A, B)$ under S^{-1} is contained in $\Lambda_{\epsilon}(A, B)$. Since $\Lambda_{\epsilon}(A, B)$ is shattered with respect to g and therefore does not intersect the dividing line $\text{Re}(z) = h$, we conclude that $\Lambda_{\epsilon/5}(\mathcal{A}, \mathcal{B})$ does not intersect the unit circle. By [Definition 4.2](#), we obtain $d_{(\mathcal{A}, \mathcal{B})} \geq \frac{2}{5}\epsilon$. Making a similar argument for the transformed pencil in line 17 or in the case of a horizontal dividing line $\text{Im}(z) = h$ yields $d_{(\mathcal{A}, \mathcal{B})} \geq \frac{2}{5}\epsilon$ for any $(\mathcal{A}, \mathcal{B})$ appearing in **EIG**. In the next step, we will use this lower bound to control the error in repeated squaring.

2. The choice of p guarantees that the error in repeated squaring is at most δ .

Consider the first call to **IRS**, which applies repeated squaring to the transformed pencil $(\mathcal{A}, \mathcal{B})$. By [Theorem 4.3](#), we know that as long as $p \geq \log_2 \left[\frac{\|(\mathcal{A}, \mathcal{B})\|_2 - d_{(\mathcal{A}, \mathcal{B})}}{d_{(\mathcal{A}, \mathcal{B})}} \right]$ then

$$\|(A_p + B_p)^{-1}A_p - P_{R, |z|>1}\|_2 \leq \|P_{R, |z|>1}\|_2 \frac{2^{p+3} \left(1 - \frac{d_{(\mathcal{A}, \mathcal{B})}}{\|(\mathcal{A}, \mathcal{B})\|_2}\right)^{2p}}{\max \left\{ 0, 1 - 2^{p+2} \left(1 - \frac{d_{(\mathcal{A}, \mathcal{B})}}{\|(\mathcal{A}, \mathcal{B})\|_2}\right)^{2p} \right\}}. \quad (4.3.6)$$

We just showed $d_{(\mathcal{A}, \mathcal{B})} \geq \frac{2}{5}\epsilon$ and

$$\|(\mathcal{A}, \mathcal{B})\|_2 \leq \|\mathcal{A}\|_2 + \|\mathcal{B}\|_2 \leq 2\|A\|_2 + (|h-1| + |h+1|)\|B\|_2 \leq 42n^\alpha, \quad (4.3.7)$$

so to satisfy $p \geq \log_2 \left[\frac{\|(\mathcal{A}, \mathcal{B})\|_2 - d_{(\mathcal{A}, \mathcal{B})}}{d_{(\mathcal{A}, \mathcal{B})}} \right]$ it is sufficient to take $p \geq \log_2 \left(\frac{105n^\alpha}{\epsilon} - 1 \right)$. Similarly, to eliminate the maximum from the denominator of (4.3.6) it is sufficient to take $p \geq -2 \log_2 \left(\log_2 \left(\frac{105n^\alpha}{105n^\alpha - \epsilon} \right) \right)$ provided $p > 6$ (which allows us to simplify the bounds by assuming $\log_2(p+2) < \frac{1}{2}p$).

With this, we can now turn to bounding the right hand side of (4.3.6). First, we upper bound $\|P_{R, |z|>1}\|_2$. Recall,

$$P_{R, |z|>1} = V \begin{pmatrix} 0 & 0 \\ 0 & I_r \end{pmatrix} V^{-1} = \sum_{j=m-r+1}^m v_j w_j^H \quad (4.3.8)$$

for $r = \text{rank}(P_{R, |z|>1})$ and V a matrix that diagonalizes $B^{-1}A$. v_i and w_i^H are the columns of V and rows of V^{-1} respectively, scaled so that $w_i^H v_i = 1$ with v_{m-r+1}, \dots, v_m corresponding to eigenvalues

of (A, B) to the right of $\text{Re}(z) = h$. Since $\Lambda_\epsilon(A, B)$ is shattered with respect to g , each of these eigenvalues $\lambda_{m-r+1}, \dots, \lambda_m$ is contained in a separate grid box of g . If Γ_i is the contour of the grid box containing λ_i , this means

$$v_j w_j^H = \frac{1}{2\pi i} \oint_{\Gamma_j} (z - B^{-1}A)^{-1} dz \quad (4.3.9)$$

and therefore

$$P_{R, |z|>1} = \frac{1}{2\pi i} \sum_{j=m-r+1}^m \oint_{\Gamma_j} (z - B^{-1}A)^{-1} dz = \frac{1}{2\pi i} \sum_{j=m-r+1}^m \oint_{\Gamma_j} (zB - A)^{-1} B dz. \quad (4.3.10)$$

Thus, by the triangle inequality,

$$\|P_{R, |z|>1}\|_2 \leq \frac{1}{2\pi} \sum_{j=m-r+1}^m \left\| \oint_{\Gamma_j} (zB - A)^{-1} B dz \right\|_2. \quad (4.3.11)$$

Moreover, applying the ML inequality to each term in this sum, we have

$$\|P_{R, |z|>1}\|_2 \leq \frac{1}{2\pi} \sum_{j=m-r+1}^m 4\omega \sup_{z \in \Gamma_j} \|(zB - A)^{-1} B\|_2 \leq \frac{2\omega \|B\|_2}{\pi} \sum_{j=m-r+1}^m \sup_{z \in \Gamma_j} \|(A - zB)^{-1}\|_2. \quad (4.3.12)$$

Since shattering guarantees $\Lambda_\epsilon(A, B) \cap \Gamma_j = \emptyset$ and therefore $\|(A - zB)^{-1}\|_2 \leq \frac{1}{\epsilon(1+|z|)} \leq \frac{1}{\epsilon}$ for all $z \in \Gamma_j$, we conclude $\|P_{R, |z|>1}\|_2 \leq \frac{2\omega r \|B\|_2}{\pi \epsilon}$. Finally using the fact that $\|B\|_2 \leq 3n^\alpha$ and $r \leq m$, we have a final upper bound $\|P_{R, |z|>1}\|_2 \leq \frac{6n^\alpha m \omega}{\pi \epsilon}$.

Combining this bound with $d_{(\mathcal{A}, \mathcal{B})} \geq \frac{2}{5}\epsilon$ and $\|(\mathcal{A}, \mathcal{B})\|_2 \leq 42n^\alpha$, (4.3.6) becomes

$$\|(A_p + B_p)^{-1} A_p - P_{R, |z|>1}\|_2 \leq \frac{6n^\alpha m \omega}{\pi \epsilon} \cdot \frac{2^{p+3} \left(1 - \frac{\epsilon}{105n^\alpha}\right)^{2^p}}{1 - 2^{p+2} \left(1 - \frac{\epsilon}{105n^\alpha}\right)^{2^p}} \quad (4.3.13)$$

for p sufficiently large (i.e., following the bounds derived above). Thus, we obtain $\|(A_p + B_p)^{-1} A_p - P_{R, |z|>1}\|_2 \leq \delta$ by taking

$$\frac{6n^\alpha m \omega}{\pi \epsilon} \cdot \frac{2^{p+3} \left(1 - \frac{\epsilon}{105n^\alpha}\right)^{2^p}}{1 - 2^{p+2} \left(1 - \frac{\epsilon}{105n^\alpha}\right)^{2^p}} \leq \delta \quad (4.3.14)$$

which is equivalent to

$$2^p \left[\frac{p+2}{2^p} + \log_2 \left(1 - \frac{\epsilon}{105n^\alpha}\right) \right] \leq \log_2 \left(\frac{\delta \pi \epsilon}{12n^\alpha m \omega + \delta \pi \epsilon} \right). \quad (4.3.15)$$

Using again the assumption that $p > 6$ and further taking $p \geq -2 \log_2 \left(-\frac{1}{2} \log_2 \left(1 - \frac{\epsilon}{105n^\alpha}\right)\right)$ to ensure $\frac{p+2}{2^p} \leq -\frac{1}{2} \log_2 \left(1 - \frac{\epsilon}{105n^\alpha}\right)$, we get the desired accuracy as long as

$$2^{p-1} \log_2 \left(1 - \frac{\epsilon}{105n^\alpha}\right) \leq \log_2 \left(\frac{\delta \pi \epsilon}{12n^\alpha m \omega + \delta \pi \epsilon} \right) \quad (4.3.16)$$

which yields a final bound $p \geq 1 + \log_2 \left[\log_2 \left(\frac{\delta \pi \epsilon}{12n^\alpha m \omega + \delta \pi \epsilon} \right) / \log_2 \left(1 - \frac{\epsilon}{105n^\alpha}\right) \right]$.

In the preceding analysis, we derived the following four bounds on p :

- $p \geq \log_2 \left(\frac{105n^\alpha}{\epsilon} - 1 \right)$ [to allow us to apply [Theorem 4.3](#)].
- $p \geq -2 \log_2 \left(\log_2 \left(\frac{105n^\alpha}{105n^\alpha - \epsilon} \right) \right)$ [to eliminate the maximum from the error bound].
- $p \geq -2 \log_2 \left(-\frac{1}{2} \log_2 \left(1 - \frac{\epsilon}{105n^\alpha}\right) \right)$ [to simplify the upper bound in (4.3.6)].

- $p \geq 1 + \log_2 \left[\log_2 \left(\frac{\delta \pi \epsilon}{12n^\alpha m \omega + \delta \pi \epsilon} \right) / \log_2 \left(1 - \frac{\epsilon}{105n^\alpha} \right) \right]$ [to ensure an error of at most δ given the other three bounds].

Since the third bound is always at least as large as the second and since we also assumed $p > 6$, we conclude that $\|(A_p + B_p)^{-1}A_p - P_{R,|z|>1}\|_2 \leq \delta$ for the p chosen in line 7 of **EIG**. Note that since $\|\mathcal{A}^H\|_2 = \|\mathcal{A}\|_2$, $\|\mathcal{B}^H\|_2 = \|\mathcal{B}\|_2$, $d_{(\mathcal{A}^H, \mathcal{B}^H)} = d_{(\mathcal{A}, \mathcal{B})}$, and $\Lambda_\epsilon(A^H, B^H)$ is shattered with respect to the grid $g^H = \{\bar{z} : z \in g\}$, the same argument guarantees that running repeated squaring on \mathcal{A}^H , and \mathcal{B}^H has error at most δ . Similarly, the same results hold for the other transformed pencils in lines 14 and 17 since in all cases $\|(\mathcal{A}, \mathcal{B})\|_2 \leq 42n^\alpha$ and $d_{(\mathcal{A}, \mathcal{B})} \geq \frac{2}{5}\epsilon$.

3. A dividing line that sufficiently splits the spectrum exists.

A dividing line sufficiently splits the spectrum if it separates at least $\frac{1}{5}m$ of the m eigenvalues of (A, B) . Suppose that no vertical line of g does this. In this case, there exists adjacent vertical lines between which more than $\frac{3}{5}m$ eigenvalues lie. Since no eigenvalues share the same grid box, this implies that a horizontal grid line must sufficiently split the spectrum.

4. With probability at least $1 - \frac{\theta}{10n^4}$, **EIG** finds a dividing line that separates exactly k eigenvalues to the right such that $\frac{1}{5}m \leq k \leq \frac{4}{5}m$.

To obtain a lower bound on this probability, we first compute the probability that for any grid line $\text{Re}(z) = h$ the value of k at line 12 is equal to the number of eigenvalues of (A, B) to the right of the line.

Suppose (A, B) has r eigenvalues to the right of $\text{Re}(z) = h$. In this case, we know in line 10 that $(A_p + B_p)^{-1}A_p$ approaches a rank- r projector $P_{R,|z|>1}$. Now k is obtained by computing a rank-revealing factorization $U_R R_1^{-1} R_2 V = (A_p + B_p)^{-1}A_p$ via **GRURV** and then counting the diagonal entries of $R_1^{-1}R_2$ that have modulus above a certain threshold. With this in mind, write

$$R_1^{-1}R_2 = \begin{bmatrix} R_{11} & R_{12} \\ 0 & R_{22} \end{bmatrix} \quad (4.3.17)$$

for R_{11} an $r \times r$ matrix. Since we are working in exact arithmetic, **GRURV** satisfies all of the guarantees of exact-arithmetic **RURV**. In particular, extending [17, Theorem 5.2] to complex matrices,

$$\sigma_r(R_{11}) \geq \sigma_r((A_p + B_p)^{-1}A_p) \sigma_r(X_{11}) \quad (4.3.18)$$

where X_{11} is the upper left $r \times r$ block of $X = Q^H V^H$ for the SVD $(A_p + B_p)^{-1}A_p = P \Sigma Q^H$. Similarly, by [7, Lemma 4.1],

$$\|R_{22}\|_2 \leq \frac{\sigma_{r+1}((A_p + B_p)^{-1}A_p)}{\sigma_r(X_{11})}. \quad (4.3.19)$$

Now $\|(A_p + B_p)^{-1}A_p - P_{R,|z|>1}\|_2 \leq \delta$ as shown in step two above, so since the rank- r projector $P_{R,|z|>1}$ satisfies $\sigma_r(P_{R,|z|>1}) = 1$ and $\sigma_{r+1}(P_{R,|z|>1}) = 0$, we have by the stability of singular values $\sigma_r((A_p + B_p)^{-1}A_p) \geq 1 - \delta$ and $\sigma_{r+1}((A_p + B_p)^{-1}A_p) \leq \delta$. Moreover, since X is Haar unitary, we have by [9, Proposition C.3]

$$\mathbb{P} \left[\frac{1}{\sigma_r(X_{11})} \leq \frac{\sqrt{r(m-r)}}{\nu} \right] \geq 1 - \nu^2 \quad (4.3.20)$$

for any $\nu \in (0, 1]$. Applying these to (4.3.18) and (4.3.19) with $\nu = \sqrt{\frac{\theta}{10\zeta}} \frac{1}{n^2}$ for $\zeta = 2(\lceil \log_2(s) \rceil + 1)$ and $s = \max\{s_1, s_2\}$, we have

$$\sigma_r(R_{11}) \geq (1 - \delta) \sqrt{\frac{\theta}{10\zeta}} \frac{1}{n^2 \sqrt{r(m-r)}} \geq \sqrt{\frac{\theta}{10\zeta}} \frac{1 - \delta}{n^3} \quad (4.3.21)$$

and

$$\|R_{22}\|_2 \leq \delta \sqrt{r(m-r)} n^2 \sqrt{\frac{10\zeta}{\theta}} \leq \delta n^3 \sqrt{\frac{10\zeta}{\theta}} \quad (4.3.22)$$

with probability at least $1 - \frac{\theta}{10\zeta n^4}$. Since the eigenvalues of any matrix are bounded in modulus above and below by its singular values and the eigenvalues of R_{11} and R_{22} are their diagonal entries, we conclude $|R_{11}(i, i)| \geq \sqrt{\frac{\theta}{10\zeta} \frac{1-\delta}{n^3}}$ for all $1 \leq i \leq r$ while $|R_{22}(j, j)| \leq \delta n^3 \sqrt{\frac{10\zeta}{\theta}}$ for all $1 \leq j \leq m - r$ with probability at least $1 - \frac{\theta}{10\zeta n^4}$. Since the requirement in line 6 that $\delta \leq \frac{\theta}{2(\theta + 10n^6\zeta)}$ guarantees $\sqrt{\frac{\theta}{10\zeta} \frac{1-\delta}{n^3}} > \delta n^3 \sqrt{\frac{10\zeta}{\theta}}$, this implies that $k = r$ with probability at least $1 - \frac{\theta}{10\zeta n^4}$.

We have shown so far that with high probability the value of k at line 12 is equal to the number of eigenvalues to the right of the vertical dividing line selected four lines earlier. Since repeating this argument yields the same probability of success when checking a horizontal grid line and we know a dividing line that separates at least $\frac{1}{5}m$ eigenvalues must exist, we can therefore lower bound the probability that **FIG** finds a suitable line by requiring that the value of k is accurate for all lines that are checked. Since we do at most two binary searches to find a good enough grid line, we check at most ζ lines. By a union bound, we conclude that a suitable line is found, and k is computed accurately for that line, with probability at least $1 - \frac{\theta}{10n^4}$.

5. **Assuming k is computed correctly in line 12, there exists matrices $\widehat{U}_R^{(k)}, \widehat{U}_L^{(k)} \in \mathbb{C}^{k \times m}$ and $\widehat{U}_R^{(m-k)}, \widehat{U}_L^{(m-k)} \in \mathbb{C}^{(m-k) \times m}$ with orthonormal columns spanning corresponding right and left deflating subspaces of (A, B) such that**

- (a) $\|U_R^{(k)} - \widehat{U}_R^{(k)}\|_2 \leq \sqrt{\sqrt{\frac{10}{\theta}} 8n^3 \delta}$
- (b) $\|U_L^{(k)} - \widehat{U}_L^{(k)}\|_2 \leq \sqrt{\sqrt{\frac{10}{\theta}} 8n^3 \delta}$
- (c) $\|U_R^{(m-k)} - \widehat{U}_R^{(m-k)}\|_2 \leq \sqrt{\sqrt{\frac{10}{\theta}} 8n^3 \delta}$
- (d) $\|U_L^{(m-k)} - \widehat{U}_L^{(m-k)}\|_2 \leq \sqrt{\sqrt{\frac{10}{\theta}} 8n^3 \delta}$

With probability at least $1 - \frac{2\theta}{5n^4}$.

This result comes from applying [Theorem 4.7](#) twice with $\nu = \sqrt{\frac{\theta}{10n^4}}$ and taking a union bound. In both cases, we use the fact that p is large enough to guarantee error in repeated squaring is at most δ and consequently

$$\sqrt{8\sqrt{k(m-k)}} \sqrt{\frac{\delta}{\nu}} \leq \sqrt{8n\sqrt{\frac{10n^4}{\theta}} \delta} = \sqrt{\sqrt{\frac{10}{\theta}} 8n^3 \delta}. \quad (4.3.23)$$

6. **Union bound on events that guarantee success for one step.**

Let E_a, E_b, E_c , and E_d be events that correspond to the results (a), (b), (c), and (d) from step 5 and let E_k be the event that a sufficient dividing line is found and k computed accurately. We have just shown

$$\mathbb{P}(E_a \cap E_b \cap E_c \cap E_d \mid E_k) \geq 1 - \frac{2\theta}{5n^4}. \quad (4.3.24)$$

Since we also know $\mathbb{P}(E_k) \geq 1 - \frac{\theta}{10n^4}$, we conclude

$$\begin{aligned} \mathbb{P}(E_a \cap E_b \cap E_c \cap E_d \cap E_k) &= \mathbb{P}(E_a \cap E_b \cap E_c \cap E_d \mid E_k) \mathbb{P}(E_k) \\ &\geq \left(1 - \frac{2\theta}{5n^4}\right) \left(1 - \frac{\theta}{10n^4}\right) \\ &\geq 1 - \frac{\theta}{2n^4}. \end{aligned} \quad (4.3.25)$$

In the remainder of the proof, we will show that conditioning on these events guarantees success for one step of **FIG**.

7. If E_a, E_b, E_c , and E_d hold, then $\Lambda_{4\epsilon/5}(A_{11}, B_{11})$ and $\Lambda_{4\epsilon/5}(A_{22}, B_{22})$ are both shattered with respect to g .

Let $\widehat{U}_R^{(k)}, \widehat{U}_L^{(k)}, \widehat{U}_R^{(m-k)},$ and $\widehat{U}_L^{(m-k)}$ be the matrices such that $\|U_R^{(k)} - \widehat{U}_R^{(k)}\|_2, \|U_L^{(k)} - \widehat{U}_L^{(k)}\|_2,$
 $\|U_R^{(m-k)} - \widehat{U}_R^{(m-k)}\|_2,$ and $\|U_L^{(m-k)} - \widehat{U}_L^{(m-k)}\|_2$ are all bounded above by $\sqrt{\sqrt{\frac{10}{\theta}} 8n^3 \delta}$ as in step

five. Since $\delta \leq \sqrt{\frac{\theta}{10}} \frac{\epsilon^2}{7200n^{2\alpha+3}}$, we can replace this upper bound with $\frac{\epsilon}{30n^\alpha}$. With this in mind, let

$$\begin{aligned} (\widehat{A}_{11}, \widehat{B}_{11}) &= \left((\widehat{U}_L^{(k)})^H A \widehat{U}_R^{(k)}, (\widehat{U}_L^{(k)})^H B \widehat{U}_R^{(k)} \right) \\ (\widehat{A}_{22}, \widehat{B}_{22}) &= \left((\widehat{U}_L^{(m-k)})^H A \widehat{U}_R^{(m-k)}, (\widehat{U}_L^{(m-k)})^H B \widehat{U}_R^{(m-k)} \right). \end{aligned} \quad (4.3.26)$$

Note that by Lemma 4.1, $\Lambda_\epsilon(\widehat{A}_{11}, \widehat{B}_{11})$ and $\Lambda_\epsilon(\widehat{A}_{22}, \widehat{B}_{22})$ are both contained in $\Lambda_\epsilon(A, B)$ and therefore shattered with respect to g . At the same time,

$$\begin{aligned} \|A_{11} - \widehat{A}_{11}\|_2 &= \|(U_L^{(k)})^H A U_R^{(k)} - (\widehat{U}_L^{(k)})^H A \widehat{U}_R^{(k)}\|_2 \\ &= \|(U_L^{(k)})^H A U_R^{(k)} - (\widehat{U}_L^{(k)})^H A U_R^{(k)} + (\widehat{U}_L^{(k)})^H A U_R^{(k)} - (\widehat{U}_L^{(k)})^H A \widehat{U}_R^{(k)}\|_2 \\ &\leq \|(U_L^{(k)} - \widehat{U}_L^{(k)})^H A U_R^{(k)}\|_2 + \|(\widehat{U}_L^{(k)})^H A (U_R^{(k)} - \widehat{U}_R^{(k)})\|_2 \\ &\leq \|U_L^{(k)} - \widehat{U}_L^{(k)}\|_2 \|A\|_2 + \|A\|_2 \|U_R^{(k)} - \widehat{U}_R^{(k)}\|_2 \\ &\leq 6n^\alpha \frac{\epsilon}{30n^\alpha} \\ &= \frac{\epsilon}{5} \end{aligned} \quad (4.3.27)$$

and similarly $\|B_{11} - \widehat{B}_{11}\|_1 \leq \frac{\epsilon}{5}$. Thus, by Lemma 3.14, $\Lambda_{4\epsilon/5}(A_{11}, B_{11})$ is shattered with respect to g . Repeating this argument for (A_{22}, B_{22}) and $(\widehat{A}_{22}, \widehat{B}_{22})$, we conclude $\Lambda_{4\epsilon/5}(A_{22}, B_{22})$ is also shattered with respect to g .

In the preceding analysis, we showed that for one step of recursion in **FIG**, a sufficient dividing line is found, k is computed correctly, and $\Lambda_{4\epsilon/5}(A_{11}, B_{11})$ and $\Lambda_{4\epsilon/5}(A_{22}, B_{22})$ are both shattered with respect to g , and therefore also with respect to the half grids g_R and g_L , with probability at least $1 - \frac{\theta}{2n^4}$. Since multiplying by matrices with orthonormal columns will preserve the norm requirements, we conclude that the subsequent calls to **FIG** in lines 21 and 23 are valid when these events occur. Hence, each recursive step succeeds with probability at least $1 - \frac{\theta}{2n^4}$. Since the recursive tree of **FIG** has depth at most $\log_{5/4}(n)$ and each step calls **FIG** twice, a union bound implies that the first guarantee of **FIG** fails with probability at most

$$2 \cdot 2^{\log_{5/4}(n)} \frac{\theta}{2n^4} \leq 2n^4 \frac{\theta}{2n^4} = \theta. \quad (4.3.28)$$

We turn now to the second guarantee when $\sigma_n(B) \geq 1$. In this case, we will show that conditioning on the same events that ensure the first guarantee also imply the second. Since **FIG** builds the approximate eigenvectors recursively, we do this inductively.

The base case here corresponds to $m = 1$, in which case **FIG** gets the one right unit eigenvector ($v = 1$) exactly correct. Suppose now we are reconstructing the eigenvectors of (A', B') from the two sub-problems (A_{11}, B_{11}) and (A_{22}, B_{22}) it is split into. (A', B') here is any pencil obtained in the divide-and-conquer process.

Let \widehat{T} and \widetilde{T} be the invertible matrices obtained from applying **FIG** to (A_{11}, B_{11}) and (A_{22}, B_{22}) as in lines 21 and 23 of the algorithm. Since these calls to **FIG** pass the parameter $\frac{\beta}{3}$, we can assume each column of \widehat{T} or \widetilde{T} is at most $\frac{\beta}{3}$ away from a true unit right eigenvector of (A_{11}, B_{11}) or (A_{22}, B_{22}) . In addition, let

$$T = \begin{pmatrix} U_R^{(k)} & U_R^{(m-k)} \end{pmatrix} \begin{pmatrix} \widehat{T} & 0 \\ 0 & \widetilde{T} \end{pmatrix} \quad (4.3.29)$$

be the matrix of approximate eigenvectors of (A', B') computed in line 24. Finally let $\widehat{U}_R^{(k)}$ and $\widehat{U}_R^{(m-k)}$ be the true matrices approximated by $U_R^{(k)}$ and $U_R^{(m-k)}$, as in step 5 above.

Consider now a column t_i of T . It suffices to handle the case where $t_i = U_R^{(k)} \hat{t}_i$ for a column \hat{t}_i of \hat{T} , as the same argument applies exactly if $t_i = U_R^{(m-k)} \tilde{t}_i$ for \tilde{t}_i a column of \tilde{T} . By our induction hypothesis, we know there exists a true right unit eigenvector \hat{v}_i of (A_{11}, B_{11}) such that

$$\|\hat{t}_i - \hat{v}_i\|_2 \leq \frac{\beta}{3}. \quad (4.3.30)$$

Now let $(\hat{A}_{11}, \hat{B}_{11})$ be the true problem approximated by (A_{11}, B_{11}) . Conditioning on the same events used above, we know (following the same arguments as in steps 5 and 7)

$$\|A_{11} - \hat{A}_{11}\|_2, \|B_{11} - \hat{B}_{11}\|_2 \leq 6n^\alpha \|U_R^{(k)} - \hat{U}_R^{(k)}\|_2 \leq 6n^\alpha \sqrt{\frac{10}{\theta} 8n^3 \delta}, \quad (4.3.31)$$

which, applying the bound $\delta \leq \sqrt{\frac{\theta}{10} \frac{\eta^2}{288n^{2\alpha+3}}}$, becomes

$$\|A_{11} - \hat{A}_{11}\|_2, \|B_{11} - \hat{B}_{11}\|_2 \leq 6n^\alpha \sqrt{\frac{10}{\theta} 8n^3} \sqrt{\frac{\theta}{10} \frac{\eta^2}{288n^{2\alpha+3}}} = \eta. \quad (4.3.32)$$

Thus, by [Lemma 3.15](#), there exists a right unit eigenvector \bar{v}_i of $(\hat{A}_{11}, \hat{B}_{11})$ such that

$$\|\hat{v}_i - \bar{v}_i\|_2 \leq \frac{\sqrt{8}\omega}{\pi} \frac{\eta}{\epsilon(\epsilon - \eta)} (1 + \|\hat{B}_{11}^{-1} \hat{A}_{11}\|_2) \|\hat{B}_{11}\|_2. \quad (4.3.33)$$

To simplify this bound, we first observe that (again by the argument made in step 7 above) we can assume $\epsilon - \eta \geq \frac{4}{5}\epsilon$. In addition, $\|\hat{A}_{11}\|_2 \leq 3$ and $\|\hat{B}_{11}\|_2 \leq 3n^\alpha$. Finally, since $\sigma_n(B) \geq 1$ and any split of divide-and-conquer can decrease the smallest singular value by at most η (by the stability of singular values), and since the decision tree of **EIG** has depth at most $\log_{5/4}(n)$, the bound $\eta \leq \frac{1}{2 \log_{5/4}(n)}$ ensures

$$\sigma_n(\hat{B}_{11}) \geq 1 - \log_{5/4}(n)\eta \geq \frac{1}{2}. \quad (4.3.34)$$

Putting everything together, we have

$$\|\hat{v}_i - \bar{v}_i\|_2 \leq \frac{\sqrt{8}\omega}{\pi} \frac{\eta}{\frac{4}{5}\epsilon^2} \left(1 + \frac{\|\hat{A}_{11}\|_2}{\sigma_n(\hat{B}_{11})}\right) \|\hat{B}_{11}\|_2 \leq \frac{105\sqrt{8}\omega n^\alpha}{4\pi \epsilon^2} \eta \leq \frac{\beta}{3}. \quad (4.3.35)$$

since $\eta \leq \frac{4\pi}{315\sqrt{8}} \frac{\beta\epsilon^2}{\omega n^\alpha}$. Now let $v_i = \hat{U}_R^{(k)} \bar{v}_i$, which is a true right unit eigenvector of (A', B') . By construction, we have

$$\begin{aligned} \|t_i - v_i\|_2 &= \|U_R^{(k)} \hat{t}_i - \hat{U}_R^{(k)} \bar{v}_i\|_2 \\ &= \|U_R^{(k)} \hat{t}_i - U_R^{(k)} \hat{v}_i + U_R^{(k)} \hat{v}_i - \hat{U}_R^{(k)} \hat{v}_i + \hat{U}_R^{(k)} \hat{v}_i - \hat{U}_R^{(k)} \bar{v}_i\|_2 \\ &\leq \|U_R^{(k)} (\hat{t}_i - \hat{v}_i)\|_2 + \|(U_R^{(k)} - \hat{U}_R^{(k)}) \hat{v}_i\|_2 + \|\hat{U}_R^{(k)} (\hat{v}_i - \bar{v}_i)\|_2. \\ &\leq \|\hat{t}_i - \hat{v}_i\|_2 + \|U_R^{(k)} - \hat{U}_R^{(k)}\|_2 + \|\hat{v}_i - \bar{v}_i\|_2. \end{aligned} \quad (4.3.36)$$

Applying [\(4.3.30\)](#) and [\(4.3.35\)](#) to this and using the fact that $\|U_R^{(k)} - \hat{U}_R^{(k)}\|_2 \leq \frac{\beta}{3}$, we conclude

$$\|t_i - v_i\|_2 \leq \frac{\beta}{3} + \frac{\beta}{3} + \frac{\beta}{3} = \beta. \quad (4.3.37)$$

By induction, we obtain the same bound for the approximate and true eigenvectors of (A, B) . \square

The condition on the eigenvector guarantee in [Theorem 4.8](#) (i.e., that $\sigma_n(B) \geq 1$) may seem restrictive, but it reflects the use case in the following section. That is, while it is possible to adjust the parameters of **EIG** to allow for less strict lower bounds on $\sigma_n(B)$, we plan to apply **EIG** to the perturbed and scaled $(\tilde{A}, n^\alpha \tilde{B})$, where by construction $\sigma_n(n^\alpha \tilde{B}) \geq 1$ with high probability.

5 Randomized Pencil Diagonalization

We can now prove our main result, presented in the introduction as [Theorem 1.1](#). First, we state our algorithm for producing an approximate diagonalization and show it succeeds in exact arithmetic with high probability. We follow that with corresponding forward error guarantees and an evaluation of the complexity of the routine.

5.1 Diagonalization Routine

In the previous section, we constructed an eigensolver that produces approximations of the eigenvalues and eigenvectors of $(\tilde{A}, n^\alpha \tilde{B})$, contained in the outputs (D_1, D_2) and T respectively. Since the n^α scaling only changes eigenvalues and can be easily undone, this effectively yields eigenvalues/eigenvectors for (\tilde{A}, \tilde{B}) . That is, T contains approximate eigenvectors of (\tilde{A}, \tilde{B}) while the corresponding eigenvalues belong to $(n^\alpha D_1, D_2)$ or equivalently $(D_1, n^{-\alpha} D_2)$. This prompts the question: how accurate are these approximations?

Unfortunately, as noted earlier, little can be said. While perturbation results do exist for the simple eigenvalues of a regular pencil or for the eigenvalues of a regular pencil obtained by perturbing a diagonalizable one [[55](#), Theorems VI.2.2 and VI.2.6], these are typically stated in terms of a chordal metric on the Riemann sphere. Our version of Bauer-Fike ([Theorem 2.20](#)) provides a route to some Euclidean norm bounds, which we state below, but its dependence on the the smallest singular value of B means it is only useful if B is far from singular. This reflects a reality of our algorithm: **EIG** always produces a set of finite eigenvalues, and we cannot identify which ones are close to true finite eigenvalues of (A, B) and which ones are meant to be infinite.

Instead, we leverage **EIG** to produce an approximate diagonalization of (A, B) . Recall from [Section 2](#) that if B is invertible and T contains right eigenvectors of (A, B) then $S = BT$ produces a diagonalization of the pencil such that $S^{-1}AT = D_1$ and $S^{-1}BT = I$. Using again the fact that \tilde{B} is invertible almost surely, we conclude that if T is the output of **EIG** then it and $\tilde{B}T$ should approximately diagonalize (\tilde{A}, \tilde{B}) . Assuming $\|A - \tilde{A}\|_2$ and $\|B - \tilde{B}\|_2$ are small, this produces an approximate diagonalization of (A, B) . We state **RPD**, a routine that wraps around **EIG** to produce this diagonalization, as [Algorithm 6](#) below.

Algorithm 6 Randomized Pencil Diagonalization (**RPD**)

Input: $A, B \in \mathbb{C}^{n \times n}$ and $\varepsilon < 1$ a desired accuracy.

Requires: $\|A\|_2, \|B\|_2 \leq 1$

Output: Nonsingular S, T and diagonal D such that $\|A - SDT^{-1}\|_2, \|B - ST^{-1}\|_2 \leq \varepsilon$ with high probability.

- 1: $\gamma = \frac{\varepsilon}{16}$
 - 2: $\alpha = \frac{\lceil 2 \log_n(1/\gamma) + 3 \rceil}{2}$
 - 3: $\epsilon = \gamma^5 / (64n^{\frac{11\alpha+25}{3}} + \gamma^5)$
 - 4: $\beta = \frac{\varepsilon \gamma^2}{24(1+4\gamma)} n^{-3\alpha-5}$
 - 5: $\omega = \frac{\gamma^4}{4} n^{-\frac{8\alpha+13}{3}}$
 - 6: Draw two independent Ginibre matrices $G_1, G_2 \in \mathbb{C}^{n \times n}$
 - 7: $(\tilde{A}, \tilde{B}) = (A + \gamma G_1, B + \gamma G_2)$
 - 8: Draw z uniformly from the box of side length ω cornered at $-4 - 4i$
 - 9: $g = \text{grid}(z, \omega, \lceil 8/\omega \rceil, \lceil 8/\omega \rceil)$
 - 10: $[T, D_1, D_2] = \mathbf{EIG}(n, \tilde{A}, n^\alpha \tilde{B}, \epsilon, \alpha, g, \beta, 1/n)$
 - 11: **for** $i = 1 : n$ **do**
 - 12: $D(i, i) = n^\alpha \frac{D_1(i, i)}{D_2(i, i)}$
 - 13: **end for**
 - 14: $S = \tilde{B}T$
 - 15: **return** S, T, D
-

Note that the assumption $\|A\|_2, \|B\|_2 \leq 1$ is essentially made for convenience; we can obtain a diagonalization of any pencil (A, B) via **RPD** by first normalizing the matrices accordingly. In [Theorem 5.1](#), we show that **RPD** produces an approximate diagonalization with the given accuracy in exact arithmetic, thereby

proving the bulk of our main result, [Theorem 1.1](#). For reference, [Figure 4](#) provides a high level overview of **RPD**, including the details of its call to **EIG**.

Theorem 5.1. *For any $A, B \in \mathbb{C}^{n \times n}$ with $\|A\|_2, \|B\|_2 \leq 1$, the outputs of exact-arithmetic **RPD** satisfy*

$$\|A - SDT^{-1}\|_2, \|B - ST^{-1}\|_2 \leq \varepsilon$$

with probability at least

$$\left[1 - \frac{82}{n} - \frac{531441}{16n^2}\right] \left[1 - \frac{1}{n} - 4e^{-n}\right] \left[1 - \frac{1}{n}\right].$$

Proof. Consider the perturbed and scaled pencil $(\tilde{A}, n^\alpha \tilde{B})$. By [Theorem 3.12](#) and its proof, with probability at least $\left(1 - \frac{82}{n} - \frac{531441}{16n^2}\right) \left(1 - \frac{n^{2-2\alpha}}{\gamma^2} - 4e^{-n}\right)$ we have the following:

1. $\|G_1\|_2, \|G_2\|_2 \leq 4$,
2. $\|\tilde{A}\|_2 \leq 3$,
3. $\|n^\alpha \tilde{B}\|_2 \leq 3n^\alpha$,
4. $\sigma_n(n^\alpha \tilde{B}) \geq 1$,
5. $\Lambda(\tilde{A}, n^\alpha \tilde{B}) \subseteq B_3(0)$,
6. $\kappa_V(n^{-\alpha} \tilde{B}^{-1} \tilde{A}) \leq \frac{n^{\alpha+2}}{\gamma}$,
7. $\Lambda_\epsilon(\tilde{A}, n^\alpha \tilde{B})$ is shattered with respect to the grid g (for ϵ as in line 3).

Conditioning on these events, we observe that 2, 3, and 7 ensure that the call to **EIG** in line 10 is valid, meaning with probability at least $1 - \frac{1}{n}$ we can add the guarantees of [Theorem 4.8](#) to our list:

8. Each eigenvalue of (D_1, D_2) shares a grid box of g with a true eigenvalue of $(\tilde{A}, n^\alpha \tilde{B})$.
9. Since $\sigma_n(n^\alpha \tilde{B}) \geq 1$ (item 4) each column t_i of T satisfies $\|t_i - v_i\|_2 \leq \beta$ for v_i a true unit right eigenvector of $(\tilde{A}, n^\alpha \tilde{B})$.

By the definition of conditional probability, all nine of these events occur simultaneously with probability at least

$$\left[1 - \frac{82}{n} - \frac{531441}{16n^2}\right] \left[1 - \frac{n^{2-2\alpha}}{\gamma^2} - 4e^{-n}\right] \left[1 - \frac{1}{n}\right]. \quad (5.1.1)$$

Since the choice of α in line 2 guarantees

$$\frac{n^{2-2\alpha}}{\gamma^2} \leq \frac{1}{n} \quad (5.1.2)$$

(5.1.1) can be bounded from below by

$$\left[1 - \frac{82}{n} - \frac{531441}{16n^2}\right] \left[1 - \frac{1}{n} - 4e^{-n}\right] \left[1 - \frac{1}{n}\right]. \quad (5.1.3)$$

To complete the proof we show that the nine items listed above guarantee both $\|A - SDT^{-1}\|_2 \leq \varepsilon$ and $\|B - ST^{-1}\|_2 \leq \varepsilon$. The second of these is trivial: since $\gamma = \frac{\varepsilon}{16}$ and $ST^{-1} = \tilde{B}$ we have

$$\|B - ST^{-1}\|_2 = \|B - \tilde{B}\|_2 = \|\gamma G_2\|_2 \leq 4\gamma = \frac{\varepsilon}{4} < \varepsilon. \quad (5.1.4)$$

To show the same for A and SDT^{-1} we use the following key fact. Let V be the matrix whose columns contain, in order, the true right unit eigenvectors of $(\tilde{A}, n^\alpha \tilde{B})$ guaranteed by item 9. Since \tilde{B} is invertible with probability one and (\tilde{A}, \tilde{B}) and $(\tilde{A}, n^\alpha \tilde{B})$ have the same set of eigenvectors, V diagonalizes $\tilde{B}^{-1} \tilde{A}$. Thus, there exists a diagonal matrix Λ such that $\tilde{B}^{-1} \tilde{A} = V \Lambda V^{-1}$. Moreover, since the eigenvalue of $(\tilde{A}, n^\alpha \tilde{B})$

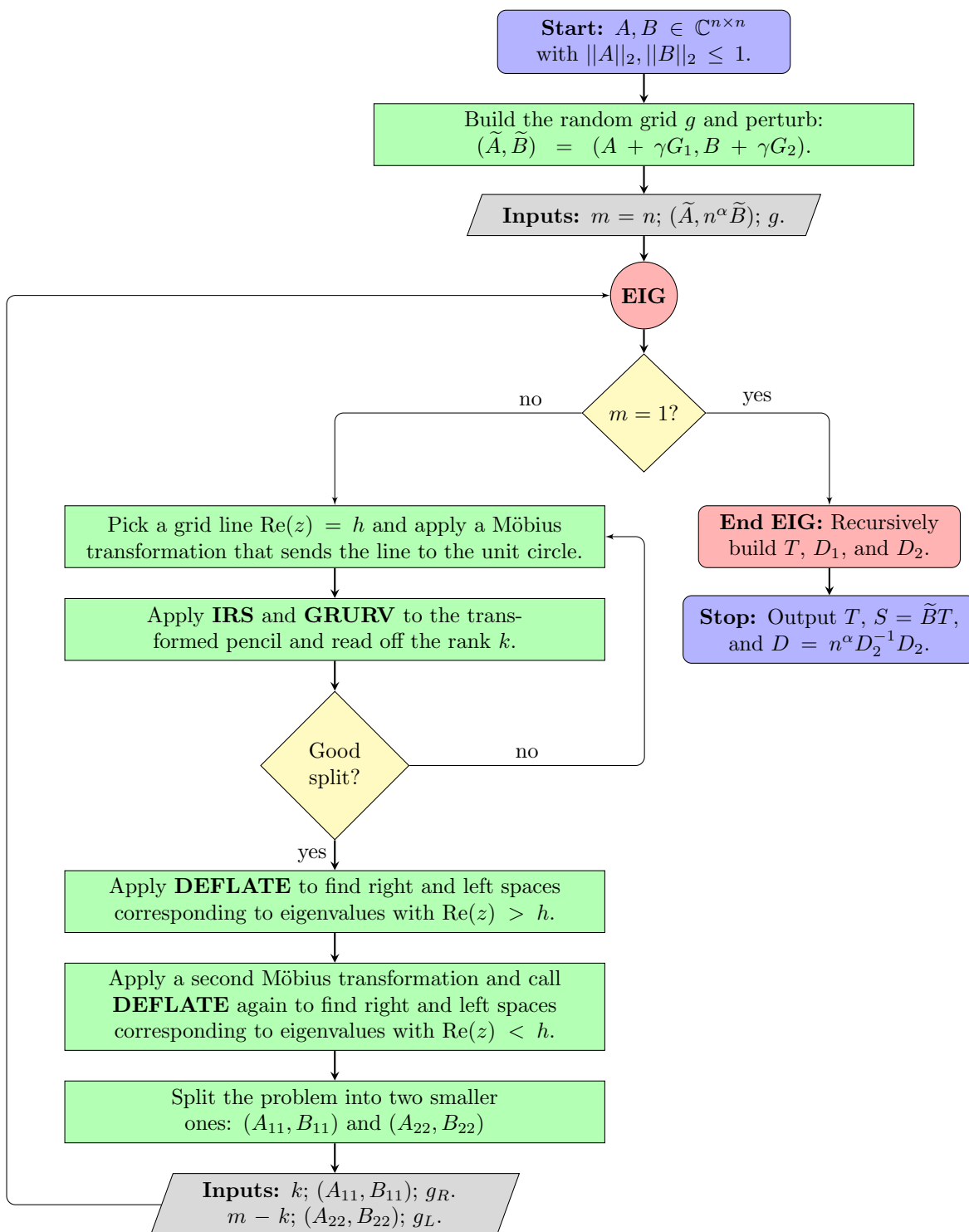


Figure 4: A diagram of **RPD** (Algorithm 6) for producing an approximate diagonalization of (A, B) . As in the pseudocode, we assume for simplicity that each split in **EIG** is made by a vertical grid line.

corresponding to v_i shares a grid box of g with the eigenvalue of (D_1, D_2) corresponding to t_i (this was how v_i was found in the proof of [Theorem 4.8](#)), each diagonal entry of Λ is at most $\sqrt{2}n^\alpha\omega$ away from the corresponding diagonal entry of $D = n^\alpha D_2^{-1} D_1$. Note that the eigenvalues of (D_1, D_2) are all contained in g , which guarantees that D_2 is invertible. With all of this in mind, expand $\|A - SDT^{-1}\|_2$ as follows:

$$\begin{aligned}
\|A - SDT^{-1}\|_2 &= \|A - \tilde{A} + \tilde{A} - SDT^{-1}\|_2 \\
&\leq \|A - \tilde{A}\|_2 + \|\tilde{A} - SDT^{-1}\|_2 \\
&\leq \|A - \tilde{A}\|_2 + \|\tilde{B}\|_2 \|\tilde{B}^{-1}\tilde{A} - TDT^{-1}\|_2 \\
&\leq 4\gamma + (1 + 4\gamma)\|V\Lambda V^{-1} - TDT^{-1}\|_2 \\
&\leq 4\gamma + (1 + 4\gamma) [\|(V - T)\Lambda V^{-1}\|_2 + \|T(\Lambda - D)V^{-1}\|_2 + \|TD(V^{-1} - T^{-1})\|_2].
\end{aligned} \tag{5.1.5}$$

To simplify this bound in terms of our parameters, we observe the following.

- Since the columns of V and T are unit vectors, $1 \leq \|V\|_2, \|T\|_2 \leq \sqrt{n}$.
- Since V diagonalizes $\tilde{B}^{-1}\tilde{A}$ and therefore also $n^{-\alpha}\tilde{B}^{-1}\tilde{A}$ and $\kappa_V(n^{-\alpha}\tilde{B}^{-1}\tilde{A}) \leq \frac{n^{\alpha+2}}{\gamma}$, [Remark 3.11](#) allows us to assume

$$\|V\|_2\|V^{-1}\|_2 \leq \frac{n^{\alpha+2}}{\gamma} \tag{5.1.6}$$

without changing probabilities. Combined with the previous point, this implies $\|V^{-1}\|_2 \leq \frac{n^{\alpha+2}}{\gamma}$.

- The columns of T and V satisfy $\|t_i - v_i\|_2 \leq \beta$ so $\|T - V\|_2 \leq \sqrt{n}\beta$
- By the stability of singular values, $\|T - V\|_2 \leq \sqrt{n}\beta$ implies $\sigma_n(T) \geq \sigma_n(V) - \sqrt{n}\beta$. Combining this with our upper bound on $\|V^{-1}\|_2$ yields

$$\|T^{-1}\|_2 \leq \frac{n^{\alpha+2}}{\gamma - n^{\frac{2\alpha+5}{2}}\beta}. \tag{5.1.7}$$

- Because each diagonal entry of Λ is at most $\sqrt{2}n^\alpha\omega$ from the corresponding diagonal entry of D , $\|\Lambda - D\|_2 \leq \sqrt{2}n^\alpha\omega$.
- Since both $(\tilde{A}, n^\alpha\tilde{B})$ and (D_1, D_2) have eigenvalues in $B_3(0)$, $\|\Lambda\|_2, \|D\|_2 \leq 3n^\alpha$.
- Finally, $\|V^{-1} - T^{-1}\|_2 = \|T^{-1}(T - V)V^{-1}\|_2 \leq \|T^{-1}\|_2\|T - V\|_2\|V^{-1}\|_2$.

Together, these imply the following bounds:

$$\|(V - T)\Lambda V^{-1}\|_2 \leq \|V - T\|_2\|\Lambda\|_2\|V^{-1}\|_2 \leq \sqrt{n}\beta \cdot 3n^\alpha \cdot \frac{n^{\alpha+2}}{\gamma} = \frac{3\beta}{\gamma} n^{\frac{4\alpha+5}{2}} \tag{5.1.8a}$$

$$\|T(\Lambda - D)V^{-1}\|_2 \leq \|T\|_2\|\Lambda - D\|_2\|V^{-1}\|_2 \leq \sqrt{n} \cdot \sqrt{2}n^\alpha\omega \cdot \frac{n^{\alpha+2}}{\gamma} = \frac{\sqrt{2}\omega}{\gamma} n^{\frac{4\alpha+5}{2}} \tag{5.1.8b}$$

$$\|TD(V^{-1} - T^{-1})\|_2 \leq \sqrt{n} \cdot 3n^\alpha \cdot \frac{n^{\alpha+2}}{\gamma - n^{\frac{2\alpha+5}{2}}\beta} \cdot \sqrt{n}\beta \cdot \frac{n^{\alpha+2}}{\gamma} = \frac{3\beta n^{3\alpha+5}}{\gamma(\gamma - n^{\frac{2\alpha+5}{2}}\beta)}. \tag{5.1.8c}$$

Now the choice of β in line 4 ensures $\beta \leq \frac{\varepsilon\gamma}{12(1+4\gamma)} n^{-\frac{4\alpha+5}{2}}$, so [\(5.1.8a\)](#) simplifies to

$$\|(V - T)\Lambda V^{-1}\|_2 \leq 3 \cdot \frac{\varepsilon\gamma}{12(1+4\gamma)n^{\frac{4\alpha+5}{2}}} \cdot \frac{n^{\frac{4\alpha+5}{2}}}{\gamma} = \frac{\varepsilon}{4(1+4\gamma)}. \tag{5.1.9}$$

Similarly, using this time the fact that $\beta < \frac{\gamma}{2} n^{-\frac{2\alpha+5}{2}}$ and therefore $\gamma - n^{\frac{2\alpha+5}{2}}\beta > \frac{\gamma}{2}$, [\(5.1.8c\)](#) becomes

$$\|TD(V^{-1} - T^{-1})\|_2 \leq \frac{6}{\gamma^2} n^{3\alpha+5} \cdot \frac{\varepsilon\gamma^2}{24(1+4\gamma)} n^{-3\alpha-5} = \frac{\varepsilon}{4(1+4\gamma)}. \tag{5.1.10}$$

Finally, $\omega = \frac{\gamma^4}{4} n^{-\frac{8\alpha+13}{3}}$ implies $\omega \leq \frac{\varepsilon\gamma}{4\sqrt{2}(1+4\gamma)} n^{-\frac{4\alpha+5}{2}}$, which allows us to upper bound (5.1.8b) as

$$\|T(\Lambda - D)V^{-1}\|_2 \leq \sqrt{2} \cdot \frac{\varepsilon\gamma}{4\sqrt{2}(1+4\gamma)n^{\frac{4\alpha+5}{2}}} \cdot \frac{n^{\frac{4\alpha+5}{2}}}{\gamma} = \frac{\varepsilon}{4(1+4\gamma)}. \quad (5.1.11)$$

Applying these to (5.1.5), we obtain

$$\|A - SDT^{-1}\|_2 \leq 4\gamma + (1+4\gamma) \left[\frac{\varepsilon}{4(1+4\gamma)} + \frac{\varepsilon}{4(1+4\gamma)} + \frac{\varepsilon}{4(1+4\gamma)} \right] = 4\gamma + \frac{3}{4}\varepsilon. \quad (5.1.12)$$

Since $\gamma = \frac{\varepsilon}{16}$ we conclude $\|A - SDT^{-1}\|_2 \leq \varepsilon$. \square

5.2 Forward Error Guarantee and Asymptotic Complexity

We might hope that [Theorem 5.1](#) can provide a forward error guarantee in terms of the eigenvector condition number $\kappa_V(A, B)$. As we demonstrate below, this is possible when the input pencil is well-behaved (in particular regular with a full set of distinct and finite eigenvalues). The resulting [Theorem 5.2](#) parallels a similar result of Banks et al. [[9](#), Proposition 1.1].

Theorem 5.2. *Let $A, B, \tilde{A}, \tilde{B} \in \mathbb{C}^{n \times n}$ with $\|A\|_2 \leq 1$. Assume that B is invertible and that the pencil (A, B) has a full set of distinct, finite eigenpairs $\{(\lambda_i, v_i)\}_{i=1}^n$. If $\|A - \tilde{A}\|_2 \leq \varepsilon\sigma_n(B)\text{gap}(A, B)$ and $\|B - \tilde{B}\|_2 \leq \varepsilon\sigma_n^2(B)\text{gap}(A, B)$ for*

$$\varepsilon \leq \frac{1}{32\kappa_V(A, B)}$$

then (\tilde{A}, \tilde{B}) has no repeated eigenvalues and any set of corresponding eigenpairs $\{(\tilde{\lambda}_i, \tilde{v}_i)\}_{i=1}^n$ satisfies

$$|\lambda_i - \tilde{\lambda}_i| \leq 4\text{gap}(A, B)\kappa_V(A, B)\varepsilon \quad \text{and} \quad \|v_i - \tilde{v}_i\|_2 \leq 24n\kappa_V(A, B)\varepsilon \quad \text{for all } i = 1, \dots, n$$

after multiplying the v_i by phases and reordering, if necessary.

Proof. We first note that $\varepsilon < \frac{1}{32\kappa_V(A, B)}$ implies

$$\|B - \tilde{B}\|_2 \leq \frac{\sigma_n^2(B)\text{gap}(A, B)}{32\kappa_V(A, B)} \leq \frac{\sigma_n(B)}{16\kappa_V(A, B)} \leq \frac{\sigma_n(B)}{2}, \quad (5.2.1)$$

where the second inequality follows from $\text{gap}(A, B) \leq 2\|B^{-1}A\|_2 \leq \frac{2}{\sigma_n(B)}$ (since $\|A\|_2 \leq 1$). Thus, [Lemma 2.13](#) guarantees $\sigma_n(\tilde{B}) \geq \sigma_n(B) - \|B - \tilde{B}\|_2 \geq \frac{\sigma_n(B)}{2}$, so \tilde{B} is invertible. With this in mind, consider the matrices $B^{-1}A$ and $\tilde{B}^{-1}\tilde{A}$, which are diagonalizable with the same eigenpairs as (A, B) and (\tilde{A}, \tilde{B}) respectively. Using again the fact that $\|A\|_2 \leq 1$, we have

$$\begin{aligned} \|B^{-1}A - \tilde{B}^{-1}\tilde{A}\|_2 &= \|B^{-1}A - \tilde{B}^{-1}A + \tilde{B}^{-1}A - \tilde{B}^{-1}\tilde{A}\|_2 \\ &\leq \|B^{-1} - \tilde{B}^{-1}\|_2\|A\|_2 + \|\tilde{B}^{-1}\|_2\|A - \tilde{A}\|_2 \\ &\leq \|\tilde{B}^{-1}\|_2\|\tilde{B} - B\|_2\|B^{-1}\|_2 + \|\tilde{B}^{-1}\|_2\|A - \tilde{A}\|_2 \\ &\leq \frac{2}{\sigma_n(B)}\varepsilon\sigma_n^2(B)\text{gap}(A, B)\frac{1}{\sigma_n(B)} + \frac{2}{\sigma_n(B)}\varepsilon\sigma_n(B)\text{gap}(A, B) \\ &\leq 4\varepsilon\text{gap}(A, B). \end{aligned} \quad (5.2.2)$$

This implies that the eigenvalues of $\tilde{B}^{-1}\tilde{A}$ belong to the $4\varepsilon\text{gap}(A, B)$ -pseudospectrum of $B^{-1}A$, and moreover we can continuously deform the eigenvalues of $B^{-1}A$ to those of $\tilde{B}^{-1}\tilde{A}$ without leaving this pseudospectrum. Since $\varepsilon < \frac{1}{4}$ and $B^{-1}A$ is diagonalizable, single matrix Bauer-Fike ([Theorem 2.15](#)) therefore implies that $\tilde{B}^{-1}\tilde{A}$, and by extension (\tilde{A}, \tilde{B}) , has a full set of distinct eigenvalues $\lambda_1, \dots, \lambda_n$. Bauer-Fike also guarantees that these eigenvalues can be ordered so that each $\tilde{\lambda}_i$ satisfies

$$|\lambda_i - \tilde{\lambda}_i| \leq 4\text{gap}(A, B)\kappa_V(B^{-1}A)\varepsilon \quad (5.2.3)$$

for a corresponding eigenvalue λ_i of $B^{-1}A$. Recalling that $\kappa_V(B^{-1}A) = \kappa_V(A, B)$, we obtain the first guarantee.

The second guarantee follows from the proof of [9, Proposition 1.1] since the requirement $\varepsilon < \frac{1}{32\kappa_V(A, B)}$ ensures by (5.2.2) that

$$\|B^{-1}A - \tilde{B}^{-1}\tilde{A}\|_2 \leq \frac{\text{gap}(B^{-1}A)}{8\kappa_V(B^{-1}A)}. \quad (5.2.4)$$

Note that while [9, Proposition 1.1] comes with norm assumptions on the matrices, these are not used in the proof of the eigenvector guarantee. \square

Banks et al. state [9, Proposition 1.1] – the single matrix counterpart to [Theorem 5.2](#) – in terms of an eigenvalue problem condition number:

$$\kappa_{\text{eig}}(A) = \frac{\kappa_V(A)}{\text{gap}(A)}. \quad (5.2.5)$$

With this in mind, we could rewrite [Theorem 5.2](#) in terms of the similar quantity

$$\frac{\kappa_V(A, B)}{\sigma_n^3(B)\text{gap}(A, B)}. \quad (5.2.6)$$

While (5.2.6) does capture some of the challenges of the generalized eigenvalue problem (i.e., it is infinite if B is singular or (A, B) has a repeated eigenvalue) it is not invariant under scaling of A and B and is therefore not suitable as a condition number for the problem. For this reason, we choose instead to state the forward error guarantees in terms of $\kappa_V(A, B)$.

The proof of [9, Proposition 1.1] relies on some basic perturbation results for individual matrices summarized in [30]. Developing corresponding results for the generalized problem may allow for a similar forward error guarantee with looser requirements on $\|A - \tilde{A}\|_2$ and $\|B - \tilde{B}\|_2$. In particular, we might hope to reduce or eliminate the factors of $\sigma_n(B)$. Absent these improvements, [Theorem 5.2](#) is fairly restrictive, requiring not only that (A, B) is regular and diagonalizable but that B is nonsingular. In part, this is a consequence of our version of Bauer-Fike, which makes many of the same assumptions and produces the same guarantees if used in the proof above. We consider a generalization to arbitrary regular pencils in [Appendix A](#). The singular pencil case is even more complex, requiring a different perturbation analysis altogether (see for example work of Demmel and Kågström [18] or Lotz and Noferini [41]).

To wrap up this section, we compute the asymptotic complexity of **RPD** in terms of n , the size of the pencil (A, B) , and ε , the accuracy of the approximate diagonalization. Throughout, we assume that we have access to black-box algorithms for multiplying two $n \times n$ matrices and computing the QR factorization of an $n \times n$ matrix, which require $T_{\text{MM}}(n)$ and $T_{\text{QR}}(n)$ arithmetic operations, respectively. For simplicity, we also assume access to QL/RQ algorithms (used in **GRURV**) that require $T_{\text{QR}}(n)$ operations.

[Proposition 5.3](#) shows that **RPD** runs in nearly matrix multiplication time. Its proof is somewhat more subtle than we have implied so far; rather than simply arguing that each step of divide-and-conquer runs in nearly matrix multiplication time and that only logarithmically many steps are needed, we apply a sharper geometric sum that leverages the shrinking problem size guaranteed by significant eigenvalue splits.

Proposition 5.3. *Exact-arithmetic **RPD** requires at most $O(\log^2(\frac{n}{\varepsilon})T_{\text{MM}}(n))$ arithmetic operations.*

Proof. We track only matrix multiplication and QR, as all other building blocks of **RPD** have smaller complexity. We begin by noting that line 2 of [Algorithm 6](#) implies $\alpha = \mathcal{O}\left(\log_n\left(\frac{1}{\gamma}\right)\right)$ and $\gamma = \Theta(\varepsilon)$, so

$$n^\alpha = \mathcal{O}\left(n^{\log_n(1/\gamma)}\right) = \mathcal{O}\left(\frac{1}{\gamma}\right) = \mathcal{O}\left(\frac{1}{\varepsilon}\right). \quad (5.2.7)$$

Meanwhile in line 3 we set

$$\epsilon > \frac{\gamma^5}{65n^{\frac{11\alpha+25}{3}}} = \Omega\left(\frac{\varepsilon^{26/3}}{n^{25/3}}\right). \quad (5.2.8)$$

Together, these imply that the number of steps of repeated squaring required at any point in the recursion can be bounded asymptotically as

$$p = \mathcal{O}\left(\log\left(\frac{n^\alpha}{\epsilon}\right)\right) = \mathcal{O}\left(\log\left(\frac{n^{25/3}}{\varepsilon^{29/3}}\right)\right) = \mathcal{O}\left(\log\left(\frac{n}{\varepsilon}\right)\right). \quad (5.2.9)$$

Consider now working through one step of divide-and-conquer. Lines 8-15 of **EIG** make up the bulk of the work, executing a search over the grid lines for one that sufficiently splits the spectrum. For each line that is checked, we make one call to **IRS** and one call to **GRURV**; each step of repeated squaring consists of one $2m \times 2m$ QR factorization and two $m \times m$ matrix multiplications, while applying **GRURV** to a product of two $m \times m$ matrices requires $3T_{\text{QR}}(m) + 2T_{\text{MM}}(m)$ operations. Combining these with (5.2.9), we conclude that each grid line checked results in

$$O\left(\log\left(\frac{n}{\epsilon}\right) [T_{\text{QR}}(2m) + 2T_{\text{MM}}(m)] + 2T_{\text{QR}}(m) + 2T_{\text{MM}}(m)\right) = O\left(\log\left(\frac{n}{\epsilon}\right) [T_{\text{QR}}(m) + T_{\text{MM}}(m)]\right) \quad (5.2.10)$$

operations. Since we check at most $O\left(\log\left(\frac{1}{\omega}\right)\right)$ grid lines each time and

$$\omega = \frac{\gamma^4}{4n^{\frac{8\alpha+13}{3}}} = \Omega\left(\frac{\epsilon^{20/3}}{n^{13/3}}\right), \quad (5.2.11)$$

lines 8-15 of **EIG** take at most

$$O\left(\log^2\left(\frac{n}{\epsilon}\right) [T_{\text{QR}}(m) + T_{\text{MM}}(m)]\right) = O\left(\log^2\left(\frac{n}{\epsilon}\right) T_{\text{MM}}(m)\right) \quad (5.2.12)$$

operations, where we simplify by noting $T_{\text{QR}}(m) = O(T_{\text{MM}}(n))$ [17, §4.1]. Since the remainder of one step of **EIG** – i.e., the subsequent calls to **DEFLATE** – has complexity equal to that of checking one grid line, we conclude that (5.2.12) is the asymptotic complexity of one step of divide-and-conquer.

To complete the proof, we sum this expression recursively. Since the $\log^2\left(\frac{n}{\epsilon}\right)$ term of (5.2.12) is independent of m , this reduces to summing $T_{\text{MM}}(m)$ over all subproblems produced by **EIG**. With this in mind, set $T_{\text{MM}}(m) = O(m^\xi)$ for $\xi \in [2, 3]$ and suppose we divide an $m \times m$ pencil into subproblems of size m_1 and m_2 . Since we enforce a significant split, we are guaranteed $\frac{1}{5}m \leq m_1, m_2 \leq \frac{4}{5}m$ and therefore

$$m_1^\xi + m_2^\xi = m_1^\xi + (m - m_1)^\xi \leq \left(\frac{4}{5}m\right)^\xi + \left(\frac{1}{5}m\right)^\xi \leq \frac{17}{25}m^\xi, \quad (5.2.13)$$

where the last inequality is obtained by applying $\xi \geq 2$. Consequently, a sum of m^ξ over all subproblems can be bounded by

$$\sum_{k=0}^{\infty} n^\xi \left(\frac{17}{25}\right)^k = n^\xi \sum_{k=0}^{\infty} \left(\frac{17}{25}\right)^k = \frac{25}{8}n^\xi \quad (5.2.14)$$

and therefore $\sum_m T_{\text{MM}}(m) = O(T_{\text{MM}}(n))$. Applying this to (5.2.12) yields the final complexity. \square

6 Numerical Examples

In this section, we consider several examples to investigate how pseudospectral divide-and-conquer performs in practice. Our first task is to adjust the parameters of **RPD** and **EIG**, as the values listed in the pseudocode of Algorithms 5 and 6 – though necessary in the proof of Theorem 5.1 – are prohibitively restrictive for implementation. Here, we make the following relaxations.

- First, we eliminate the n^α scaling, testing examples with eigenvalues exclusively (or predominantly) in $B_3(0)$.
- Extracting the main dependence on γ and n , we set $\epsilon = \beta = \omega = \gamma/n$ and we limit the number of steps of repeated squaring to $p = \lceil \log_2(n/\epsilon) \rceil$.
- Finally, we drop the factor of $1/n^3$ from the criteria used to compute k in line 12 of **EIG**.

In light of these simplifications, we present the following experiments as simply a proof of concept. Accordingly, we do not consider run times nor do we use an explicitly parallel implementation of the algorithm. Throughout, all results were obtained in Matlab version R2023a.²

²Our implementation is available here: <https://github.com/ry-schneider/Randomized.Pencil.Diagonalization>

6.1 Model Problems

We start by using **RPD** as stated (i.e., running to subproblems of size 1×1) on the following 50×50 model problems.

- 1. Planted Spectrum:** First, we consider a pencil with equally spaced, real eigenvalues in the interval $[-2, 2]$. To obtain (A, B) , we fill a diagonal matrix Λ as $\Lambda(j, j) = -2 + \frac{4}{49}(j - 1)$ and set $A = X\Lambda Y^{-1}$ and $B = XY^{-1}$ for X and Y two independent, complex Gaussian matrices. In accordance with **RPD**, we then normalize the pencil so that $\|A\|_2, \|B\|_2 \leq 1$. We can think of this example as the best-case scenario, where $\text{gap}(A, B)$ is large and B is far from singular.
- 2. Jordan Block:** Next, we consider a pencil (A, B) with $B = I$ and $A = J_{50}(0)$ for $J_{50}(0)$ a Jordan block with eigenvalue zero. In contrast to the planted spectrum example, this tests a generalized eigenvalue problem with $\text{gap}(A, B) = 0$.

We track the performance of divide-and-conquer on these examples in several ways. First and foremost, we want to verify a finite-precision counterpart to [Theorem 5.1](#): does **RPD** reliably produce accurate diagonalizations of each pencil? With this in mind, we compute diagonalization error as

$$\log_{10} \left(\max \{ \|A - SDT^{-1}\|_2, \|B - ST^{-1}\|_2 \} \right), \quad (6.1.1)$$

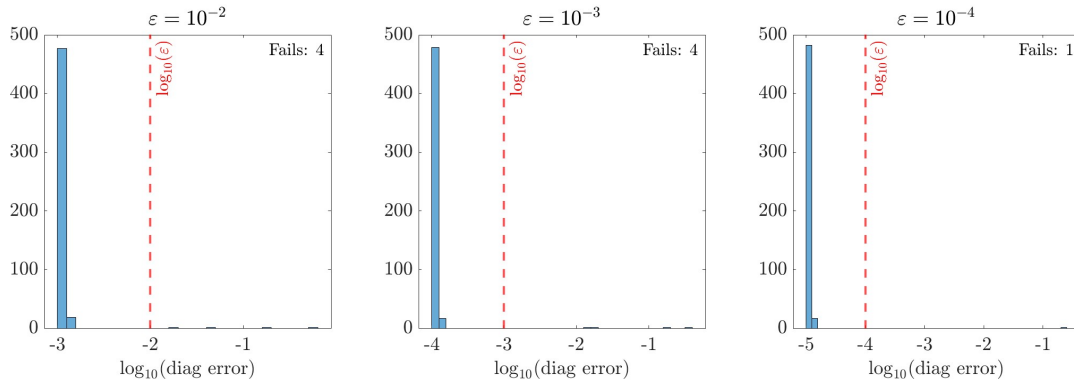
for S, D , and T the outputs of **RPD**, and we consider a run to be successful if this error is at most $\log_{10}(\varepsilon)$. Tracking the number of failed runs yields an empirical failure probability for **RPD** (with the simplifications made above). Note that (6.1.1) is only meaningful if $\|A\|_2$ and $\|B\|_2$ are roughly equal and close to one, as is the case in our examples.

Next, we want to measure the efficiency of the divide-and-conquer process. One way to do this is to catalog the relative split size at each step (i.e., k/m in **EIG**). While we know that **EIG** guarantees that the relative split is at least 0.2 and at most 0.8, divide-and-conquer is most efficient if relative splits are close to 0.5 at each step.

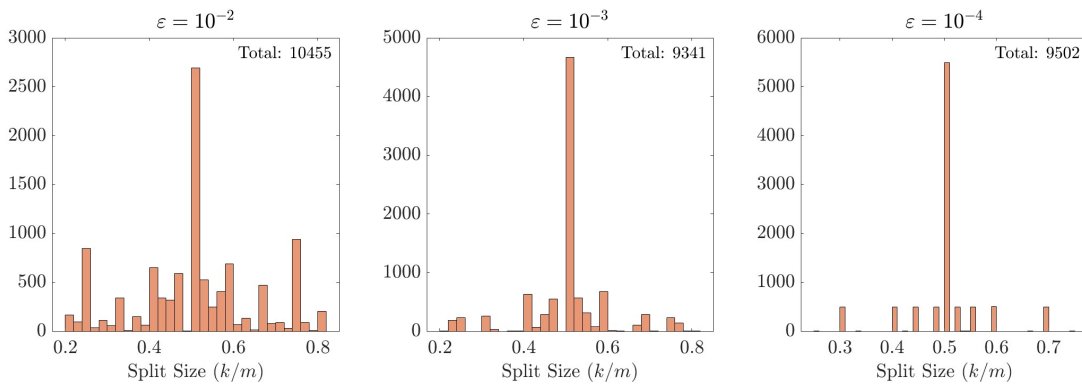
Of course, the split size tells only part of the story. Recalling the proof of [Proposition 5.3](#), **EIG** spends most of its time finding a dividing line; thus, even if splits are reliably near 50/50, the algorithm may be slow if too many lines are checked. Assuming access to $O(n^3)$ algorithms for matrix multiplication and QR, one step of our implementation requires $O(\log(\frac{n}{\varepsilon})m^3l)$ operations, where l is the number of grid lines checked and m is the size of the current subproblem. Ignoring the $\log(\frac{n}{\varepsilon})$ factor (as it will cancel in our eventual measure of efficiency) we can do a pseudo-flop count by summing m^3l over all steps with $m > 1$, and we can easily compute an optimal value for this count by requiring at each step that $l = 1$ and that the split is as close to 50/50 as possible. Dividing the actual count by the optimal one produces what we call a *relative efficiency factor* for each run, which tells us roughly how many times more work **RPD** is doing than the best-case scenario.

Histograms of each of these measures of performance are presented for both examples in [Figures 5 and 6](#). In each test, we run **RPD** 500 times and present results for decreasing values of ε . With only a handful of failed runs on each problem, the results are compelling: **RPD** reliably diagonalizes both pencils, and divide-and-conquer appears to favor near-optimal eigenvalue splits. This carries through to the relative efficiency. Our rough flop count shows that **RPD** executes only slightly more than the optimal amount of work to produce these diagonalizations. Note that the number of failed runs appears to decrease with ε . While this may seem counterintuitive, it is a byproduct of our relaxed parameters, which become more restrictive (or equivalently more sensitive) as ε shrinks.

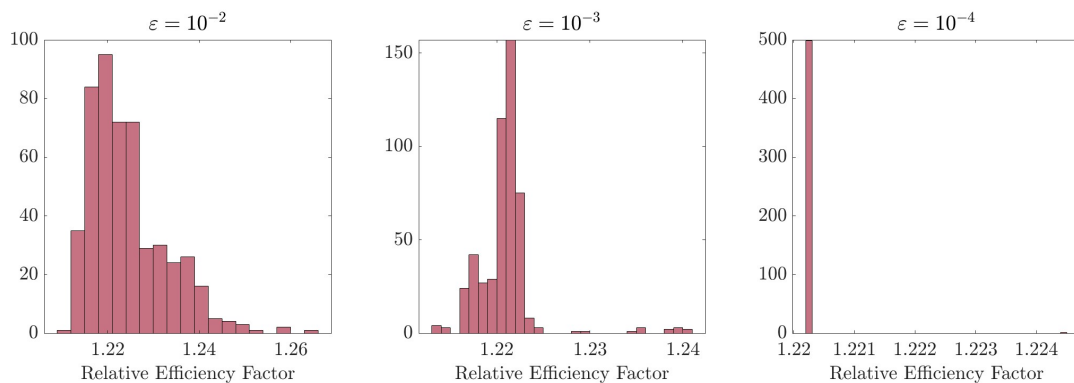
While these results are promising, we might be more interested in probing the boundaries of [Theorem 5.2](#). That is, when **RPD** succeeds, how accurate are the corresponding sets of approximate eigenvalues? With this in mind [Figure 7](#) provides eigenvalue approximation data for both model problems, where in each case we consider only approximations produced by successful runs. The results in these plots trace out nicely the challenge of extracting accurate eigenvalues from an accurate diagonalization. In the best case – the planted spectrum example – increasingly accurate diagonalizations provide correspondingly better eigenvalue approximations, as promised by [Theorem 5.2](#). The Jordan block example, on the other hand, demonstrates that when $\text{gap}(A, B) = 0$ we cannot hope to recover repeated eigenvalues with any confidence, though this is also the case for classical backwards-stable algorithms like QZ.



(a) Frequency of diagonalization error (6.1.1). We mark the $\log_{10}(\varepsilon)$ threshold for success in red and count the number of failed runs. For this example $\|A\|_2 = 1$ and $\|B\|_2 = 0.9104$.

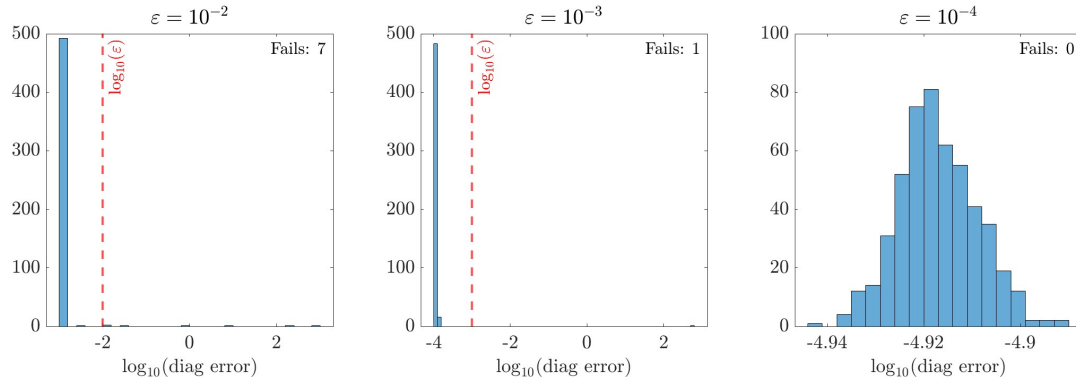


(b) Frequency of relative eigenvalue split sizes (i.e., k/m in **FIG**). We do not include subproblems with $m \leq 3$, as these can only be split in one way. Since the total number of splits is variable (and dependent on the splits themselves) we record it at the top of each plot. Dividing this total by 500 gives a rough average number of splits per run.

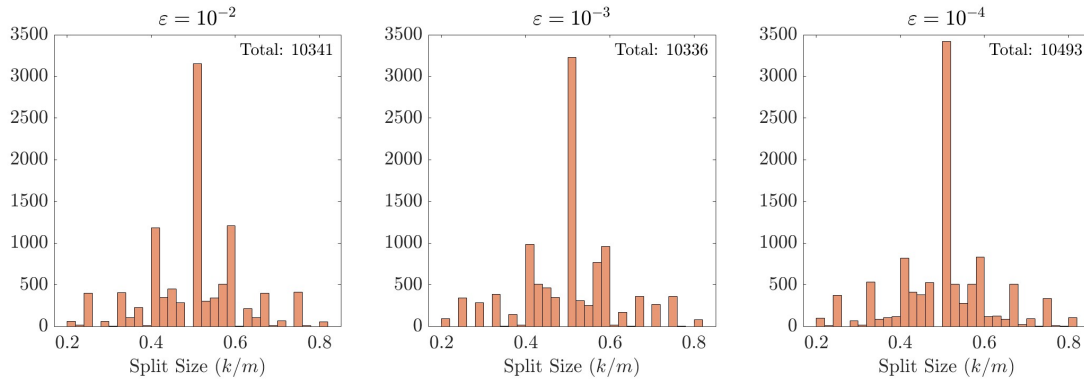


(c) Frequency of relative efficiency factor (i.e., the pseudo-flop count divided by its optimal value).

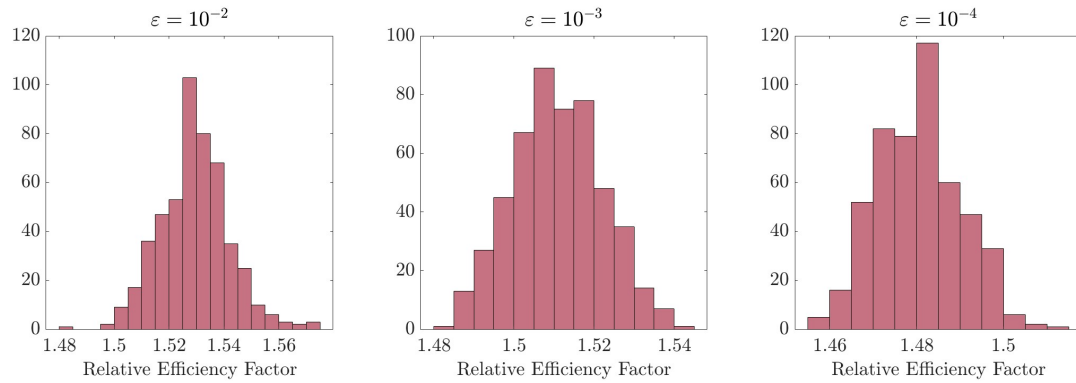
Figure 5: Performance data for **RPD** on the 50×50 planted-spectrum example with decreasing values of ε . Each plot corresponds to 500 runs of **RPD**.



(a) Same as (a) of Figure 5. For this example $\|A\|_2 = \|B\|_2 = 1$.

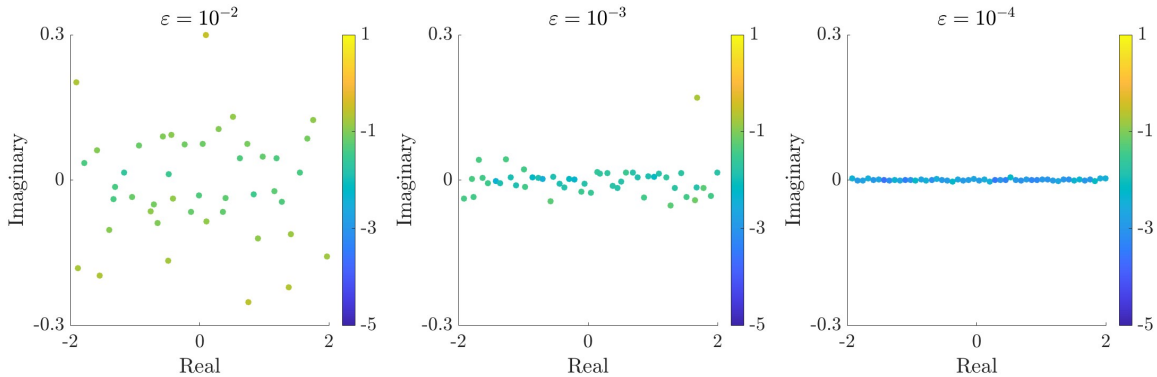


(b) Same as (b) of Figure 5.

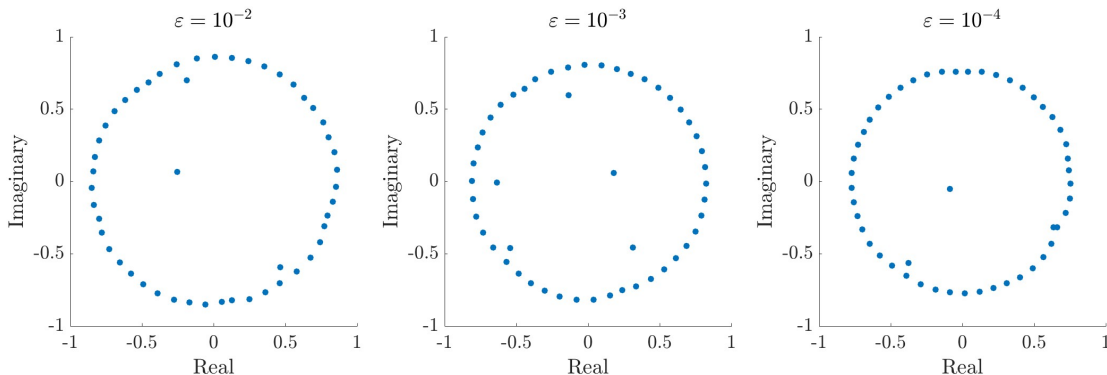


(c) Same as (c) of Figure 5

Figure 6: A repeat of Figure 5 for the 50×50 Jordan block example.



(a) Eigenvalue approximations for the planted spectrum example obtained from **RPD** with different values of ε . Each approximate eigenvalue is colored according to its accuracy, which is computed as $\log_{10} |\tilde{\lambda}_i - \lambda_i|$ for λ_i and $\tilde{\lambda}_i$ the true and approximate eigenvalues ordered by their real parts.



(b) Eigenvalue approximations for the Jordan block example obtained from **RPD** with different values of ε . The only true eigenvalue for this problem is zero.

Figure 7: Eigenvalue approximation data for **RPD** applied to the planted spectrum and Jordan block examples. We present here only results for successful runs – i.e., each set of approximate eigenvalues corresponds to a diagonalization with $\|A - SDT^{-1}\|_2 \leq \varepsilon$ and $\|B - ST^{-1}\|_2 \leq \varepsilon$.

6.2 Large n and Infinite Eigenvalues

Running **RPD** down to subproblems of size 1×1 is useful from a theoretical perspective but unlikely to be done in practice. We turn next to a more realistic use case, where n is large and only a few splits are made before passing off to **QZ**. In this setting, we test the algorithm on pencils with an eigenvalue at infinity (i.e., where B is singular). To do this, we construct a 1000×1000 pencil by drawing A and B randomly, computing a singular value decomposition $B = U\Sigma V^H$, and setting

$$B = B - \sigma_{\min}(B)uv^H \tag{6.2.1}$$

for u and v the last columns of U and V , respectively. By construction, this forces B to be singular without changing its remaining singular values (and critically ensuring its norm remains comparable to A). As in the previous examples, we normalize A and B before calling **RPD**.

Remark 6.1. Because we omit the n^α scaling on this example, the perturbed pencil (\tilde{A}, \tilde{B}) is very likely to have an eigenvalue outside of the shattering grid. While this appears problematic it is ultimately harmless. When only a handful of splits are needed, (\tilde{A}, \tilde{B}) can have many – even a large fraction – of eigenvalues outside of the grid, and divide-and-conquer will only falter if these fall predominantly in a specific region (for example between two vertical grid lines but above all of the horizontal ones). In part, this justifies our choice to omit the n^α scaling; while it is necessary to state an algorithm that provably runs to scalar

subproblems, it is overly restrictive in practice – driving eigenvalues that are initially small closer together and necessitating a finer grid.

In addition to testing larger values of n , we also use this example to further justify our decision to avoid matrix inversion. To that end – and in light of [Proposition 3.13](#) – we compare **RPD** to an alternative algorithm that proceeds as follows:

1. Perturb to obtain (\tilde{A}, \tilde{B}) .
2. Form the product $X = \tilde{B}^{-1}\tilde{A}$.
3. Apply the single-matrix, divide-and-conquer routine of Banks et al. [[9](#), Algorithm EIG].

To ensure a fair comparison, we run both algorithms with the same perturbations (meaning the same (\tilde{A}, \tilde{B}) and the same grid. We also restrict the number of steps of the Newton iteration for the sign function – the counterpart to **IRS** used by Banks et al. – to $\lceil \log_2(n/\epsilon) \rceil$. In both cases, we run divide-and-conquer to subproblems with $m \leq 250$, at which point we default to QZ and QR, respectively, by calling Matlab’s `eig`. In the tests presented below, both algorithms averaged five splits before defaulting to `eig`.

Once again, we track diagonalization error via [\(6.1.1\)](#). Importantly, we are interested in producing a diagonalization of (A, B) even if the single-matrix algorithm of Banks et al. is used. In that case, a matrix T containing right eigenvectors (the output of single-matrix divide-and-conquer) gives rise to a corresponding matrix of left eigenvectors $S = \tilde{B}T$, which together approximately diagonalize (A, B) . This mirrors exactly how the diagonalization is obtained in **RPD**.

In addition, we record the eigenvalue error associated with each diagonalization. This is done by ordering the approximate and true eigenvalues by magnitude and computing the average, absolute error over the spectrum, excluding the eigenvalue at infinity. [Figure 8](#) records eigenvalue and diagonalization errors for both algorithms and for two choices of ϵ . Each plot corresponds to 200 trials, derived from twenty random draws of A and B run through each algorithm ten times.

When $\epsilon = 10^{-5}$ we see little difference between the algorithms; though **RPD** is slightly more accurate, both approaches produce successful diagonalizations and comparably good eigenvalue approximations. Recalling that the size of the perturbation is determined by ϵ , this appears to be a consequence of the relatively large perturbation applied to B , which ensures that \tilde{B} is well-conditioned and that the error incurred by forming $\tilde{B}^{-1}\tilde{A}$ is small. In this case – or more generally in situations where B is known to be well-conditioned – both algorithms are viable and essentially equivalent.

In contrast, when ϵ is much smaller **RPD** shows clear advantages. While neither can produce an accurate enough diagonalization – an indication that our relaxed parameters are too loose for this regime – **RPD** is consistently an order of magnitude better than its single-matrix alternative, and its corresponding eigenvalue approximations are remarkably accurate. Again this seems attributable to the conditioning of \tilde{B} ; here, forming $\tilde{B}^{-1}\tilde{A}$ not only forces divide-and-conquer to work with a poorly-conditioned matrix but also introduces error that meaningfully shifts the eigenvalues away from those of (A, B) .

Indeed, the difference in eigenvalue error present when $\epsilon = 10^{-10}$ traces a similar gap between QZ and QR, as marked on the histograms. This indicates that the poor eigenvalue recovery of Banks et al. is due primarily to the gap between the eigenvalues of $\tilde{B}^{-1}\tilde{A}$ and (A, B) , which is essentially what the error in QR represents. Consequently, we cannot hope that by improving the diagonalization produced by Banks et al. – which should be possible by adjusting the parameters – we will see a similar improvement in the eigenvalues. On this example, then, we expect that this approach will break down as ϵ becomes small; while initially decreasing ϵ may improve diagonalization and eigenvalue accuracy, \tilde{B} will eventually become poorly-conditioned enough to guarantee that the eigenvalues of $\tilde{B}^{-1}\tilde{A}$ are far from those of (A, B) . Contrast this with **RPD**, which does not suffer from the same drawback and can reproduce the finite eigenvalues of (A, B) to high accuracy.

Note that the example considered here is a larger version of the one covered by [Figure 3](#). Together, they capture the danger of operating with inversion: when \tilde{B} is poorly conditioned, not only are the pseudospectra of $\tilde{B}^{-1}\tilde{A}$ unwieldy, but the eigenvalues they collapse to may significantly stray from those of the input pencil.

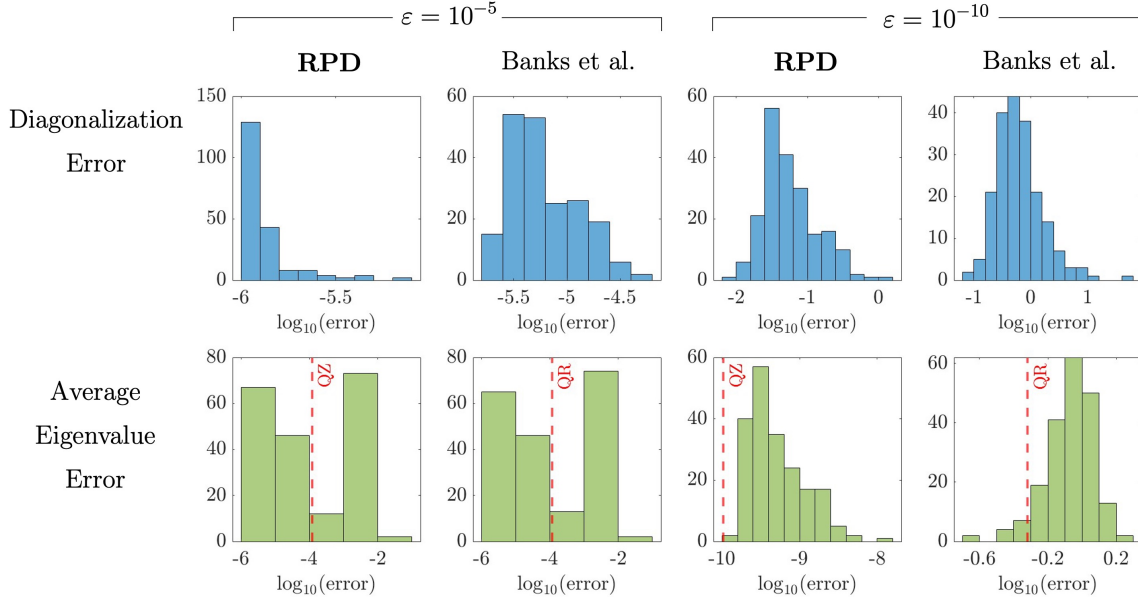


Figure 8: Performance data for **RPD** versus the single matrix, divide-and-conquer algorithm of Banks et al. [9]. Here, 1000×1000 pencils are constructed by drawing A and B randomly and subtracting a rank one matrix from B to force it to be singular (without changing its remaining singular values). For twenty random draws of A and B , we present ten runs through both algorithms, with first $\varepsilon = 10^{-5}$ and subsequently $\varepsilon = 10^{-10}$. Diagonalization error is computed according to (6.1.1) while eigenvalue accuracy is measured by ordering the true and approximate eigenvalues by magnitude and computing the average absolute error, excluding the eigenvalue at infinity. For the latter, we mark the error achieved by QZ/QR (computed in the same way) when applied to (\tilde{A}, \tilde{B}) and $\tilde{B}^{-1}\tilde{A}$, respectively.

6.3 Singular Pencils

To this point we have exclusively tested divide-and-conquer on regular pencils. Since singular pencils are a reality in many applications, we consider as a final test the following example taken from Lotz and Noferini [41]:

$$A = \begin{pmatrix} 2 & -1 & -5 & -1 \\ 6 & -2 & -11 & -2 \\ 5 & 0 & -2 & 0 \\ 3 & 1 & 3 & 1 \end{pmatrix}, \quad B = \begin{pmatrix} 1 & -1 & -4 & -2 \\ 2 & -3 & -12 & -6 \\ -1 & -3 & -11 & -6 \\ -2 & -2 & -7 & -4 \end{pmatrix}. \quad (6.3.1)$$

The singular structure of this pencil is revealed by its Kronecker canonical form [40]:

$$A - \lambda B = \begin{pmatrix} -3 & 1 & 1 & 1 \\ -8 & 3 & 2 & 0 \\ -5 & 3 & 0 & 1 \\ -2 & 2 & -1 & 1 \end{pmatrix} \begin{pmatrix} 1 - \lambda & 0 & 0 & 0 \\ 0 & -\lambda & 1 & 0 \\ 0 & 0 & -\lambda & 1 \\ 0 & 0 & 0 & 0 \end{pmatrix} \begin{pmatrix} -1 & 0 & 1 & 0 \\ 0 & 1 & -4 & -2 \\ 0 & 0 & 1 & 0 \\ 1 & -1 & 0 & 1 \end{pmatrix}^{-1}, \quad (6.3.2)$$

which indicates that (A, B) has only one simple eigenvalue at $\lambda = 1$.

Practically speaking, recovering this eigenvalue via divide-and-conquer should be difficult due to the initial perturbation made by **RPD**. In fact, Lotz and Noferini show that an arbitrarily small (nonrandom) perturbation to (A, B) can send its eigenvalues to any four points in the complex plane. In spite of this, divide-and-conquer finds the true eigenvalue to roughly five digits of precision when run with $\varepsilon = 10^{-6}$, as shown in Table 2.

Divide-and-Conquer (Algorithm 6)			
QZ [44]	Run 1	Run 2	Run 3
-2.089013	0.999997 - 0.000007i	1.000001 - 0.000008i	0.999994 - 0.000032i
1.000000	0.463026 - 0.216072i	-0.064526 + 0.383530i	0.816203 - 0.082329i
0.445724	-0.036567 - 0.391359i	-0.236744 - 0.298458i	0.178283 - 0.299444i
-0.014976	-1.987468 - 0.361121i	-1.152406 + 0.981613i	-2.368016 + 0.144692i

Table 2: Eigenvalues of the singular pencil (6.3.1) as computed by QZ and pseudospectral divide-and-conquer. We present three successful runs of **RPD**, each with $\varepsilon = 10^{-6}$.

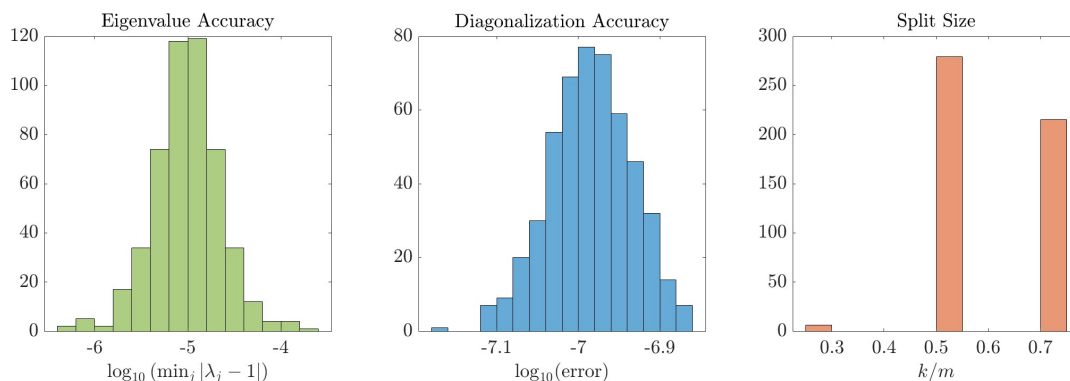


Figure 9: Statistics for 500 runs of **RPD** applied to a normalized version of the singular pencil (6.3.1) with $\|A\|_2 = 0.6940$, $\|B\|_2 = 1$, and $\varepsilon = 10^{-6}$. For the first plot, $\{\lambda_i\}_{1 \leq i \leq 4}$ are the approximate eigenvalues obtained via divide-and-conquer. Once again, no runs defaulted to calling `eig`. As in the previous examples, we consider only splits on subproblems with $m > 3$ for the third histogram; as a result, it records only the first split of each run, and the total number of splits is 500 (the number of runs).

Of course, QZ also finds $\lambda = 1$ to a remarkable 14 digits of precision. Motivated by this observation, Lotz and Noferini develop a theory of weak condition numbers to help explain the apparent stability of this eigenvalue. The results in Table 2 reflect the spirit of these condition numbers; though perturbations exist that produce arbitrary eigenvalues, a typical random one is likely to yield an eigenvalue near one.³ Randomization has another advantage here: while QZ always produces the same three spurious “eigenvalues,” divide-and-conquer does not – meaning multiple runs can help distinguish true eigenvalues from fake. Finally, we provide in Figure 9 a few empirical statistics for 500 runs of **RPD** on a normalized version of (A, B) .

7 Conclusion

In this paper, we have constructed an inverse-free routine for producing an approximate diagonalization of any matrix pencil (A, B) . The method, which rests on a divide-and-conquer eigensolver for the generalized eigenvalue problem, involves several threads of randomness. The most important of these is a random perturbation made to the input matrices, which regularizes the problem and allows the divide-and-conquer process to succeed with high probability. Leveraging this result, our approach produces a provably accurate approximate diagonalization (in a backward-error sense) for any input pencil in exact arithmetic, again with high probability. Moreover, the algorithm runs in nearly matrix multiplication time, establishing

³Earlier work of Demmel and Kågström [18] took a different approach to establishing the stability of QZ on singular pencils, demonstrating that QZ will preserve Kronecker canonical form, and therefore successfully recover true eigenvalues, provided round-off errors are small enough. This nevertheless cannot explain the strong performance of **RPD**, as Gaussian perturbations *will* change the Kronecker structure of the pencil with high probability.

$O(\log^2(\frac{n}{\varepsilon})T_{\text{MM}}(n))$ as an upper bound on the complexity of producing – without relying on inversion – an exact-arithmetic diagonalization of an $n \times n$ pencil with backward error ε . Replacing B with the identity, this provides another nearly matrix multiplication time algorithm for diagonalizing a single matrix, representing an inverse-free counterpart to the algorithm of Banks et al. [9].

For interested readers, we note that there are a number of open problems and next steps related to this work, which we discuss briefly below.

- **Finite-Precision Analysis:** The most immediate open question concerns a floating-point stability bound for **RPD**. While we expect that the method will succeed with similar guarantees in finite precision if stated properly, we have not yet completed an end-to-end analysis. [Appendix B](#) explores some of the work done in this direction.
- **Hermitian/Deterministic Variants:** Throughout, we made no assumptions on the matrices of our pencil. Nevertheless, much attention has been paid to the Hermitian eigenvalue problem, where A is Hermitian and B is Hermitian positive definite, meaning a version of the method adapted to that setting may be worth developing. The main difference there is the use of **DEFLATE**, as the left and right eigenspaces of a Hermitian pencil are the same. More generally, we might hope to devise a deterministic way to produce the pseudospectral shattering result central to the algorithm.
- **Perturbation Results for the Generalized Eigenvalue Problem:** In completing this work, we found that many of the useful perturbation results for the single-matrix eigenvalue problem do not have counterparts for the generalized problem. In particular, there is a lack of results stated in ways that are practical for numerical purposes (i.e., using the Euclidean norm as opposed to a chordal metric). We hope that this work inspires more research in this direction, and we expect that developing better tools may improve the analysis presented here.

8 Acknowledgements

This work was supported by NSF grant DMS 2154099 and by Graduate Fellowships for STEM Diversity (GFSD). We thank Jess Banks, Jorge Garza-Vargas, and Nikhil Srivastava for their advice and feedback as well as Anne Greenbaum for helpful correspondence. We also thank two anonymous referees for their detailed comments, corrections, and suggestions, which have improved the quality of the paper.

A Alternative Versions of Bauer-Fike for Matrix Pencils

In this appendix, we discuss alternative formulations of [Theorem 2.20](#). As mentioned above, our version of Bauer-Fike is stated for easy use in the proof of [Theorem 3.12](#) and therefore appears somewhat unusual compared to existing perturbation results for the generalized eigenvalue problem. Nevertheless, it is essentially the same as standard bounds, as we demonstrate below. To do this, we introduce common notation from perturbation theory as presented in Stewart and Sun [55].

We begin by re-casting each eigenvalue λ as an ordered pair $\langle \alpha, \beta \rangle$ such that $\lambda = \frac{\alpha}{\beta}$. In this notation, solutions to the generalized eigenvalue problem satisfy $\beta Av = \alpha Bv$. The main benefit of representing eigenvalues in this way is the natural inclusion of those at infinity, which now correspond to $\beta = 0$. Moreover, this definition links nicely with matrix pencil diagonalization; if $(A, B) = (SD_1T^{-1}, SD_2T^{-1})$, each diagonal entry of D_1 and D_2 contains a corresponding α and β . Note that if (A, B) is regular, we can never have $\alpha = \beta = 0$.

Of course, there are infinitely many choices of α and β that yield the same eigenvalue λ . For this reason, we can think of each eigenvalue $\langle \alpha, \beta \rangle$ as a projective line – i.e., the subspace spanned by $(\alpha \ \beta)^T$. Accordingly, we measure distance between two eigenvalues $\langle \alpha_1, \beta_1 \rangle$ and $\langle \alpha_2, \beta_2 \rangle$ with the chordal metric:

$$\chi(\langle \alpha_1, \beta_1 \rangle, \langle \alpha_2, \beta_2 \rangle) = \frac{|\alpha_1\beta_2 - \beta_1\alpha_2|}{\sqrt{|\alpha_1|^2 + |\beta_1|^2} \sqrt{|\alpha_2|^2 + |\beta_2|^2}}. \tag{A.0.1}$$

Dividing both the numerator and denominator of (A.0.1) by $|\beta_1\beta_2|$, we observe that if $\lambda_1 = \frac{\alpha_1}{\beta_1}$ and $\lambda_2 = \frac{\alpha_2}{\beta_2}$ then

$$\chi(\langle \alpha_1, \beta_1 \rangle, \langle \alpha_2, \beta_2 \rangle) = \frac{|\lambda_1 - \lambda_2|}{\sqrt{|\lambda_1|^2 + 1} \sqrt{|\lambda_2|^2 + 1}}. \quad (\text{A.0.2})$$

In other words, the chordal distance between $\langle \alpha_1, \beta_1 \rangle$ and $\langle \alpha_2, \beta_2 \rangle$ is half the Euclidean distance between the images of λ_1 and λ_2 under the stereographic projection. This ensures that the distance between any two eigenvalues is at most one, including eigenvalues at infinity.

Though perturbation results in terms of χ originate with Stewart [53], the first version of Bauer-Fike stated in terms of the chordal distance for general matrices is due to Elsner and Sun [23], which we summarize below.

Theorem A.1 (Elsner and Sun 1982). *Let (A, B) be a diagonalizable pencil with eigenvalues $\langle \alpha_i, \beta_i \rangle$. If T is any matrix of right eigenvectors of (A, B) and $\langle \tilde{\alpha}_i, \tilde{\beta}_i \rangle$ are the eigenvalues of the regular pencil (\tilde{A}, \tilde{B}) , then*

$$\max_i \min_j \chi(\langle \alpha_i, \beta_i \rangle, \langle \tilde{\alpha}_j, \tilde{\beta}_j \rangle) \leq \kappa(T) \|(AA^H + BB^H)^{-1/2}\|_2 \|(A - \tilde{A}, B - \tilde{B})\|_2$$

While Theorem A.1 is more general than Theorem 2.20, the two results are essentially the same under the assumptions made in Section 2.2. To demonstrate this, suppose that (A, B) is diagonalizable and that B is nonsingular with $\epsilon < \sigma_n(B)$. If $z \in \Lambda_\epsilon(A, B)$ then z is an eigenvalue of a pencil (\tilde{A}, \tilde{B}) with $\|A - \tilde{A}\|_2, \|B - \tilde{B}\|_2 \leq \epsilon$. Thus, if λ is the eigenvalue of (A, B) closest to z , Theorem A.1 and (A.0.2) imply

$$\frac{|z - \lambda|}{\sqrt{|z|^2 + 1} \sqrt{|\lambda|^2 + 1}} \leq \sqrt{2} \epsilon \kappa(T) \|(AA^H + BB^H)^{-1/2}\|_2 \quad (\text{A.0.3})$$

or, equivalently,

$$|z - \lambda| \leq \sqrt{2} \epsilon \kappa(T) \|(AA^H + BB^H)^{-1/2}\|_2 \sqrt{|z|^2 + 1} \sqrt{|\lambda|^2 + 1}. \quad (\text{A.0.4})$$

Applying Lemma 2.19 to bound $|z|$ and $|\lambda|$ and noting $\|(AA^H + BB^H)^{-1/2}\|_2 = \frac{1}{\sigma_n(A, B)}$, we conclude that $\Lambda_\epsilon(A, B)$ is contained in balls around the eigenvalues of (A, B) of radius

$$\sqrt{2} \epsilon \frac{\kappa(T)}{\sigma_n(A, B)} \left[1 + \left(\frac{\epsilon \|B^{-1}\|_2 + \|B^{-1}A\|_2}{1 - \epsilon \|B^{-1}\|_2} \right)^2 \right]. \quad (\text{A.0.5})$$

On one hand, the $\sigma_n(A, B)$ in (A.0.5) is an improvement over the factor of $\|B^{-1}\|_2$ in Theorem 2.20, as $\sigma_n(A, B) \geq \sigma_n(B)$. At the same time, we pay the price in an additional factor of $\sqrt{2}$ and the square on the piece coming from Lemma 2.19. Since $\sigma_n(A, B) \geq \sigma_n(A)$, (A.0.5) is likely a better bound if we know that A is far from singular, though in the proof of Theorem 3.12 the only bounds on $\sigma_n(A)$ available are the same as those for $\sigma_n(B)$. This means that, up to constants, a proof of shattering using Theorem A.1 is the same as the one given above. In particular, Elsner and Sun's result cannot be used to improve the dependence of ϵ on n . Similarly, it would not change Theorem 5.2.

Nevertheless, there is an important benefit of the generality of Theorem A.1: the ability to control changes in the finite eigenvalues of a pencil with some at infinity. Up to this point, we have pursued a standard Bauer-Fike result that bounds $\Lambda_\epsilon(A, B)$ by a union of balls around the eigenvalues of (A, B) . Because we know $\Lambda_\epsilon(A, B)$ is unbounded if B is singular or $\epsilon > \sigma_n(B)$, Theorem 2.20 and the alternate version (A.0.5) do not consider the case where B is singular. This ultimately carries through to our forward error bound Theorem 5.2, which similarly requires that B is invertible. While we know that we can't obtain any kind of forward error guarantees for the infinite eigenvalues of (A, B) with singular B , we would like to extend Theorem 5.2 to the finite eigenvalues if possible. Theorem A.1 offers one way to do this, producing the following proposition.

Proposition A.2. *Let (A, B) be a regular, diagonalizable pencil and let (\tilde{A}, \tilde{B}) be a nearby pencil with $\|A - \tilde{A}\|_2, \|B - \tilde{B}\|_2 \leq \epsilon$. Suppose that $\langle \alpha, \beta \rangle$ and $\langle \tilde{\alpha}, \tilde{\beta} \rangle$ are eigenvalues of (A, B) and (\tilde{A}, \tilde{B}) , where $\langle \alpha, \beta \rangle$ is the closest eigenvalue of (A, B) to $\langle \tilde{\alpha}, \tilde{\beta} \rangle$ in the chordal metric χ . If $\lambda = \frac{\alpha}{\beta}$ and $\tilde{\lambda} = \frac{\tilde{\alpha}}{\tilde{\beta}}$ are both finite, then*

$$|\lambda - \tilde{\lambda}| \leq \sqrt{2} \epsilon \frac{\kappa_V(A, B)}{\sigma_n(A, B)} \sqrt{|\lambda|^2 + 1} \sqrt{|\tilde{\lambda}|^2 + 1}.$$

Proof. This follows directly from [Theorem A.1](#), noting that we can replace $\kappa(T)$ with $\kappa_V(A, B)$ by taking an infimum. \square

Of course, this result is only useful if we can bound $|\lambda|$ and $|\tilde{\lambda}|$, which is not necessarily straightforward. We do note, however, that $\sigma_n(A, B)$ is guaranteed to be nonzero since (A, B) is regular.

To finish this section, we summarize other known variants of Bauer-Fike for the generalized eigenvalue problem (though this is by no means an exhaustive list). First, we note that [Theorem A.1](#) is the version stated by Stewart and Sun [[55](#), Theorem VI.2.6] rewritten in terms of the canonical angle between the row spaces of (A, B) and (\tilde{A}, \tilde{B}) . Stewart and Sun also include a version that swaps $\kappa(T)$ for $\|T\|_2\|S^{-1}\|_2$, where $(S^{-1}AT, S^{-1}BT)$ is a diagonalization of (A, B) with the columns of S^{-1} and T normalized appropriately (see [[55](#), Theorem VI.2.7]). This yields the simpler bound

$$\max_i \min_j \chi \left(\langle \alpha_i, \beta_i \rangle, \langle \tilde{\alpha}_j, \tilde{\beta}_j \rangle \right) \leq \|S^{-1}\|_2 \|T\|_2 \|(A - \tilde{A}, B - \tilde{B})\|_2. \quad (\text{A.0.6})$$

Note however that $\|S^{-1}\|_2$ hides a dependence on the conditioning of A and B (recall for example that we construct our diagonalization above by taking $S = BT$).

Minor improvements on [Theorem A.1](#) can be found in work of Elsner and Lancaster [[22](#)]. Meanwhile, Chu [[14](#)] stated their own version of Bauer-Fike consisting of four separate bounds, depending on whether the initial and perturbed eigenvalues are finite/infinite, which was subsequently generalized to matrix polynomials [[15](#)]. Finally, we note a recent sharp version of Shi and Wei [[52](#)] stated in terms of the sign-complex spectral radius.

B Finite-Precision Analysis

In this appendix, we analyze key building blocks of **EIG** and **RPD** in finite-precision arithmetic. We first outline our model of floating-point computation before proving results for shattering and **GRURV**. A rigorous stability bound for **IRS** under similar assumptions is covered in [[51](#)].

While a full end-to-end analysis of **RPD** remains open, these bounds suggest that it likely requires provably lower precision than methods built on inversion, in particular its single-matrix counterpart of Banks et al. (see the discussion in [[51](#), Chapter 6]).

B.1 Black-Box Assumptions

Throughout, we assume a floating-point arithmetic where

$$fl(x \circ y) = (x \circ y)(1 + \Delta), \quad |\Delta| \leq \mathbf{u} \quad (\text{B.1.1})$$

for basic operations $\circ \in \{+, -, \times, \div\}$ and a machine precision $\mathbf{u}(\varepsilon, n)$, which is a function of the desired accuracy ε and the size of the problem n . We assume that \sqrt{x} can be evaluated in this way as well. [\(B.1.1\)](#) is a standard formulation for finite-precision computations (see for example [[35](#)]).

Throughout, we can think of \mathbf{u} as inverse polynomial in n . In practice, we choose \mathbf{u} based on our error analysis to ensure either true backward stability or, if that's not possible, the slightly weaker logarithmic stability of Demmel, Dumitriu, and Holtz [[17](#)]. With this in mind, we further assume access to black-box algorithms for Gaussian sampling, matrix multiplication, and QR/QL, which we summarize below. These follow Banks et al. [[9](#)] to allow for easy connection with their floating-point bounds.

Assumption B.1 (Gaussian Sampling). There exists a c_N -stable Gaussian sampler $N(\sigma)$ that takes $\sigma \in \mathbb{R}_{\geq 0}$ and outputs $N(\sigma)$ satisfying $|N(\sigma) - \mathcal{N}| \leq c_N \sigma \mathbf{u}$ for some $\mathcal{N} \sim \mathcal{N}(0, \sigma^2)$.

Assumption B.2 (Matrix Multiplication). There exists a $\mu_{MM}(n)$ -stable $n \times n$ multiplication algorithm $MM(\cdot, \cdot)$ satisfying

$$\|MM(A, B) - AB\|_2 \leq \mu_{MM}(n) \mathbf{u} \|A\|_2 \|B\|_2$$

in $T_{MM}(n)$ arithmetic operations.

Assumption B.3 (QR Factorization). There exists a $\mu_{QR}(n)$ -stable $n \times n$ QR algorithm $QR(\cdot)$ satisfying

1. $[Q, R] = \mathbf{QR}(A)$
2. R is exactly upper triangular
3. There exist A' and unitary Q' such that $A' = Q'R$ with

$$\|Q' - Q\|_2 \leq \mu_{\mathbf{QR}}(n)\mathbf{u} \quad \text{and} \quad \|A' - A\|_2 \leq \mu_{\mathbf{QR}}(n)\mathbf{u}\|A\|_2,$$

in $T_{\mathbf{QR}}(n)$ arithmetic operations.

For simplicity, we further assume access to a QL algorithm $\mathbf{QL}(\cdot)$ that satisfies similar guarantees as in [Assumption B.3](#) with the same parameter $\mu_{\mathbf{QR}}(n)$. Note that for these routines we can always guarantee a truly triangular result in finite-precision by forcing entries above/below the diagonal to be zero. Finally, we include a black-box inversion algorithm to allow us to quantify the benefit of working inverse-free.

Assumption B.4 (Matrix Inversion). There exists a $(\mu_{\mathbf{INV}}(n), c_{\mathbf{INV}})$ -stable $n \times n$ inversion algorithm $\mathbf{INV}(\cdot)$ satisfying

$$\|\mathbf{INV}(A) - A^{-1}\|_2 \leq \mu_{\mathbf{INV}}(n)\mathbf{u}\kappa_2(A)^{c_{\mathbf{INV}} \log(n)}\|A^{-1}\|_2$$

in $T_{\mathbf{INV}}(n)$ arithmetic operations.

Before proceeding with our analysis, we pause to note that the assumptions listed above are all compatible with fast matrix multiplication [17], meaning the bounds cover any implementation that uses a fast matrix multiplication routine, including [16, 56, 63, 64].

B.2 Finite-Precision Shattering

In this section, we consider how floating-point computations impact pseudospectral shattering. We start with $\Lambda_\epsilon(\tilde{A}, n^\alpha \tilde{B})$. A straightforward extension of [9, Theorem 3.13] implies the following finite-precision counterpart to [Theorem 3.12](#).

Theorem B.5. *Let $A, B \in \mathbb{C}^{n \times n}$ with $\|A\|_2, \|B\|_2 \leq 1$ and let $0 < \gamma < \frac{1}{2}$. Further, let $\omega = \frac{\gamma^4}{4} n^{-\frac{8\alpha+13}{3}}$ and construct the grid $g = \text{grid}(z, \omega, \lceil 8/\omega \rceil, \lceil 8/\omega \rceil)$ for $\alpha > 0$ and z chosen uniformly at random from the square with bottom left corner $-4 - 4i$ and side length ω . On a floating-point machine with precision \mathbf{u} , suppose $G_1, G_2 \in \mathbb{C}^{n \times n}$ satisfy $G_k(i, j) = N(\frac{1}{\sqrt{n}})$ for $1 \leq i, j \leq n$ and $k = 1, 2$. If $\tilde{A} = A + \gamma G_1$ and $\tilde{B} = B + \gamma G_2$ (again in finite precision) then $\Lambda_\epsilon(\tilde{A}, n^\alpha \tilde{B})$ is shattered with respect to g for*

$$\epsilon = \frac{1}{2} \cdot \frac{\gamma^5}{64n^{\frac{11\alpha+25}{3}} + \gamma^5}$$

with probability at least $\left[1 - \frac{82}{n} - \frac{531441}{16n^2}\right] \left[1 - \frac{n^{2-2\alpha}}{\gamma^2} - 4e^{-n}\right]$ provided

$$\mathbf{u} \leq \frac{1}{2(3 + c_N)n^{\alpha+\frac{1}{2}}} \cdot \frac{\gamma^5}{64n^{\frac{11\alpha+25}{3}} + \gamma^5}.$$

Proof. Following the proof of [9, Theorem 3.13], \tilde{A} and \tilde{B} are at most $(3+c_N)\sqrt{n}\mathbf{u}$ away (in the spectral norm) from their exact-arithmetic counterparts. Accommodating the n^α scaling on \tilde{B} and recalling that shattering is achieved in exact arithmetic for $\epsilon = \frac{\gamma^5}{64n^{\frac{11\alpha+25}{3}} + \gamma^5}$ with probability at least $\left[1 - \frac{82}{n} - \frac{531441}{16n^2}\right] \left[1 - \frac{n^{2-2\alpha}}{\gamma^2} - 4e^{-n}\right]$, [Lemma 3.14](#) implies that it is sufficient to take

$$(3 + c_N)n^{\alpha+\frac{1}{2}}\mathbf{u} \leq \frac{1}{2} \cdot \frac{\gamma^5}{64n^{\frac{11\alpha+25}{3}} + \gamma^5}, \tag{B.2.1}$$

which is equivalent to the listed requirement on \mathbf{u} . □

We consider next $\tilde{B}^{-1}\tilde{A}$. In this case, we must account for error incurred by inverting \tilde{B} and multiplying by \tilde{A} on top of the error already baked into \tilde{A} and \tilde{B} . With this in mind, we first prove an intermediate result.

Lemma B.6. Suppose $A_1, A_2, B_1, B_2 \in \mathbb{C}^{n \times n}$ with $\|A_1 - A_2\|_2, \|B_1 - B_2\|_2 \leq \delta$ for $\delta < \sigma_n(B_1)$. Then

$$\|B_1^{-1}A_1 - B_2^{-1}A_2\|_2 \leq \delta \|B_1^{-1}\|_2 \left(1 + \frac{\|A_1\|_2 + \delta}{\sigma_n(B_1) - \delta}\right).$$

Proof. We have

$$\begin{aligned} \|B_1^{-1}A_1 - B_2^{-1}A_2\|_2 &= \|B_1^{-1}A_1 - B_1^{-1}A_2 + B_1^{-1}A_2 - B_2^{-1}A_2\|_2 \\ &\leq \|B_1^{-1}\|_2 \|A_1 - A_2\|_2 + \|B_1^{-1} - B_2^{-1}\|_2 \|A_2\|_2 \\ &\leq \delta \|B_1^{-1}\|_2 + \|B_1^{-1}\|_2 \|B_2 - B_1\|_2 \|B_2^{-1}\|_2 \|A_2\|_2 \\ &\leq \delta \|B_1^{-1}\|_2 \left(1 + \frac{\|A_2\|_2}{\sigma_n(B_2)}\right) \\ &\leq \delta \|B_1^{-1}\|_2 \left(1 + \frac{\|A_1\|_2 + \delta}{\sigma_n(B_1) - \delta}\right), \end{aligned} \tag{B.2.2}$$

where the last inequality follows from stability of singular values. \square

Combining [Lemma B.6](#) with [Assumption B.2](#) and [Assumption B.4](#) yields the following finite-precision counterpart to [Proposition 3.13](#).

Theorem B.7. Let $A, B \in \mathbb{C}^{n \times n}$ with $\|A\|_2, \|B\|_2 \leq 1$ and let $\gamma \in (0, \frac{1}{2})$. Further let $\omega = \frac{\gamma^4}{4} n^{-\frac{8\alpha+13}{3}}$ and construct the grid $g = \text{grid}(z, \omega, \lceil 8/\omega \rceil, \lceil 8/\omega \rceil)$ for $\alpha > 0$ and z chosen uniformly at random from the square with bottom left corner $-4 - 4i$ and side length ω . On a floating-point machine with precision \mathbf{u} , suppose $G_1, G_2 \in \mathbb{C}^{n \times n}$ satisfy $G_k(i, j) = N(\frac{1}{\sqrt{n}})$ for $1 \leq i, j \leq n$ and $k = 1, 2$. If $\tilde{A} = A + \gamma G_1, \tilde{B} = B + \gamma G_2$ (again in finite precision) and further

$$M = \text{MM}(\text{INV}(\tilde{B}), \tilde{A}),$$

then $\Lambda_\epsilon(n^{-\alpha}M)$ is shattered with respect to g for

$$\epsilon = \frac{\gamma^5}{32} n^{-\frac{11\alpha+25}{3}}$$

with probability at least $\left[1 - \frac{82}{n} - \frac{531441}{16n^2}\right] \left[1 - \frac{n^{2-2\alpha}}{\gamma^2} - 4e^{-n}\right]$ provided

$$\mathbf{u} \leq \frac{1}{21\mu_{\text{INV}}(n)} \cdot \frac{1}{(6n^\alpha + 1)^{c_{\text{INV}} \log(n)}} \cdot \frac{\gamma^5}{64} n^{-\frac{11\alpha+25}{3}}.$$

Proof. Set $(A_2, B_2) = (\tilde{A}, \tilde{B})$ and let (A_1, B_1) be the corresponding exact-arithmetic pencil (perturbed with true Ginibre matrices). Further let $X = n^{-\alpha}B_1^{-1}A_1$ and $X' = n^{-\alpha}B_2^{-1}A_2$. Here, X is the exact-arithmetic product covered by [Proposition 3.13](#) while X' is the exact product corresponding to (A_2, B_2) , equivalently a floating-point version of X that assumes exact inversion and matrix multiplication. Throughout, we assume access to the events that guarantee shattering in [Proposition 3.13](#), in particular $\sigma_n(B_1) \geq n^{-\alpha}$, and $\|A_1\|_2, \|B_1\|_2 \leq 3$, which occur with probability at least $\left[1 - \frac{82}{n} - \frac{531441}{16n^2}\right] \left[1 - \frac{n^{2-2\alpha}}{\gamma^2} - 4e^{-n}\right]$.

As in the proof of [Theorem B.5](#), we start by noting $\|A_1 - A_2\|_2, \|B_1 - B_2\|_2 \leq (3 + c_N)\sqrt{n}\mathbf{u}$. Since $\mathbf{u} \leq \frac{1}{2(3+c_N)n^{\alpha+\frac{1}{2}}}$ and therefore $(3 + c_N)\sqrt{n}\mathbf{u} \leq \frac{1}{2n^\alpha} < \sigma_n(B_1)$, [Lemma B.6](#) implies

$$\|X - X'\|_2 \leq 2(3 + c_N)\sqrt{n}\mathbf{u}(1 + 3n^\alpha). \tag{B.2.3}$$

With this in mind, we next seek a bound on $\|n^{-\alpha}M - X'\|_2$. To do this, let $C = \text{INV}(B_2)$. Applying [Assumption B.4](#), we have

$$\|C - B_2^{-1}\|_2 \leq \mu_{\text{INV}}(n)\mathbf{u}\kappa_2(B_2)^{c_{\text{INV}} \log(n)} \|B_2^{-1}\|_2. \tag{B.2.4}$$

By the stability of singular values, $\|B_2\|_2 \leq 3 + (3 + c_N)\sqrt{n}\mathbf{u}$ and $\sigma_n(B_2) \geq n^{-\alpha} - (3 + c_N)\sqrt{n}\mathbf{u}$, so this can be simplified to

$$\begin{aligned} \|C - B_2^{-1}\|_2 &\leq \mu_{\text{INV}}(n)\mathbf{u} \left(\frac{(3 + (3 + c_N)\sqrt{n}\mathbf{u})n^\alpha}{1 - [(3 + c_N)\sqrt{n}\mathbf{u}]n^\alpha} \right)^{c_{\text{INV}} \log(n)} \cdot \frac{n^\alpha}{1 - [(3 + c_N)\sqrt{n}\mathbf{u}]n^\alpha} \\ &\leq \mu_{\text{INV}}(n)\mathbf{u}(6n^\alpha + 1)^{c_{\text{INV}} \log(n)}(2n^\alpha), \end{aligned} \quad (\text{B.2.5})$$

where we again use the fact that $(3 + c_N)\sqrt{n}\mathbf{u} \leq \frac{1}{2n^\alpha}$. Now $M = \mathbf{M}\mathbf{M}(C, A_2)$, so by [Assumption B.2](#)

$$\|M - CA_2\|_2 \leq \mu_{\text{MM}}(n)\mathbf{u}\|C\|_2\|A_2\|_2. \quad (\text{B.2.6})$$

Bounding $\|C\|_2$ via [\(B.2.5\)](#) as

$$\|C\|_2 \leq \|B_2^{-1}\|_2 + \mu_{\text{INV}}(n)\mathbf{u}(6n^\alpha + 1)^{c_{\text{INV}} \log(n)}(2n^\alpha) \leq 2n^\alpha \left[1 + \mu_{\text{INV}}(n)\mathbf{u}(6n^\alpha + 1)^{c_{\text{INV}} \log(n)} \right] \quad (\text{B.2.7})$$

and further noting $\|A_2\|_2 \leq \|A\|_1 + (3 + c_N)\sqrt{n}\mathbf{u} \leq 3 + (3 + c_N)\sqrt{n}\mathbf{u}$, we conclude

$$\begin{aligned} \|M - CA_2\|_2 &\leq \mu_{\text{MM}}(n)\mathbf{u}(6n^\alpha + 1) \left[1 + \mu_{\text{INV}}(n)\mathbf{u}(6n^\alpha + 1)^{c_{\text{INV}} \log(n)} \right] \\ &= \mu_{\text{MM}}(n)\mathbf{u}(6n^\alpha + 1) + \mu_{\text{MM}}(n)\mu_{\text{INV}}(n)\mathbf{u}^2(6n^\alpha + 1)^{c_{\text{INV}} \log(n)+1}. \end{aligned} \quad (\text{B.2.8})$$

Putting everything together, we have

$$\begin{aligned} \|n^{-\alpha}M - X'\|_2 &= \|n^{-\alpha}M - n^{-\alpha}CA_2 + n^{-\alpha}CA_2 - n^{-\alpha}B_2^{-1}A_2\|_2 \\ &\leq n^{-\alpha}\|M - CA_2\|_2 + n^{-\alpha}\|C - B_2^{-1}\|_2\|A_2\|_2 \\ &\leq 7 \left[\mu_{\text{MM}}(n)\mathbf{u} + \mu_{\text{MM}}(n)\mu_{\text{INV}}(n)\mathbf{u}^2(6n^\alpha + 1)^{c_{\text{INV}} \log(n)} + \mu_{\text{INV}}(n)\mathbf{u}(6n^\alpha + 1)^{c_{\text{INV}} \log(n)} \right] \end{aligned} \quad (\text{B.2.9})$$

after applying $n^{-\alpha}(6n^\alpha + 1) \leq 7$ and $\|A_2\|_2 \leq 3 + (3 + c_N)\sqrt{n}\mathbf{u} \leq \frac{7}{2}$ to simplify constants. The last term in this expression clearly dominates; assuming each piece of [\(B.2.9\)](#) is bounded by the last one, we obtain

$$\|n^{-\alpha}M - X'\|_2 \leq 21\mu_{\text{INV}}(n)\mathbf{u}(6n^\alpha + 1)^{c_{\text{INV}} \log(n)}. \quad (\text{B.2.10})$$

Combining this with [\(B.2.3\)](#) yields our final error bound:

$$\|n^{-\alpha}M - X\|_2 \leq 21\mu_{\text{INV}}(n)\mathbf{u}(6n^\alpha + 1)^{c_{\text{INV}} \log(n)} + 2(3 + c_N)\sqrt{n}\mathbf{u}(1 + 3n^\alpha). \quad (\text{B.2.11})$$

Since [Proposition 3.13](#) implies that $\Lambda_\epsilon(X)$ is shattered for $\epsilon = \frac{\gamma^5}{16}n^{-\frac{11\alpha+25}{3}}$, we ensure shattering for $\Lambda_\epsilon(n^{-\alpha}M)$ with $\epsilon = \frac{\gamma^5}{32}n^{-\frac{11\alpha+25}{3}}$ by requiring that each piece of [\(B.2.11\)](#) is bounded by $\frac{\gamma^5}{64}n^{-\frac{11\alpha+25}{3}}$, which is guaranteed as long as

$$\mathbf{u} \leq \frac{1}{21\mu_{\text{INV}}(n)} \cdot \frac{1}{(6n^\alpha + 1)^{c_{\text{INV}} \log(n)}} \cdot \frac{\gamma^5}{64}n^{-\frac{11\alpha+25}{3}}. \quad (\text{B.2.12})$$

Note that this requirement on \mathbf{u} satisfies the assumptions used throughout the proof. \square

Comparing [Theorem B.7](#) with [Theorem B.5](#) makes clear the practical cost of forming $\tilde{B}^{-1}\tilde{A}$. In particular, finite-precision shattering for the pencil requires $O(\log(n/\epsilon))$ bits of precision versus $O(\log(n/\epsilon) + \log^2(n))$ for $n^{-\alpha}\tilde{B}^{-1}\tilde{A}$, where the polylog increase in the latter is rooted in the logarithmic stability of [INV](#). This captures rigorously the phenomenon displayed in [Figure 3](#).

B.3 Two-Matrix GRURV

In our algorithm, [EIG](#) only ever applies [GRURV](#) to a pair of matrices in one of the following ways: [GRURV](#)(2, $A_1, A_2, -1, 1$) or [GRURV](#)(2, $A_1, A_2, 1, -1$). Under the floating-point setting established above, the first of these proceeds as follows.

[GRURV](#)(2, $A_1, A_2, -1, 1$):

1. $[U_2, R_2, V] = \mathbf{RURV}(A_2)$
2. $X = \mathbf{MM}(A_1^H, U_2)$
3. $[U, R_1^H] = \mathbf{QL}(X)$

There are three sources of error here: \mathbf{RURV} in step one, matrix multiplication in step two, and \mathbf{QL} in step three. The latter two are controlled by [Assumption B.2](#) and [Assumption B.3](#) respectively. To control error in finite precision \mathbf{RURV} , we use work of Banks et al. [[9](#), Lemma C.17] (which is itself built on [Assumption B.1](#)). Under the additional assumptions

$$4\|A_2\|_2 \max\{c_N\mu_{\mathbf{MM}}(n)\mathbf{u}, c_N\mu_{\mathbf{QR}}(n)\mathbf{u}\} \leq \frac{1}{4} \leq \|A_2\|_2 \quad \text{and} \quad 1 \leq \min\{\mu_{\mathbf{MM}}(n), \mu_{\mathbf{QR}}(n), c_N\} \quad (\text{B.3.1})$$

this yields the following.

Theorem B.8. *Given $A_1, A_2 \in \mathbb{C}^{n \times n}$, let $[U, R_1, R_2, V] = \mathbf{GRURV}(2, A_1, A_2, -1, 1)$ on a floating-point machine with precision \mathbf{u} satisfying (B.3.1). Then there exist $\tilde{A}_1, \tilde{A}_2 \in \mathbb{C}^{n \times n}$ and unitary $\tilde{U}, \tilde{V} \in \mathbb{C}^{n \times n}$ such that $\tilde{A}_1^{-1}\tilde{A}_2 = \tilde{U}R_1^{-1}R_2\tilde{V}$ and*

1. \tilde{V} is Haar distributed.
2. $\|U - \tilde{U}\|_2 \leq \mu_{\mathbf{QR}}(n)\mathbf{u}$.
3. $\|A_1 - \tilde{A}_1\|_2 \leq [\mu_{\mathbf{QR}}(n)\mathbf{u} + \mu_{\mathbf{MM}}(n)\mathbf{u}(1 + \mu_{\mathbf{QR}}(n)\mathbf{u}) + \mu_{\mathbf{QR}}(n)\mathbf{u}(1 + \mu_{\mathbf{MM}}(n)\mathbf{u})(1 + \mu_{\mathbf{QR}}(n)\mathbf{u})] \|A_1\|_2$.
4. For every $1 > \alpha > 0$ and $t > 2\sqrt{2} + 1$, the event that both
 - $\|V - \tilde{V}\|_2 \leq \frac{8tn^{3/2}}{\alpha} c_N\mu_{\mathbf{QR}}(n)\mathbf{u} + \frac{10n^2}{\alpha}\mathbf{u}$
 - $\|A_2 - \tilde{A}_2\|_2 \leq \left(\frac{9tn^{3/2}}{\alpha} c_N\mu_{\mathbf{QR}}(n)\mathbf{u} + 2\mu_{\mathbf{MM}}(n)\mathbf{u} + \frac{10n^2}{\alpha} c_N\mathbf{u} \right) \|A_2\|_2$

occurs with probability at least $1 - 2e\alpha^2 - 2e^{-t^2n}$.

Proof. Beginning with finite-precision guarantees for \mathbf{RURV} , [[9](#), Lemma C.17] implies that there exists unitary matrices \tilde{U}_2 and \tilde{V} and a matrix \tilde{A}_2 such that $\tilde{A}_2 = \tilde{U}_2 R_2 \tilde{V}$, where \tilde{V} is Haar distributed and $\|U_2 - \tilde{U}_2\|_2, \|V - \tilde{V}\|_2$, and $\|A_2 - \tilde{A}_2\|_2$ can all be controlled. In particular,

$$\|U_2 - \tilde{U}_2\|_2 \leq \mu_{\mathbf{QR}}(n)\mathbf{u}. \quad (\text{B.3.2})$$

Consequently, [Assumption B.2](#) guarantees that in step two above

$$\|X - A_1^H U_2\|_2 \leq \mu_{\mathbf{MM}}(n)\mathbf{u} \|U_2\|_2 \|A_1\|_2 \leq \mu_{\mathbf{MM}}(n)\mathbf{u}(1 + \mu_{\mathbf{QR}}(n)\mathbf{u}) \|A_1\|_2. \quad (\text{B.3.3})$$

Lastly, [Assumption B.3](#) implies that there exists a unitary matrix \tilde{U} and a matrix \tilde{X} such that $\tilde{X} = \tilde{U}R_1^H$ with

$$\|X - \tilde{X}\|_2 \leq \mu_{\mathbf{QR}}(n)\mathbf{u} \|X\|_2. \quad (\text{B.3.4})$$

With this in mind, let $\tilde{A}_1 = \tilde{U}_2 \tilde{X}^H$. By construction, we have

$$\tilde{A}_1^{-1} \tilde{A}_2 = (\tilde{U}_2 \tilde{X}^H)^{-1} \tilde{U}_2 R_2 \tilde{V} = (R_1 \tilde{U}^H)^{-1} R_2 \tilde{V} = \tilde{U} R_1^{-1} R_2 \tilde{V}, \quad (\text{B.3.5})$$

which means $\tilde{U} R_1^{-1} R_2 \tilde{V}$ is a generalized rank-revealing factorization of $\tilde{A}_1^{-1} \tilde{A}_2$. Now the distance between A_2 and \tilde{A}_2 follows directly from [[9](#), Lemma C.17], as does the analogous result for \tilde{V} . Additionally, we observe

$$\begin{aligned} \|A_1 - \tilde{A}_1\|_2 &= \|A_1 - \tilde{U}_2 \tilde{X}^H\|_2 \\ &\leq \|A_1^H \tilde{U}_2 - \tilde{X}\|_2 \\ &= \|A_1^H \tilde{U}_2 - A_1^H U_2 + A_1^H U_2 - X + X - \tilde{X}\|_2 \\ &\leq \|A_1^H (\tilde{U}_2 - U_2)\|_2 + \|A_1^H U_2 - X\|_2 + \|X - \tilde{X}\|_2 \\ &\leq \|A_1\|_2 \mu_{\mathbf{QR}}(n)\mathbf{u} + \mu_{\mathbf{MM}}(n)\mathbf{u}(1 + \mu_{\mathbf{QR}}(n)\mathbf{u}) \|A_1\|_2 + \mu_{\mathbf{QR}}(n)\mathbf{u} \|X\|_2. \end{aligned} \quad (\text{B.3.6})$$

Since (B.3.3) implies

$$\begin{aligned}
\|X\|_2 &\leq \mu_{\text{MM}}(n)\mathbf{u}(1 + \mu_{\text{QR}}(n)\mathbf{u})\|A_1\|_2 + \|A_1^H U_2\|_2 \\
&\leq \mu_{\text{MM}}(n)\mathbf{u}(1 + \mu_{\text{QR}}(n)\mathbf{u})\|A_1\|_2 + \|A_1\|_2(1 + \mu_{\text{QR}}(n)\mathbf{u}) \\
&= (1 + \mu_{\text{MM}}(n)\mathbf{u})(1 + \mu_{\text{QR}}(n)\mathbf{u})\|A_1\|_2,
\end{aligned} \tag{B.3.7}$$

this becomes

$$\|A_1 - \tilde{A}_1\|_2 \leq [\mu_{\text{QR}}(n)\mathbf{u} + \mu_{\text{MM}}(n)\mathbf{u}(1 + \mu_{\text{QR}}(n)\mathbf{u}) + \mu_{\text{QR}}(n)\mathbf{u}(1 + \mu_{\text{MM}}(n)\mathbf{u})(1 + \mu_{\text{QR}}(n)\mathbf{u})] \|A_1\|_2. \tag{B.3.8}$$

Finally recalling (B.3.2), we have all of the listed bounds. \square

While [Theorem B.8](#) applies explicitly to $\mathbf{GRURV}(2, A_1, A_2, -1, 1)$ it also covers $\mathbf{GRURV}(2, A_1, A_2, 1, -1)$; the latter only swaps \mathbf{RURV} and \mathbf{QL} for \mathbf{RULV} and \mathbf{QR} , thereby providing the same guarantees since \mathbf{QR} and \mathbf{QL} satisfy essentially the same assumptions.

References

- [1] B. Adlerborn, B. Kågström, and D. Kressner. A parallel QZ algorithm for distributed memory HPC systems. *SIAM Journal on Scientific Computing*, 36(5):C480–C503, 2014.
- [2] M. Aizenman, R. Peled, J. Schenker, M. Shamis, and S. Sodin. Matrix regularizing effects of Gaussian perturbations. *Communications in Contemporary Mathematics*, 19(03):1750028, 2017.
- [3] L. M. Anguas, M. I. Bueno, and F. M. Dopico. A comparison of eigenvalue condition numbers for matrix polynomials. *Linear Algebra and its Applications*, 564:170–200, 2019.
- [4] Z. Bai, J. Demmel, and M. Gu. An inverse free parallel spectral divide and conquer algorithm for nonsymmetric eigenproblems. *Numerische Mathematik*, 76:279–308, 1997.
- [5] Z. D. Bai. Circular law. *The Annals of Probability*, 25(1):494–529, 1997.
- [6] G. Ballard, J. Demmel, and I. Dumitriu. Minimizing Communication for Eigenproblems and the Singular Value Decomposition. Technical Report UCB/EECS-2011-14, EECS Department, University of California, Berkeley, Feb 2011.
- [7] G. Ballard, J. Demmel, I. Dumitriu, and A. Rusciano. A Generalized Randomized Rank-Revealing Factorization. arXiv:1909.06524, 2019.
- [8] G. Ballard, J. Demmel, O. Holtz, and O. Schwartz. Minimizing communication in numerical linear algebra. *SIAM Journal on Matrix Analysis and Applications*, 32:866–901, 2011.
- [9] J. Banks, J. Garza-Vargas, A. Kulkarni, and N. Srivastava. Pseudospectral Shattering, the Sign Function, and Diagonalization in Nearly Matrix Multiplication Time. *Foundations of Computational Mathematics*, 23:1959–2047, 2023.
- [10] J. Banks, A. Kulkarni, S. Mukherjee, and N. Srivastava. Gaussian regularization of the pseudospectrum and Davies’ conjecture. *Communications on Pure and Applied Mathematics*, 74:2114–2131, 2021.
- [11] F. L. Bauer and C. T. Fike. Norms and exclusion theorems. *Numerische Mathematik*, 2(1):137–141, 1960.
- [12] A. Beavers and E. Denman. A new similarity transformation method for eigenvalues and eigenvectors. *Mathematical Biosciences*, 21(1):143–169, 1974.
- [13] T. F. Chan. Rank revealing QR factorizations. *Linear Algebra and its Applications*, 88-89:67–82, 1987.
- [14] E. K. Chu. Exclusion theorems and the perturbation analysis of the generalized eigenvalue problem. *SIAM Journal on Numerical Analysis*, 24(5):1114–1125, 1987.

- [15] E. K. Chu. Perturbation of eigenvalues for matrix polynomials via the Bauer-Fike theorems. *SIAM Journal on Matrix Analysis and Applications*, 25(2):551–573, 2003.
- [16] D. Coppersmith and S. Winograd. Matrix multiplication via arithmetic progressions. *Journal of Symbolic Computation*, 9(3):251–280, 1990.
- [17] J. Demmel, I. Dumitriu, and O. Holtz. Fast linear algebra is stable. *Numerische Mathematik*, 108:59–91, 2007.
- [18] J. W. Demmel and B. Kågström. Computing stable eigendecompositions of matrix pencils. *Linear Algebra and its Applications*, 88-89:139–186, 1987.
- [19] F. M. Dopico and V. Noferini. Root polynomials and their role in the theory of matrix polynomials. *Linear Algebra and its Applications*, 584:37–78, 2020.
- [20] A. Edelman. Eigenvalues and condition numbers of random matrices. *SIAM Journal on Matrix Analysis and Applications*, 9(4):543–560, 1988.
- [21] A. Edelman and N. R. Rao. Random matrix theory. *Acta Numerica*, 14:233–297, 2005.
- [22] L. Elsner and P. Lancaster. The spectral variation of pencils of matrices. *Journal of Computational Mathematics*, 3(3):262–274, 1985.
- [23] L. Elsner and J. Sun. Perturbation theorems for the generalized eigenvalue problem. *Linear Algebra and its Applications*, 48:341–357, 1982.
- [24] T. Ericsson and A. Ruhe. The spectral transformation Lánczos method for the numerical solution of large sparse generalized symmetric eigenvalue problems. *Mathematics of Computation*, 35:1251–1268, 1980.
- [25] B. Farrell and R. Vershynin. Smoothed analysis of symmetric random matrices with continuous distributions. *Proceedings of the American Mathematical Society*, 144, 2012.
- [26] R. D. Fierro, P. C. Hansen, and P. S. K. Hansen. UTV tools: Matlab templates for rank-revealing UTV decompositions. *Numerical Algorithms*, 20:165–194, 1999.
- [27] G. D. Forney, Jr. Minimal bases of rational vector spaces, with applications to multivariable linear systems. *SIAM Journal on Control*, 13(3):493–520, 1975.
- [28] V. Frayssé, M. Gueury, F. Nicoud, and V. Toumazou. Spectral portraits for matrix pencils. Technical Report, CERFACS, 1996.
- [29] J. D. Gardiner and A. J. Laub. A generalization of the matrix-sign-function solution for algebraic Riccati equations. *International Journal of Control*, 44(3):823–832, 1986.
- [30] A. Greenbaum, R.-C. Li, and M. L. Overton. First-order perturbation theory for eigenvalues and eigenvectors. *SIAM Review*, 62(2):463–482, 2020.
- [31] M. Gu and S. C. Eisenstat. Efficient algorithms for computing a strong rank-revealing QR factorization. *SIAM Journal on Scientific Computing*, 17(4):848–869, 1996.
- [32] M. R. Guarracino, C. Cifarelli, O. Seref, and P. M. Pardalos. A classification method based on generalized eigenvalue problems. *Optimization Methods and Software*, 22(1):73–81, 2007.
- [33] E. Hairer and G. Wanner. *Solving Ordinary Differential Equations II. Stiff and Differential-Algebraic Problems*, volume 14 of *Springer Verlag Series in Computational Mathematics*. 1996.
- [34] D. J. Higham and N. J. Higham. Structured backward error and condition of generalized eigenvalue problems. *SIAM Journal on Matrix Analysis and Applications*, 20(2):493–512, 1998.
- [35] N. J. Higham. *Accuracy and Stability of Numerical Algorithms*. Society for Industrial and Applied Mathematics, Second edition, 2002.

- [36] M. E. Hochstenbach, C. Mehl, and B. Plestenjak. Solving singular generalized eigenvalue problems by a rank-completing perturbation. *SIAM Journal on Matrix Analysis and Applications*, 40(3):1022–1046, 2019.
- [37] R. A. Horn and C. R. Johnson. *Matrix Analysis*. Cambridge University Press, Second edition, 2012.
- [38] Y. Hua and T. Sarkar. Matrix pencil method for estimating parameters of exponentially damped/undamped sinusoids in noise. *IEEE Transactions on Acoustics, Speech, and Signal Processing*, 38(5):814–824, 1990.
- [39] B. Kågström and D. Kressner. Multishift variants of the QZ algorithm with aggressive early deflation. *SIAM Journal on Matrix Analysis and Applications*, 29(1):199–227, 2007.
- [40] L. Kronecker. *Algebraische Reduction der Schaaren bilinearer Formen*. Sitzungsberichte der Preussischen Akademie der Wissenschaften. 1890.
- [41] M. Lotz and V. Noferini. Wilkinson’s bus: Weak condition numbers, with an application to singular polynomial eigenproblems. *Foundations of Computational Mathematics*, 20:1439–1473, 2020.
- [42] A. N. Malyshev. Parallel algorithm for solving some spectral problems of linear algebra. *Linear Algebra and its Applications*, 188-189:489–520, 1993.
- [43] O. Mangasarian and E. Wild. Multisurface proximal support vector machine classification via generalized eigenvalues. *IEEE Transactions on Pattern Analysis and Machine Intelligence*, 28(1):69–74, 2006.
- [44] C. B. Moler and G. W. Stewart. An algorithm for generalized matrix eigenvalue problems. *SIAM Journal on Numerical Analysis*, 10(2):241–256, 1973.
- [45] J. D. Roberts. Linear model reduction and solution of the algebraic Riccati equation by use of the sign function. *International Journal of Control*, 32(4):677–687, 1980.
- [46] R. Roy and T. Kailath. ESPRIT-estimation of signal parameters via rotational invariance techniques. *IEEE Transactions on Acoustics, Speech, and Signal Processing*, 37(7):984–995, 1989.
- [47] M. Rudelson and R. Vershynin. The Littlewood–Offord problem and invertibility of random matrices. *Advances in Mathematics*, 218(2):600–633, 2008.
- [48] T. Sakurai and H. Sugiura. A projection method for generalized eigenvalue problems using numerical integration. *Journal of Computational and Applied Mathematics*, 159(1):119–128, 2003.
- [49] A. H. Sameh and J. A. Wisniewski. A trace minimization algorithm for the generalized eigenvalue problem. *SIAM Journal on Numerical Analysis*, 19(6):1243–1259, 1982.
- [50] A. Sankar, D. A. Spielman, and S.-H. Teng. Smoothed analysis of the condition numbers and growth factors of matrices. *SIAM Journal on Matrix Analysis and Applications*, 28(2):446–476, 2006.
- [51] R. Schneider. Pseudospectral Divide-and-Conquer for the Generalized Eigenvalue Problem. PhD Thesis, 2024.
- [52] X. Shi and Y. Wei. A sharp version of Bauer–Fike’s theorem. *Journal of Computational and Applied Mathematics*, 236(13):3218–3227, 2012.
- [53] G. W. Stewart. Gershgorin theory for the generalized eigenvalue problem $Ax = \lambda Bx$. *Mathematics of Computation*, 29(130):600–606, 1975.
- [54] G. W. Stewart. Updating a rank-revealing ULV decomposition. *SIAM Journal on Matrix Analysis and Applications*, 14(2):494–499, 1993.
- [55] G. W. Stewart and J. Sun. *Matrix Perturbation Theory*. Computer Science and Scientific Computing. Elsevier Science, 1990.

- [56] V. Strassen. Gaussian elimination is not optimal. *Numerische Mathematik*, 13:354–356, 1969.
- [57] T. Tao and V. Vu. Random matrices: the distribution of the smallest singular values. *Geometric and Functional Analysis*, 20, 04 2009.
- [58] L. N. Trefethen and M. Embree. *Spectra and Pseudospectra: The Behavior of Nonnormal Matrices and Operators*. Princeton University Press, 2020.
- [59] P. Van Dooren. Reducing subspaces: Definitions, properties and algorithms. In B. Kågström and A. Ruhe, editors, *Matrix Pencils*, pages 58–73, Berlin, Heidelberg, 1983. Springer Berlin Heidelberg.
- [60] R. Vershynin. *High-Dimensional Probability: An Introduction with Applications in Data Science*. Cambridge Series in Statistical and Probabilistic Mathematics. Cambridge University Press, 2018.
- [61] R. C. Ward. The combination shift QZ algorithm. *SIAM Journal on Numerical Analysis*, 12(6):835–853, 1975.
- [62] D. S. Watkins. Performance of the QZ algorithm in the presence of infinite eigenvalues. *SIAM Journal on Matrix Analysis and Applications*, 22(2):364–375, 2000.
- [63] V. V. Williams. Multiplying Matrices Faster than Coppersmith-Winograd. In *Proceedings of the Forty-Fourth Annual ACM Symposium on Theory of Computing*, STOC '12, page 887–898. Association for Computing Machinery, 2012.
- [64] V. V. Williams, Y. Xu, Z. Xu, and R. Zhou. New Bounds for Matrix Multiplication: from Alpha to Omega. arXiv:2307.07970, 2023.